Title
The hypoxanthine-Guanine-Xanthine phosphoribosyltransferase in Tritrichomonas foetus

Author
Chin, Marian Susan

Publication Date
1995

Peer reviewed|Thesis/dissertation

The Hypoxanthine-Guanine-Xanthine Phosphoribosyltransferase in Tritrichomonas foetus

by

Marian Susan Chin

DISSERTATION

Submitted in partial satisfaction of the requirements for the degree of

DOCTOR OF PHILOSOPHY

in

Pharmaceutical Chemistry

in the

GRADUATE DIVISION

of the

UNIVERSITY OF CALIFORNIA

San Francisco

Date **University Librarian**

Degree Conferred: . . . . . .

For my family,

whose unwavering belief in my capabilities made this possible.

ACKNOWLEDGMENTS

I need to express my gratitude to my advisor, Dr. C. C. Wang, for the opportunity of conducting my thesis work in his laboratory and for his guidance during the course of this work. I am grateful also to Dr. Alice Wang for teaching me basic laboratory techniques and for her kindness to me when my mother died. The work described in this dissertation would not have been possible without the advice and friendship of many of my laboratory associates, and I would like to thank each of them for what they have taught me: Dr. Ted "What is the control?" White for teaching me the importance of carrying out controlled experiments; Dr. Sydney P. Craig, III for his scientific enthusiasm and the many discussions concerning possible methods useful to isolating either the *T. foetus* HGXPRTase gene or the *G. lamblia* GPRTase gene; Dr. Joanne "What are you waiting for?" Beck for her friendship, encouragement, *T. foetus* cDNA library and for being the other person working with *T. foetus*; Dr. Ling Yuan for his advice on protein purification and enzyme kinetics; Dr. Liz Hedstrom for advice on complementation and for answering all my "dumb" questions about enzyme kinetics; Dr. Tien "Just do it" Nguyen for advice and discussions on enzyme kinetics; Dr. Jürg "The Swiss" Sommer and Dr. Shaobing "The Genius" Hua for their advice on molecular biology techniques; Dr. John Somoza for sharing the results of the mass spectrometry experiments with me and for helping me to print Figure 1.10; Dr. Doug Kuntz, Dr. Patricia Doyle, Dr. Jamil Kanaaneh, Dr. Martha Mytomba, Dr. Dechao Yu, Mr. Jorge Huerte, Mr. George Lai, Ms. Kathy Shen and Ms. Juan Wang for their friendship and encouragement. I want to thank Dr. Kathy Bass, Dr. Jessica Krakow and Dr. Tiina Sepp for their friendship and our discussions on non-scientific topics which helped me to hang on to my sanity during my graduate education.

To my roommates, Dr. Suzanna Chan, Dr. Emily Chen, Dr. Tracey Moore and Dr. Irene Tan, thanks for your friendship, encouragement and late night talks--I could not have done this without you, and a special thanks to Tracey for suggesting that I try complementation. To my church family, thanks for your concerns and prayers (Rom. 12:15), and a special thanks to the Super Saturday gang (Mia Yee, Dickson Ng, Ka Yan Liu and Elana Chin). To my "brothers", Tat Wong and Gary Dea, thanks for your prayers and for your help in setting up my computer system (there was no way that this could have been written on my old "putt-putt" MacPlus). To Dr. Darren Wong, thanks for your friendship, for the many discussions about food and music, for encouraging me to play the violin again (I regret that we never had the time to put the Brahms Violin and Piano Sonata in G together) and for being my resource person regarding the formatting of this dissertation. To Ms. Carolyn Koo (soon to be Dr. Carolyn Koo), thanks for holding up the walls of the 11th floor with me--I never could have done it without you--thank you for your friendship, for listening to me rattle on about experiments and helping me to find the flaw in my logic, for proofreading my orals proposal, my manuscript, my CV and this dissertation, for help with printing some of the figures in this dissertation, for the Price Club runs and intense baking sessions.

Most of all I want to thank my family, Mr. Eddie Chin, Ms. Marcella Chin, Mr. Matthew Chin and Dr. Linda Chun for their love, support and prayers during my graduate education--you are the best family anyone could ask for. Thank you for not asking me, "When are you going to be done?" every time you saw me. Marcy, thanks for being there for my late night despair calls, and Happy Father's Day Dad!

The majority of the material discussed in Chapter One is derived from the article: "Isolation, Sequencing and Expression of the Gene Encoding

Hypoxanthine-Guanine-Xanthine Phosphoribosyltransferase of *Tritrichomonas foetus*", published in the journal Molecular and Biochemical Parasitology, (1994), 63, 221-229. Permission from the publisher regarding the inclusion of this work in this doctoral dissertation has been obtained (see letter following the Acknowledgement section).

As J. S. Bach noted at the beginning of all his works "Jesu Juva", I also begin the description of my graduate work with this phrase, and after several years, I conclude my work as Bach did with "Soli Deo Gloria".

ELSEVIER
SCIENCE

Amsterdam Publishing
Division

Sara Burgerhartstraat 25
1055 KV Amsterdam
The Netherlands

P.O. Box 521
1000 AM Amsterdam
The Netherlands

Tel (+31) 20 5862 833
Fax (+31) 20 5862 722

Dr. Marian Chin
Department of Pharmaceutical Chemistry
Box 0446
University of California
San Francisco, CA 94143-0446
U.S.A.

Direct Line: (20) 4852 605
FAX: (20) 4852 722

Amsterdam, 9 March 1995

Dear Dr. Chin,

Thank you for your letter of 1st March 1995, copy herewith enclosed, containing your request for permission to include material from the article; "*Isolation, sequencing and expression of the gene encoding hypoxanthine-guanine-xanthine phophoribosyltransferase of Tritrichomonas foetus*", published in our journal **Molecular and Biochemical Parasitology, Vol. 63 (1994), pp. 221-229**, in your doctoral dissertation.

We are pleased to grant you, and University Microfilms International, permission to reproduce material from the above-mentioned article in your dissertation, provided that full acknowledgement is given to the original source of publication, and that your work is not distributed commercially.

Yours sincerely,
ELSEVIER SCIENCE B.V.
Amsterdam Publishing Division

Ms Tonny Smit
Rights & Permissions

Imprints:
Elsevier
Pergamon
North-Holland
Excerpta Medica

Bankers: Hollandsche Bank-Unie
Rotterdam 62.30.60.493
HR Amsterdam 158992

ABSTRACT

Tritrichomonas foetus, an anaerobic, flagellated protozoan parasite, is the causative agent of one of the major reproductive diseases of cattle. Hypoxanthine-guanine-xanthine phosphoribosyltransferase (HGXPRTase) is an enzyme essential in the nucleic acid metabolism of *T. foetus* because the parasite is unable to synthesize purine nucleotides *de novo* and relies on the HGXPRTase activities for its purine requirements. As a result of its critical role in the purine salvage pathway of *T. foetus*, this enzyme has been proposed as a potential target for structure-based inhibitor design.

Initially, a cDNA clone encoding part of the HGXPRTase was isolated by complementation of an *Escherichia coli* mutant, SØ609, with a cDNA library of *T. foetus*. The full-length genomic clone was then isolated and identified to have an open reading frame of 549 bp encoding an 183-amino acid sequence with an estimated size of 21.1 kDa. Northern blot analysis identified a single mRNA band of approximately 700-800 bases, and Southern blot analysis indicated that this is a single copy gene. The amino acid sequence is only 27.3% identical to that of the human HGPRTase but is 35-40% identical with prokaryotic HGPRTases. The *T. foetus* HGXPRTase was subsequently cloned into the pBAce vector for expression in *E. coli*. This construct yields approximately 50% of the total cellular protein of the transformed *E. coli*. The enzyme has been purified to homogeneity and was found to have the same molecular weight as the native enzyme, a pI of 4.8 and specific activities of 2856 nmol IMP/min-mg protein, 2496 nmol GMP/min-mg protein and 1567 nmol XMP/min-mg protein.

Initial velocity studies of the *T. foetus* HGXPRTase show that the enzyme follows a sequential kinetic mechanism. The simplest mechanistic model supported by the product inhibition studies is an ordered bi-bi mechanism where

TABLE OF CONTENTS:

LIST OF TABLES:

Table **Page**

LIST OF FIGURES:

INTRODUCTION

Of the parasitic trichomonads only a few, such as *Trichomonas vaginalis*, *Trichomonas gallinae* and *Tritrichomonas foetus*, are pathogenic in mammals and birds (Levine, 1961). Most trichomonads inhabit the digestive tracts of the host organism, and those found in the large intestine are commensal and nonpathogenic. Of the pathogenic species, both *T. vaginalis* and *T. foetus* are found in the urogenital tract of their hosts, and *T. gallinae* is found in the upper digestive tract (esophagus and crop) of its host. *T. foetus*, the causative agent of bovine urogenital trichomoniasis, is an anaerobic protozoan parasite. The taxonomic classification of *T. foetus* is given below:

kingdom: *Protista*

phylum: *Parabasala*

subphylum: *Sarcomastigophora*

superclass: *Mastigophora*

class: *Zoomastigophorea*

order: *Trichomonadida*

family: *Trichomonadidae*

subfamily: *Tritrichomonadidae*

Trichomonads are believed to have branched very early from the eukaryotic tree, just after *Giardia lamblia* (Sogin, *et al.*, 1989) but before the Euglenozoa. Comparison of the small subunit rRNA (SSU rRNA) sequences agrees with this theory (Sogin, 1989; Sogin, 1991). The early divergence of the trichomonads is upheld by the molecular lengths of *Tritrichomonas foetus* rDNA repeating unit and SSU rRNA (Champney, *et al.*, 1992).

MORPHOLOGY

The morphology of *T. foetus* has been studied extensively by Wenrich and Emmerson (Weinrich and Emmerson, 1933) and by Kirby (Kirby, 1951) (see Fig. I.1). The body of the parasite is spindle- to pear-shaped, approximately 9-25 μm long and 3-15 μm wide in fixed and stained preparations. The dimensions are larger for live specimens, 15-22.5 μm long and 4.5-10 μm wide, since the trichomonad cell shrinks significantly when treated with fixatives (Abraham and Honigberg, 1964). It has three anterior flagella of nearly equal length (11-17 μm), and a posterior flagellum about as long as the anterior flagella (16 μm).

Members of the *Trichomonadidae* family possess a unique cytoskeletal structure, the costa, which supports the undulating membrane. Reports (Lemoine, *et al.*, 1983; Sledge, *et al.*, 1978) have suggested that the costa is composed of carbohydrates, but cytochemical and costa fraction enrichment techniques indicate that the costa contains mainly proteins (Benchimol, *et al.*, 1982; Monteiro-Leal, *et al.*, 1993). The "accessory filament" and the attached part of the recurrent flagellum form the external margin of the undulating membrane. The undulating membrane of *T. foetus* differs from that found in other *Trichomonadinae* because it consists of two distinct physical structures: a proximal part, containing the proximal marginal lamella, and a distal part enclosing the distal marginal lamella in its ventral area and the microtubules of the recurrent flagellum in its dorsal area. Other structures observed by light microscopy include the axostyle, pelta and kinetosomes, which are all structures composed of a network of microtubules (Benchimol, 1994). Weinrich and Emmerson (Weinrich and Emmerson, 1933) found the ellipsoidal or ovoid nucleus located slightly posterior to the anterior end of the cell. With cryotechniques, Benchimol (Benchimol, 1994), found the nucleus at different locations in frozen *T. foetus* cells and proposed that the nucleus is in transient

motion prior to freeze fixation. Examination of *T. foetus* with cryotechniques also reveals that the surface of the parasite has hair-like structures projecting out from the plasma membrane (Benchimol, 1994).

T. foetus also possess lysosomes and Golgi bodies, and instead of mitochondria, they possess hydrogenosomes. The paracostal and paraaxostylar granules observed with light microscopy (Honigberg, *et al.*, 1971) correspond to the hydrogenosomes. Benchimol and de Souza (Benchimol and de Souza, 1983) found that the hydrogenosomal envelope consists of two membranes, and a peripheral vesicle is often found associated with this organelle. The hydrogenosome contains enzymes responsible for the production of acetate, CO_2 and H_2 from pyruvate and malate under anaerobic conditions (Müller, 1993), and the peripheral vesicle is believed to function in the regulation of intracellular calcium (Chapman, *et al.*, 1985). Glycogen granules are found throughout the cytoplasm and are especially abundant within the axostyle.

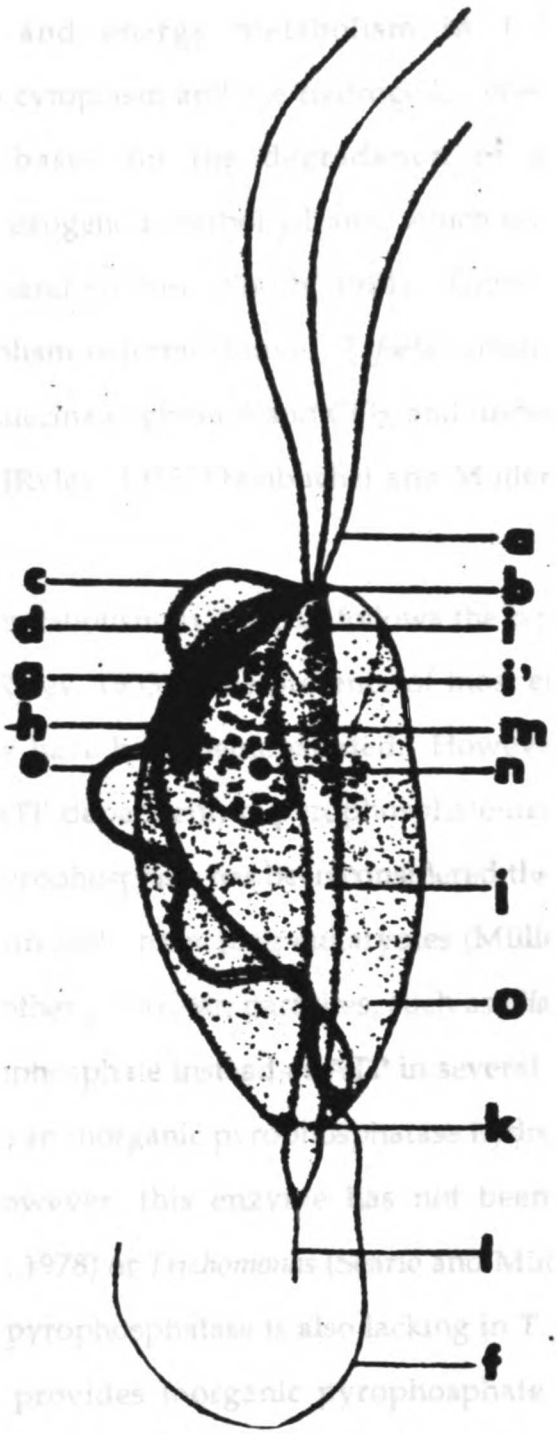

Figure I.1. Line diagram of fixed and stained *Tritrichomonas foetus* (Kirby, 1951).

Key to symbols in Fig. I.1: a, anterior flagella; b, kinetosomal complex; c, recurrent flagellum at the margin of the undulating membrane; d, undulating membrane; e, "accessory filament;" f, free posterio flagellum; g, costa; h, parabasal body; i, capitulum of the axostyle; i', ventral extension of the axostylar capitulum; j, trunk of the axostyle; k, periaxostylar ring; l, terminal filamentous extension of the axostyle; m, nucleus; n, nucleolus; o, undifferentiated cytoplasm.

CARBOHYDRATE METABOLISM

Carbohydrate and energy metabolism in *T. foetus* occurs in two compartments, the cytoplasm and the hydrogenosome. Energy metabolism in trichomonads is based on the degradation of glycogen (endogenous carbohydrate) and exogenous carbohydrates, which include glucose, galactose, mannose, maltose and sucrose (Shorb, 1964). Under aerobic and anaerobic conditions, metabolism is fermentative. *T. foetus* consumes carbohydrates and produces acetate, succinate, glycerol and CO_2, and under anaerobic conditions it also produces H_2 (Ryley, 1955; Steinbuchel and Müller, 1986; Steinbuchel and Müller, 1986).

Carbohydrate metabolism in *T. foetus* follows the typical glycolytic pathway (Lindblom, 1961; Ryley, 1955). The presence of most enzymes of the Embden-Meyerhof pathway have been demonstrated. However, phosphofructokinase instead of being ATP-dependent, is pyrophosphate-dependent (Mertens, *et al.*, 1989). Inorganic pyrophosphate has been considered the high energy compound equivalent of ATP in early branching eukaryotes (Müller, 1992). In addition to the trichomonads other protozoan parasites, such as *Giardia* and *Entamoeba*, also use inorganic pyrophosphate instead of ATP in several reactions (Müller, 1992). In most organisms, an inorganic pyrophosphatase hydrolyzes any PP_i generated in the cytosol; however, this enzyme has not been detected in *Entamoeba* (McLaughlin, *et al.*, 1978) or *Trichomonas* (Searle and Müller, 1991), and it is likely that this cytosolic pyrophosphatase is also lacking in *T. foetus*. Thus, the lack of pyrophosphatase provides inorganic pyrophosphate for glycolysis in these protozoan parasites. Mertens (Mertens, 1991) believes that the overall ATP yield of glycolysis is increased when inorganic pyrophosphate is used in these reactions. In both the glycolytic pathway and in further metabolism of pyruvate, ATP is generated by substrate-level phosphorylation only. Conversion of

phosphoenol pyruvate (PEP) to succinate is accomplished by the actions of the following cytosolic enzymes: PEP carboxykinase, malate dehydrogenase, fumarate hydratase and fumarate reductase (Müller and Lindmark, 1974). Succinate dehydrogenase activity has not been detected. Glycerol is converted from dihydroxyacetone phosphate by cytosolic glycerol-3-phosphate dehydrogenase and glycerol-3-phosphatase (Steinbuchel and Müller, 1986). Pyruvate is converted to acetate in the hydrogenosome through the actions of pyruvate:ferrodoxin oxidoreductase, acetate:succinate CoA-transferase and succinate thiokinase (Steinbuchel and Müller, 1986). Electrons produced by the consumption of carbohydrates are used to reduce protons and several glycolytic intermediates. Under aerobic conditions, electrons can also be transferred to O_2. Since cytochromes and cytochrome oxidase are not found in trichomonads, compounds which may function as electron carriers include Fe-S proteins, pyridine nucleotides and flavins (Lloyd, *et al.*, 1979).

Trichomonads also lack an active tricarboxylic acid cycle (Shorb, 1964), and instead of mitochondria they have hydrogenosomes--organelles in which the conversion of pyruvate to acetate and the production of H_2 and ATP occurs (Müller, 1993). Steinbuchel and Müller (Steinbuchel and Müller, 1986) postulate that metabolism of cytosolic malate and glycerol-3-phosphate may occur in the hydrogenosome. The following enzyme activities have also been found associated with the hydrogenosome: glycerol-3-phosphate dehydrogenase, superoxide dismutase, adenylate kinase, NADH oxidase, ferredoxins and NAD:ferredoxin oxidoreductase (Gutteridge and Coombs, 1977; Lindmark and Müller, 1974; Linstead and Bradley, 1988; McLaughlin, *et al.*, 1978; Ryley, 1955). Hydrogenosomeless trichomonads have been cultured (Steinbuchel and Müller, 1986), and metabolism in these mutants is cytosolic with production of ethanol,

but no H_2, acetate or succinate. Carbohydrate metabolism in *T. foetus* is shown schematically below in Figure I.2.

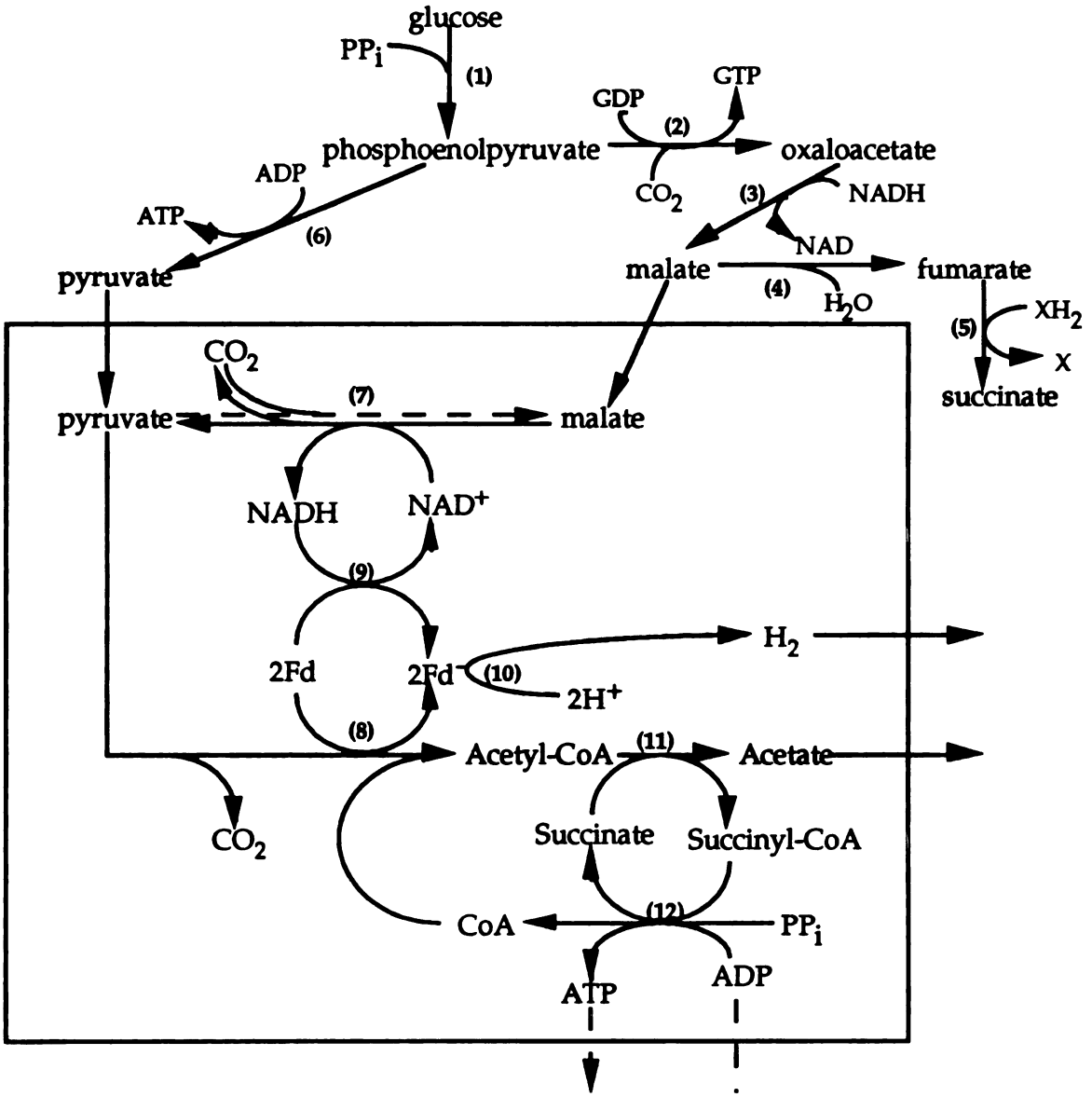

Figure I.2. Hypothetical scheme of carbohydrate metabolism of *Tritrichomonas foetus* (Lindmark and Müller, 1976; Mertens, *et al.*, 1989; Müller, 1993).

Only glycolytic steps differing from the usual glycolytic path are indicated. (1) PP_i phosphofructokinase; (2) phosphoenolpyruvate carboxykinase (GDP); (3) malate dehydrogenase (NAD); (4) fumarate hydratase; (5) fumarate reductase; (6) pyruvate kinase; (7) malate dehydrogenase (decarboxylating) (NAD); (8) pyruvate:ferredoxin oxidoreductase; (9) NAD:ferredoxin oxidoreductase; (10) H_2:ferredoxin oxidoreductase; (11) acetate:succinate CoA-transferase; (12) succinate thiokinase; Fd, ferredoxin; XH_2, unknown reducing agent. The box represents the hydrogenosome.

PURINE AND PYRIMIDINE METABOLISM

Many protozoan parasites have been discovered to be incapable of *de novo* purine nucleotide biosynthesis (Fish, *et al.*, 1982; Gutteridge and Gaborak, 1979; Krug, *et al.*, 1989; Marr, *et al.*, 1978; Schwartzman and Pfefferkorn, 1982; Wang and Aldritt, 1983; Wang and Simashkevich, 1981). Studies by Wang *et al.* (Wang, *et al.*, 1983) found that *T. foetus* is unable to incorporate radiolabeled glycine or formate into nucleotides. Instead, this trichomonad incorporates purine bases and purine nucleosides into the nucleotide pool. Adenine and inosine are first converted to hypoxanthine which then enters the nucleotide pool as IMP. Unlike *T. vaginalis*, which include only adenosine kinase and guanosine kinase in its purine salvage networks, the following enzyme activities have been noted in the purine salvage pathway of *T. foetus*: adenine deaminase, inosine phosphorylase, hypoxanthine phosphoribosyltransferase, adenosine kinase, xanthine phosphoribosyltransferase, guanine phosphoribosyltransferase, guanosine phosphorylase, guanosine phosphotransferase, guanine deaminase, adenosine deaminase and adenosine phosphorylase (see Fig. I.3). Work by Beck and Wang (Beck and Wang, 1993) has demonstrated that the hypoxanthine phosphoribosyltransferase, guanine phosphoribosyltransferase and xanthine phosphoribosyltransferase activities resides on a single protein.

Pyrimidine metabolism in anaerobic flagellates differs from most parasitic protozoa. Although most parasitic protozoa are capable of *de novo* pyrimidine biosynthesis, the anaerobic flagellates, *Giardia lamblia* (Lindmark and Jarroll, 1982) and *T. vaginalis* (Hill, *et al.*, 1981) were found to be pyrimidine auxotrophs. Studies by Wang *et al.* (Wang, *et al.*, 1983) found that *T. foetus* failed to incorporate bicarbonate, aspartate or orotate into pyrimidine nucleotides or nucleic acids; thus, it is also a pyrimidine auxotroph. In *T. foetus*, uracil, uridine and cytidine are salvaged by uracil phosphoribosyltransferase, with uridine and

cytidine converted by uridine phosphorylase and cytidine deaminase to uracil, which enters the nucleotide pool as UMP. Uridine phosphotransferase activity has also been detected. Uracil and uridine cannot be converted to TMP since radiolabeled uracil and uridine are not found in *T. foetus* DNA, and extracts of *T. foetus* lack dihydrofolate reductase and thymidylate synthetase activities. Thymidine salvage is accomplished with thymidine phosphotransferase and is not associated with salvage of other pyrimidines. The pyrimidine salvage pathway is shown in Fig. I.4.

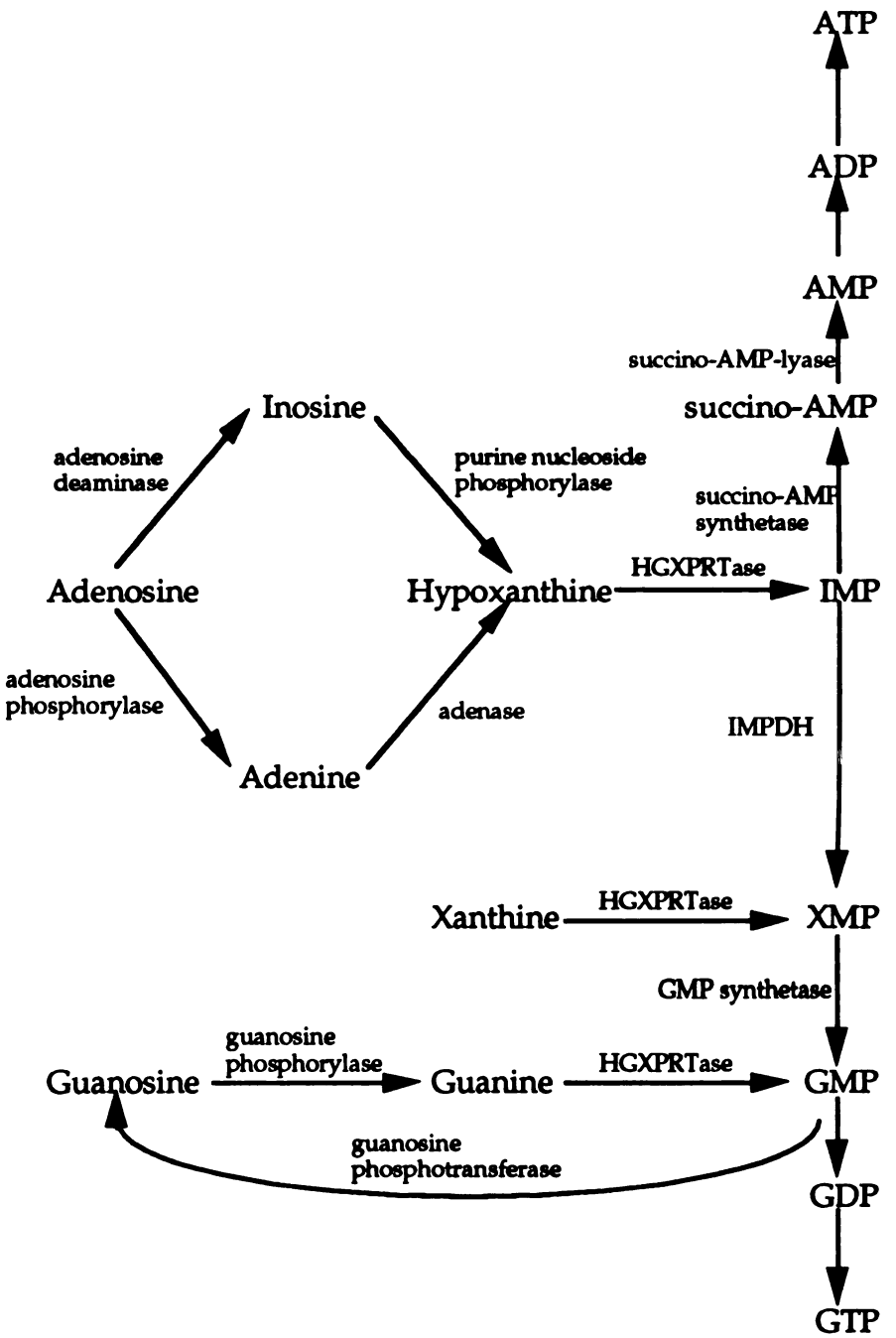

Figure I.3. Purine salvage pathways of *Tritrichomonas foetus* (Wang, *et al.*, 1983).

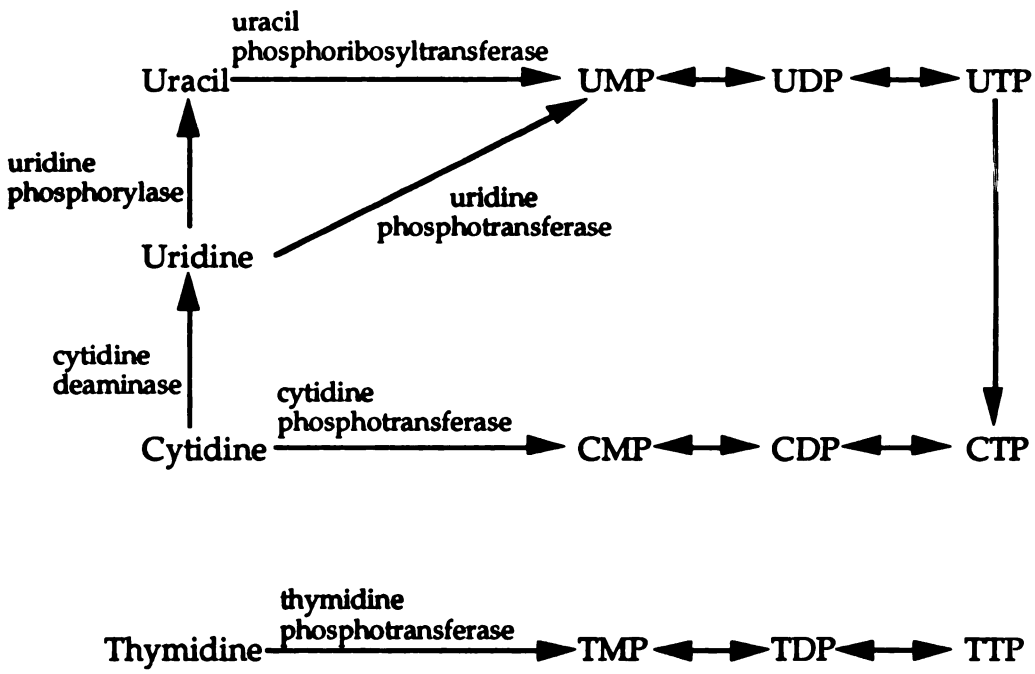

Figure I.4. Pyrimidine salvage pathways of *Tritrichomonas foetus* (Wang, *et al.*, 1983).

TRICHOMONIASIS

Bovine urogenital trichomoniasis is a venereal disease of worldwide distribution (Fitzgerald, 1986; Morgan, 1946). Reports show that 26% of beef herds in the western United States were infected (Johnson, 1964), and the incidence of within-herd infection in the western United States ranges from 5.8 to 38.5% (Kimsey, *et al.*, 1980; Skirrow, *et al.*, 1985). Estimates of as high as 51% of old bulls in Australia (Clark, *et al.*, 1974) and 71% of all cattle examined at a Nigeria abattoir were infected with *T. foetus* (Akinboade, 1980). Estimates of the dollar loss in the United States due to bovine trichomoniasis have ranged from $2.5 million to $62.4 million dollars per year (Fitzgerald, 1986; Wilson, *et al.*, 1979).

Transmission of *T. foetus* from bulls to cows occurs during coitus. Bulls are the active carriers of the disease. Bulls younger than 4 years are less susceptible to becoming infected; however, older bulls appear to be more susceptible to infection and once infected they remain infected for life if left untreated (Christensen, *et al.*, 1977). In infected bulls, the parasite is found throughout the preputial cavity and on the surface of the penis (Parsonson, *et al.*, 1974). Bulls are typically asymptomatic, but acute infection occurs with mucopurulent discharge and swelling of the prepuce which subsides about two weeks after infection (Honigberg, 1978).

Clinical signs of trichomoniasis in cows may include vaginal discharges, irregularities in the estrous cycle and delayed conceptions (Honigberg, 1978). Fourteen to 18 days after infection the trichomonads are found in large numbers in the vagina (Hammond and Bartlett, 1945). The parasites invade the uterus by migrating through the cervix. Morgan (Morgan, 1946) states that the primary site

of infection is the uterus, but parasites may remain in the vagina causing low-grade endometritis, in addition to uterine, cervical and vaginal catarrh. Fertilization may be prevented by endometritis and uterine catarrh; however, abortion usually occurs if an infected cow conceives. Honigberg (Honigberg, 1978) describes the abortions as being either complete or incomplete. The former occurs when both the fetus and placental membranes are expelled, and the latter occurs if the fetus is expelled, but the placental membranes are retained in the uterus. In cases of complete abortion, cows recover and can conceive later on. If the membranes are not removed in cases of incomplete abortions, chronic catarrh and purulent endometrosis develop and cause destruction of the uterine mucosa, leading to permanent sterility.

PATHOGENESIS

The pathology of *T. foetus* infection in heifers was studied by Parsonson *et al.* (Parsonson, *et al.*, 1976), and hemorrhagic placentomes and partial placental detachment were observed as evidence of impending abortion in two of 11 pregnant animals. Invasion of placental and fetal tissues was not observed. Histopathological studies of fetal and placental tissues by Rhyan *et al.* (Rhyan, *et al.*, 1988) and by Burgess and Knoblock (Burgess and Knoblock, 1989) found that *T. foetus* can invade the placenta and cause placentitis, and the parasite was also found in the fetal tissue.

The pathogenicity of *T. foetus* has also been studied in tissue culture (Burgess, *et al.*, 1990; Corbeil, *et al.*, 1989; Filho and de Souza, 1988; Florent, 1947; Hogue, 1938; Kulda and Honigberg, 1969). Three hypotheses have been proposed to explain the cytotoxic effect of trichomonads. Hogue (Hogue, 1938) suggested that cell damage was caused by parasitic toxins. However, Florent (Florent, 1947) thought that the pathological changes observed were due to depletion of

nutrients by trichomonads. Work by Kulda and Honigberg (Kulda and Honigberg, 1969) agrees with the hypothesis of Hogue (Hogue, 1938). *T. foetus* was found to have neuraminidase (Romanowska and Watkins, 1963), hyaluronidase (Timofeev, 1962) as well as the following hydrolases (glycosidases): α- and β-glucosidases, α- and β-galactosidases, α- and β-N-acetylglucosaminidases, α- and β-fucosidases, and α-rhamnosidases (Harrap and Watkins, 1970; Stealey and Watkins, 1972; Watkins, 1959; Watkins and Morgan, 1954). The biological significance of these hydrolases has yet to be determined. Both neuraminidase and hyaluronidase have been postulated to be involved in events leading to abortion and sterility (Müller and Saathoff, 1972), but more research is needed to verify this hypothesis. Work by Lockwood *et al.* has found that *T. foetus* contains multiple forms of cysteine proteinases (Lockwood, *et al.*, 1987). Preliminary results indicate that the cysteine proteinases found in the media differ from the intracellular cysteine proteinases of the trichomonads. These intracellular and extracellular proteinases may play a role in fulfilling the amino acid requirements of these urogenital parasites, or they may be involved in the pathogenicity of the trichomonads.

Adhesion to epithelial cells is another mechanism of tissue damage that was proposed by Filho *et al.* (Filho and de Souza, 1988) and by Corbeil *et al.* (Corbeil, *et al.*, 1989). Both groups of researchers noted that *T. foetus* adhered to epithelial monolayers. Adherence is accomplished initially by the posterior flagellum which is followed by the cell body of the trichomonad. Both Filho *et al.* (Filho and de Souza, 1988) and Burgess *et al.* (Burgess, *et al.*, 1990) propose that the pathogenic effects exerted by the trichomonads could be caused by secretion of proteases and release of lytic factors, in addition to adhesion. Therefore, a combination of factors may be responsible for the tissue damage caused by trichomonads.

DRUG THERAPY

Most of the early treatment for bovine trichomoniasis focused on treating the bull, and little research focused on the treatment of heifers/cows since the infection in females is self-limiting (Fitzgerald, 1986). Earlier treatment of bulls included ointment and salves. Bartlett (Bartlett, 1948) reported that Bovoflavin-Salbe, an ointment containing trypaflavine and surfen, cured seven out of eight infected bulls. Salves of acriflavine or berenil (Fitzgerald, *et al.*, 1963) were also used in treating infected animals. Because all of the topical treatments are expensive, time-consuming and tedious, another mode of therapy would be more practical.

Many systemic agents have been tested *in vitro* and *in vivo* (in experimental animals) against *T. foetus*, and they include the following: metronidazole; dimetridazole; iponidazole; tinidazole; 1-propargyl-5-nitroimidazole; 2-nitroimidazoles; 1[(2,4-dinitropyrryl)-ethyl]-2-methylimidazole; 1,2-,4-alkyl-substituted 5-nitroimidazoles; aminitrozole, 1-substituted 2,4-dinitropyrroles; various 2-(nitro-heterocyclic-benzimidazoles, benzoxazoles, and benzothiazoles; nitrofurans, bis(thiosemicarbazones) and bis(methylthiosemicarbazones); and substituted dithiocarbamates and bis-(thiocarbamoyl)disulfides (Michaels, 1968). Dimetridazole has been found to be effective when used orally or intravenously to treat *T. foetus* infected cattle (McLoughlin, 1965; McLoughlin, 1968; McLoughlin, 1970); however, oral administration requires larger doses and repeated handling of the animal, and some animals developed respiratory difficulty and ataxia with intravenous administration of dimetridazole.

Strains of *T. foetus* which are resistant to dimetridazole have developed (McLoughlin, 1967). The dimetridazole resistant strain was also cross-resistant to metronidazole and amintrozole. Nitroimidazole compounds enter the cell by

diffusion, and the nitro group of the compounds is reduced inside the anaerobic cells (Ings, *et al.*, 1974; Moreno, *et al.*, 1983; Müller, 1983), forming the following proposed intermediates: nitro-free radical, nitroso, nitroso-free radical and hydroxylamine derivative (see scheme below).

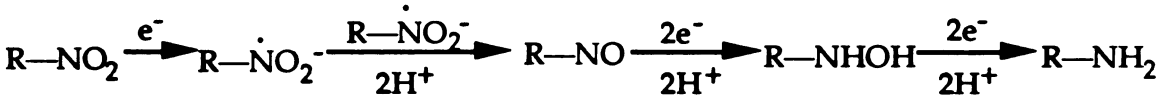

Intact *T. foetus* cells, anaerobic homogenates of *T. foetus* or anaerobic *T. foetus* hydrogenosomes are all capable of forming the nitro-free radical of metronidazole (DoCampo, *et al.*, 1984; Moreno, *et al.*, 1983). The electron donors are proposed to be ferredoxin proteins of low redox potential, and Lindmark and Müller (Lindmark and Müller, 1976) hypothesize that the reduction occurs by a nonenzymatic chemical reaction of the reduced ferredoxin with the nitroimidazole. The toxic effects of nitroimidazole compounds are believed to be due to the interaction of a reactive metabolite of the nitroimidazoles with DNA or protein (Moreno, *et al.*, 1983; Müller, 1983). Ings *et al.* (Ings, *et al.*, 1974) hypothesizes that the DNA-drug complex can no longer be used as a primer for DNA and RNA polymerases; therefore, all nucleic acid synthesis is inhibited.

Work by Cerkasovová *et al.* has demonstrated that anaerobic metronidazole resistance in *T. foetus* develops with loss of pyruvate:ferredoxin oxidoreductase and hydrogenase (Cerkasovová, *et al.*, 1984). Therefore, the parasite is resistant to metronidazole because it lacks the enzyme machinery to form the reactive drug species. Cerkasovová and coworkers also noted that the metronidazole-resistant cells were smaller in size and contained less protein than the metronidazole-sensitive cells. Thus, these mutant cells can survive without the principle metabolic pathway of the hydrogenasomes. However, the mutant trichomonads appear to grow at a slower rate than the drug-sensitive strain

(Kulda, *et al.*, 1984). Resistance of an organism to a drug can be reversed by simultaneously administering a second drug. For example, resistance to streptomycin in bacteria was prevented with concurrent administration of quinacrine (De Courcy and Sevag, 1967). However, use of quinacrine in conjunction with dimetridazole in trichomonad infected hamsters did not prevent resistance to dimetridazole from occurring (McLoughlin and Chute, 1969). Acriflavine had been used with some success in reversing drug resistance in bacteria (Mitsuhashi, *et al.*, 1961; Watanabe and Fukasawa, 1961) and *Eimeria tenella* (McLoughlin and Chute, 1968). Nevertheless, acriflavine did not cause a reversion of the dimetridazole-resistant strain to a dimetridazole-sensitive strain of *T. foetus* (McLoughlin and Chute, 1969).

Ipronidazole was another nitroimidazole compound used to treat bovine trichomoniasis, and it lacked the side effects associated with dimetridazole (Fitzgerald, 1986; Skirrow and BonDurant, 1988; Skirrow, *et al.*, 1985; Williams, *et al.*, 1987). However, both dimetridazole and ipronidazole were removed from use in the United States by the Food and Drug Administration because of suspected carcinogenic effects (Ames, *et al.*, 1973; Herrick, 1990; Rustia and Shubik, 1972). Presently there are no systemic medications available in the United States to treat bovine urogenital trichomoniasis.

HGPRTases

Phosphoribosyltransferases (PRTases) are enzymes which catalyze purine, pyrimidine and pyridine nucleotide biosynthesis, in addition to histidine and tryptophan biosynthesis. These enzymes require a divalent metal ion, share α-D-5-phosphoribosyl-1-pyrophosphate (PRPP) as a substrate and release pyrophosphate from ribose with inversion of the anomeric carbon (Musick, 1981). Musick (Musick, 1981) also reports that PRTases are acidic proteins with

pH optima that are generally alkaline, and amino acid residues involved in catalysis and binding appear to be cysteine and lysine, respectively. Since all PRTases utilize PRPP, it has been proposed that these enzymes may share a common structure which may resemble a nucleotide-binding domain (Musick, 1981).

Hypoxanthine-guanine phosphoribosyltransferase (HGPRTase E.C.2.4.2.8) is one member of the PRTase family (Musick, 1981). This enzyme catalyzes the Mg^{2+}-dependent transfer of phosphoribose from PRPP to the purine bases hypoxanthine, guanine and xanthine, forming pyrophosphate, IMP, GMP and XMP, respectively. In mammals HGPRTase is important in purine metabolism even though mammals can obtain purine nucleotides by *de novo* synthesis. However, mutations which affect expression of HGPRTase or alter the ability of the enzyme to bind substrates, result in hyperuricemia which is clinically expressed as gout (Chinault and Caskey, 1984). When HGPRTase activity is lacking, the metabolic disease is called Lesch-Nyhan syndrome (Rosenbloom, *et al.*, 1967; Seegmiller, *et al.*, 1967). This disorder is characterized by hyperuricemia, uric acid nephrolithiasis, growth and mental retardation, choreoathetosis, spasticity, hyperreflexia and self-mutilation. Lesch-Nyhan syndrome is an X-linked disorder (Lesch and Nyhan, 1964). Hyperuricemia results because the lack of HGPRTase causes PRPP to accumulate which activates glutamine amidotransferase. This in turn increases *de novo* purine biosynthesis, and without HGPRTase, the purine bases can only be oxidized to uric acid (Kelley and Wyngaarden, 1983; Seegmiller, 1980). The CNS defects manifested in Lesch-Nyhan syndrome may be caused by loss of central dopaminergic neurons (Lloyd, *et al.*, 1981; Breese, *et al.*, 1990). HGPRTase$^-$ mice do not exhibit any of the neurobehavioral abnormalities associated with Lesch-Nyhan syndrome (Jinnah, *et al.*, 1992); nevertheless, the lack of HGPRTase in these mutants is still

associated with a specific deficit in basal ganglia dopamine systems (Jinnah, *et al.*, 1994). Several hypotheses have been proposed to explain how the HGPRTase deficiency may lead to the decrease in brain dopamine levels, such as depletion of some purine essential during development or accumulation of a toxic purine metabolite which may destroy dopaminergic fibers (Jinnah, *et al.*, 1994), reduction in the number of branches of striatal dopamine terminals (Lloyd, *et al.*, 1981), reduction in GTP levels which may decrease the availability of the cofactor tetrahydrobiopterin for tyrosine hydroxylase (Goldstein, *et al.*, 1986; Watts, 1985) and misregulation of dopamine receptors (Goldstein, *et al.*, 1985; Goldstein, *et al.*, 1986; Watts, 1985). Jinnah *et al.* have not found any evidence of purine depletion or accumulation of a toxic purine metabolite in the HGPRTase$^-$ mice (Jinnah, *et al.*, 1993), and there is very little experimental evidence which proves or disproves any of the other hypotheses.

Unlike mammalian cells, parasitic protozoa are unable to synthesize purine nucleotides from PRPP, amino acids and formate. All parasitic protozoa studied to date, including *Plasmodium lophurae* (Walsh and Sherman, 1968), *Leishmania donovani* (Marr, *et al.*, 1978), *Leishmania braziliensis* (Marr, *et al.*, 1978), *Entamoeba histolytica* (Berens, *et al.*, 1981), *Eimeria tenella* (Wang and Simashkevich, 1981), *Toxoplasma gondii* (Krug, *et al.*, 1989; Schwartzman and Pfefferkorn, 1982), *Trypanosoma cruzi* (Berens, *et al.*, 1981), *Trypanosoma brucei* (Fish, *et al.*, 1982), *Giardia lamblia* (Wang and Aldritt, 1983), *Trichomonas vaginalis* (Miller and Linstead, 1983) and *Tritrichomonas foetus* (Wang, *et al.*, 1983), must fulfill their need for purine nucleotides through purine salvage pathways. Although all organisms possess purine salvage networks, the combination of salvage enzymes which make up the pathways used by parasites varies from parasite to parasite. For example, *T. vaginalis* and *E. histolytica* rely on purine nucleoside phosphorylases/kinases for purine salvage (Lo and Wang, 1985; Miller and

Linstead, 1983). *P. lophurae, L. donovani, L. braziliensis, E. tenella, T. gondi, T. cruzi, T. brucei, G. lamblia* and *T. foetus* rely on purine phosphoribosyltransferases (Berens, *et al.*, 1981; Fish, *et al.*, 1982; Krug, *et al.*, 1989; Marr, *et al.*, 1978; Schwartzman and Pfefferkorn, 1982; Walsh and Sherman, 1968; Wang and Aldritt, 1983; Wang and Simashkevich, 1981; Wang, *et al.*, 1983), and these parasites, with the exception of *G. lamblia*, are able to convert IMP to AMP and GMP. *G. lamblia* uses a guanine phosphoribosyltransferase to salvage guanine and adenine phosphoribosyltransferase to salvage adenine (Wang and Aldritt, 1983), and interconversion of GMP and AMP does not occur in *G. lamblia*, *T. vaginalis* or *E. histolytica* (Lo and Wang, 1985; Miller and Linstead, 1983). Since purine salvage pathways are crucial for the survival of these protozoan parasites, enzymes in this pathway, such as purine phosphoribosyltransferases, may be useful as targets for the design of structure-based inhibitors for parasitic chemotherapy.

If HGPRTase is a potential target for inhibitor design, detailed kinetic and structural analyses of both host and parasitic HGPRTases are essential since defects in the mammalian enzyme are responsible for metabolic disorders. These studies may reveal differences in the active sites and catalytic mechanisms which can be used to selectively inhibit the parasitic enzymes. Kinetic analyses of the human (Giacomello and Salerno, 1978) and schistosomal (Yuan, *et al.*, 1992) enzymes have revealed differences in their kinetic mechanisms. Both enzymes follow a sequential kinetic mechanism with Mg_2PRPP as the first substrate to bind to the enzyme. However, the release of products differ in these two enzymes, with products released randomly by the human enzyme and products released in an ordered fashion ($MgPP_i$ first and Mg-complexed purine nucleotide last) by the schistosomal enzyme.

Three PRTases, glutamine-5-phosphoribosyl-1-pyrophosphate amidotransferase (amido-PRTase), orotate phosphoribosyltransferase (OPRTase) and HGPRTase, have been examined crystallographically (Eads, *et al.*, 1994; Scapin, *et al.*, 1994; Smith, *et al.*, 1994). Even though the similarity of the amino acid sequences is low between these three enzymes, the three dimensional structures are similar. All three enzymes have a core α/β structure that resembles the nucleotide-binding fold of dehydrogenases, except that the β-sheet is composed of five β-strands instead of six. Both HGPRTase and amido-PRTase have four α-helices that surround these five β-strands, whereas OPRTase has three α-helices. These three PRTases also lack the Gly-X-X-Gly-X-Gly sequence motif associated with the mononucleotide binding sites (Schulz, 1992). The sequence motif proposed as the PRPP binding site (Hershey and Taylor, 1986) is found in a strand and loop region of the core structure in these three PRTases. For both the OPRTase and HGPRTase, the electron density of the loop is poor. Both Eads *et al.* (Eads, *et al.*, 1994) and Scapin *et al.* (Scapin, *et al.*, 1994) propose that this loop may move during catalysis. Specificity for the nitrogenous base is determined by amino acid residues located at the carboxyl end of HGPRTase, the amino terminal "hood" region of OPRTase, and a separate domain (NH_2 domain) in amido-PRTase. Thus, the crystallographic studies of these three PRTases have revealed common structural features of this family of enzymes (α/β core) and residues involved in substrate binding.

RESEARCH GOALS

Since *T. foetus* is an auxotroph for purine nucleotides, HGXPRTase is essential to the survival of this trichomonad and can serve as a target for inhibitor design. Characterization of the *T. foetus* HGXPRTase by kinetic and structural studies is necessary prior to designing inhibitors specific for the trichomonad enzyme. The goal of my research was to clone the gene encoding the *T. foetus* HGXPRTase, and to characterize the enzyme by steady-state kinetic analyses. We anticipated that the results of these studies would reveal differences between the trichomonad and mammalian enzymes which would be useful for inhibitor design. Characterization of the enzyme using conventional protein purification techniques would be difficult since the yield of HGXPRTase from *T. foetus* is 0.8 mg per two liters of mid-logrithmic parasites (Beck and Wang, 1993). Cloning the *T. foetus* HGXPRTase gene for expression in *E. coli* would supply sufficient quantities for enzyme characterization. After assessing the feasibility of many different techniques to identify the *T. foetus* HGXPRTase gene, I was able to clone this gene using functional complementation. Chapter 1 describes the cloning and characterization of the *T. foetus* HGXPRTase gene. Chapter 2 describes the successful expression of the *T. foetus* HGXPRTase gene in *E. coli*. The recombinant protein was purified to apparent homongeneity and characterized. There were no differences in the measured characteristics between the native and recombinant *T. foetus* enzymes. Chapter 3 presents the results of initial velocity studies and product inhibition studies of the recombinant enzyme.

CHAPTER 1: CLONING AND SEQUENCING OF THE HYPOXANTHINE-GUANINE-XANTHINE PHOSPHORIBOSYLTRANSFERASE GENE FROM *TRITRICHOMONAS FOETUS*

INTRODUCTION

Early attempts to isolate a DNA clone encoding *Tritrichomonas foetus* HGXPRTase using heterologous probes, the polymerase chain reaction and screening a cDNA expression library were unsuccessful. We finally resorted to the method of complementation which has been used successfully to clone genes encoding enzymes in metabolic pathways, such as the gene encoding glucose phosphate isomerase from *Plasmodium falciparum* (Kaslow and Hill, 1990)and the *URA*5 gene from *Cryptococcus neoformans* (Edman and Kwon-Chong, 1990). In *Escherichia coli* purine nucleotides can be either synthesized *de novo* or salvaged from the environment (see Fig. 1.1) (Neuhard and Nygaard, 1987). When purine *de novo* synthesis or salvage are blocked by mutations, *E. coli* is unable to survive on minimal media supplemented with a particular purine base. For instance, the *E. coli* mutant, SØ609 (Jochimsen, *et al.*, 1975), has a mutation in the *de novo* purine synthetic pathway (*pur H,J*) and 3 mutations in the purine salvage pathway (*Δgpt, hpt and pup*), which makes it incapable of growing on minimal medium supplemented with hypoxanthine, guanine or xanthine, but it will be able to grow on minimal medium supplemented with adenine. If SØ609 is transformed with cDNA encoding the *T. foetus* HGXPRTase and expresses the active enzyme, the bacterium should be able to survive on minimal media supplemented with either hypoxanthine, guanine or xanthine.

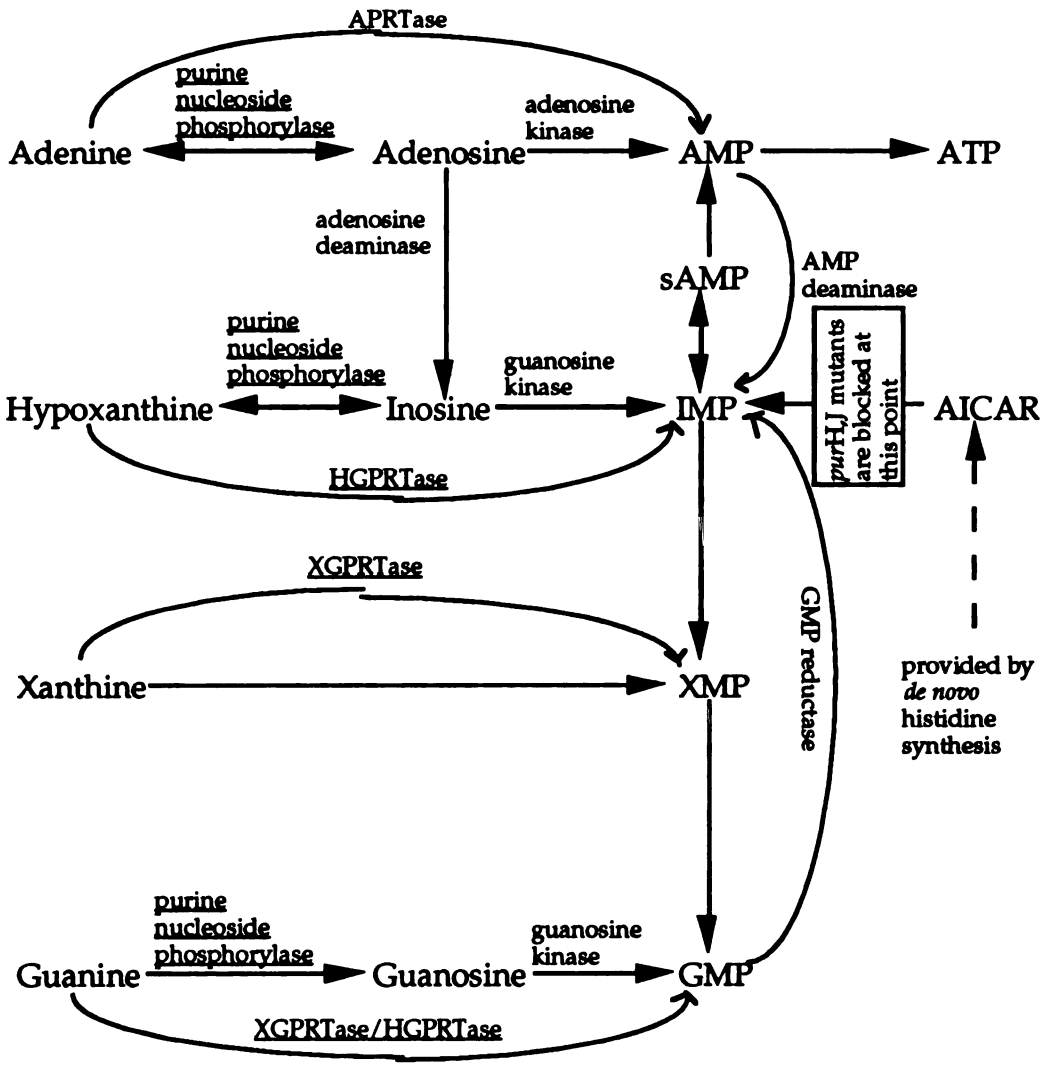

Figure 1.1. The Purine Salvage Pathway of *E. coli* (Neuhard and Nygaard, 1987).

Enzymes missing in the mutants SØ609 and SØ606 are underlined.

MATERIALS AND METHODS

Materials: *Tritrichomonas foetus* strain KV_1, ATCC30924, were cultured in Diamond's TYM media (Diamond, 1957) (see Appendix A). The cDNA library, genomic DNA and poly(A^+) RNA blot from *T. foetus* strain KV_1, were obtained from Dr. Joanne Beck. The *Escherichia coli* strain used for complementation,

SØ609 (F^- *ara*, Δ*pro-gpt-lac*, *thi*, *hpt*, *pup*, *pur*H,J, *str*A), was obtained from Dr. Per Nygaard (University Institute of Biological Chemistry B, Copenhagen, Denmark). The *E. coli* strains used to rescue the phagemid and plasmid forms of the cDNA library were: XL1-Blue (*end*A1, *hsd*R17(r_k^-, m_k^+), *sup*E44, *thi*-1, λ^-, *rec*A1, *gyr*A96, *rel*A1, (*lac*$^-$) [F', *pro*AB, *lac*1qZDM15, Tn10(tet^R)] (Stratagene, La Jolla, CA) and DH5αF' (F' ø80d*lac*ZDM15, D(*lac*ZYA-argF)U169, *end* A1, *rec*A1, *hsd*R17(r_k^-,m_k^+), *thi*-1, *sup*E44, λ^-, *gyr*A96, *rel*A1)(Gibco/BRL, Gaithersburg, MD). The DH5αF' strain was also used as a host for subcloning procedures. All restriction endonucleases were purchased from New England Biolabs (Beverly, MA) or Gibco/BRL (Gaithersburg, MD). [8-^{14}C]hypoxanthine (57.0 mCi/mmole), [8-^{14}C]guanine (55.0 mCi/mmole) and [8-^{14}C]xanthine (59.0 mCi/mmole) were obtained from ICN (Costa Mesa, CA). [α^{32}P]dCTP and [γ^{32}P]ATP were purchased from NEN (Burbank, CA). Bacto-tryptone and vitamin-free Casamino acids were purchased from Difco (Detroit, MI). Bacto-yeast extract was purchased from Becton Dickinson and Co. (Cockeysville, MD). All other reagents were from Sigma Chemical Co. (St Louis, MO), and of the highest purity available.

Library construction, phagemid rescue and plasmid generation

A phagemid library of *T. foetus* cDNA was obtained by coinfecting *E. coli* XL1-Blue cells with 10^8 PFU of the lambda phage library and 10^{10} PFU of the R408 helper phage in 45 ml of LB media (Short, *et al.*, 1988). After 6 hrs at 37°C the culture was heated at 70°C for 20 min and centrifuged to remove cellular debris. The supernatant containing rescued phagemids gave a titer of $1.5x10^5$ CFU/μl on ampicillin containing plates.

A plasmid library was generated by transforming *E. coli* DH5aF' competent cells with the rescued phagemids (Short, *et al.*, 1988). LB media was inoculated

with the phagemid transformed bacteria by overlaying the bacterial lawn with 3 ml of LB media/plate for 5 min at room temperature, transferring the LB media to a 50 ml centrifuge tube, adding ampicillin to 50-75 mg/L and incubating overnight at 37°C. Plasmids were recovered by alkaline lysis (Sambrook, *et al.*, 1989).

A genomic library of *T. foetus* was constructed with 16-20 Kb fragments generated by partial digestion of genomic DNA from *T. foetus* strain KV_1 with MboI and ligated into the phage vector λEMBL3 (Stratagene, La Jolla, CA) following the manufacturer's instructions.

Construction of the positive control plasmid, pSmc.2"

pSmc2, the plasmid containing the full-length cDNA encoding the *Schistosoma mansoni* HGPRTase (Craig, *et al.*, 1988), was first digested with XbaI and BclI, and the overhanging ends were filled in using the Klenow large fragment DNA polymerase and deoxynucleotides to create blunt ends for religation. The plasmid was then cut with EcoRI, the overhanging ends were filled in (as described above) and the ends religated. The resulting plasmid was designated pBSmc2" (see Fig. 1.2).

Complementation

E. coli strain SØ609 were made competent following the method of Hanahan (Hanahan, 1983). Forty-five micrograms of the plasmid library were mixed with 100 µl suspension of SØ609 competent cells, incubated on ice for 30 min, followed by a heat shock at 42°C for 45 sec, and incubated on ice for 2 min. After growth in 0.5 ml SOC medium (bacto-tryptone 20 g/L, bacto-yeast extract 5 g/L, NaCl 0.5 g/L, 2.5 mM KCl, 10 mM $MgCl_2$, and 20 mM glucose) for 1 hr, the cells were washed with M9CA medium (Na_2HPO_4 6 g/L, KH_2PO_4 3 g/L, NaCl 0.5 g/L, NH_4Cl 1 g/L, 2 mM $MgSO_4$, 0.1 mM $CaCl_2$, 0.2% glucose and

0.2% vitamin-free casamino acids) and spread onto selective media plates (M9CA agar plates supplemented with 1.5 μM thiamine, 20 mg/L guanine, 50 mg/L ampicillin and isopropyl-β-D-thiogalactopyranoside (IPTG)). Plates were incubated at 37°C. Colonies appearing on these plates were restreaked onto fresh selective media plates. SØ609 cells containing pBSmc2", were used as a positive control, and SØ609 cells containing pBluescript (Stratagene, La Jolla, CA) with no insert were used as a negative control.

Southern and Northern Hybridizations

Approximately 6 μg of *T. foetus* genomic DNA were digested with appropriate restriction endonucleases, separated on a 0.8% agarose/Tris-borate-buffered gel and transferred to Nytran membrane (Schleicher & Schuell, Keene, N.H.) by the method of Southern (Southern, 1975). *T. foetus* genomic DNA was also digested with decreasing concentrations of the restriction enzyme, EcoRI, separated on a 0.8% agarose/Tris-borate-buffered gel and transferred to Nytran membrane as described above. A cDNA fragment was labeled with digoxigenin-dUTP by random priming using the Genius kit (Boehringer Mannheim, Indianapolis, IN) and hybridized to the blot in 5xSSC (750 mM NaCl, 75 mM sodium citrate), 50% formamide at 50°C. The blot was washed twice at room temperature in 1xSSC + 0.1% sodium dodecyl sulfate (SDS), followed by a 30 min. wash in 1xSSC + 0.1% SDS at 50°C and a 30 min. wash in 0.1xSSC + 0.1% SDS at 50°C. The blot was developed following the manufacturer's recommendations (see Appendix B) and exposed to X-ray film.

T. foetus poly(A^+) RNA was resolved on a MOPS-formaldehyde-agarose gel and transferred onto nitrocellulose (Micron Separations Inc., Westborough, MA) (Sambrook, *et al.*, 1989). The poly(A^+) RNA blot was probed with a ^{32}P random prime labeled cDNA fragment under stringent conditions in 5xSSC, 50%

formamide at 55°C. The blot was washed three times at room temperature and once for a 20 min. wash in 5xSSC + 0.1% SDS at 65°C and exposed to X-ray film.

Cloning the full-length gene

The *T. foetus*-λEMBL3 library was screened using the ^{32}P random prime labeled cDNA fragment under the same hybridization conditions used for the Southern. The DNA of one purified phage clone was digested with restriction endonucleases, fractionated on an agarose gel, transferred to nitrocellulose and probed with the random prime labeled cDNA fragment under the same stringency used to screen the library. The fragment that hybridized to the probe was subcloned into Bluescript KS+ and Bluescript KS- plasmids (Stratagene, La Jolla, CA).

DNA Sequencing

Single-stranded template was generated from cloned DNA following the protocol recommended by Stratagene (La Jolla, CA) (see Appendix C). Both single-stranded and double-stranded DNA were sequenced using the Sequenase 2.0 kit (U. S. Biochemical Corp., Cleveland, OH). Sequencing primers were synthesized by the Biomolecular Resource Center at the University of California, San Francisco. Programs designed by the Biocomputational laboratory at University of California, San Francisco were used for sequence analysis.

Primer Extension

Total RNA from *T. foetus* strain KV_1 was isolated as described by Wang and Wang (Wang and Wang, 1985) (see Appendix A), and poly(A^+) RNA was purified on oligo(dT)cellulose columns. The primer, 5'-GTTATAGAGAACTCTCTCAAGGT-CGTCCAT-3', was designed to hybridize to nucleotides 19-48 (Fig. 1.8). Primer extension was carried out as described (Sambrook, *et al.*, 1989). The primer was labeled using [$\gamma^{32}P$]ATP and

polynucleotide kinase, mixed with poly(A^+) RNA and allowed to anneal at 42°C overnight. Reverse transcriptase and deoxynucleotides were added for the extension reaction.

Enzyme Assay

M9CA supplemented with 1.5 μM thiamine, 20 mg/L guanine, 75 mg/L ampicillin and 10 mM IPTG was inoculated with bacteria cells containing the plasmid of interest and incubated at 37°C with aeration. Bacteria cells from 3 ml of the culture were pelleted, resuspended in 100 μl TE buffer, 0.9 mM PRPP and 3 mg/ml lysozyme, incubated at 37°C for 15 min. and freeze-thawed three times to lyse cells. Cell debris was removed by microcentrifugation, and the supernatant was assayed for enzyme activity. Five microliters of the supernatant were added to 20 μl of a reaction mixture of 0.3 M Tris-HCl pH 7.8, 18 mM $MgCl_2$, 0.5 mM PRPP containing either 17.5 μM ^{14}C-hypoxanthine, 18.2 μM ^{14}C-guanine, or 17 μM ^{14}C-xanthine, incubated at 37°C for 5 min and stopped with 1 mM hypoxanthine and 1 mM IMP. Twenty microliters of the reaction mixture was spotted on a PEI cellulose sheet which was developed with 5 mM NH_4Ac pH 4.5, dried and exposed to X-ray film (Yuan, *et al.*, 1990).

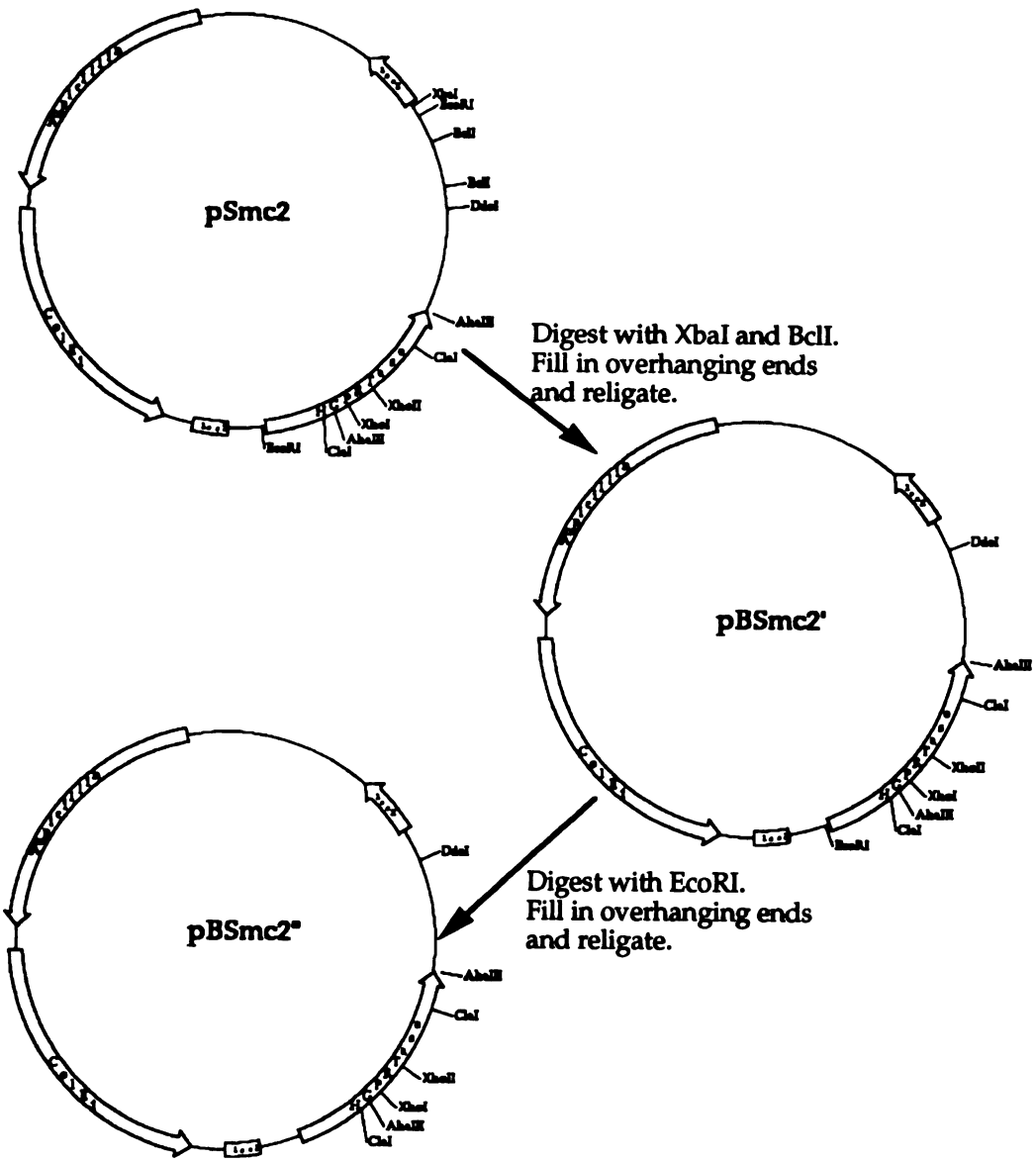

Figure 1.2. Construction of pBSmc2" from pSmc2.

RESULTS

Cloning T. foetus HGXPRTase by complementation

A cDNA library of *T. foetus* was constructed in the lambda vector ZAP II. Double stranded plasmids were generated from the library by rescuing phagemids and transforming *E. coli* DH5αF' cells with the phagemids. Plasmids were isolated from the transformed *E. coli* DH5αF', used to transform competent *E. coli* SØ609, and the transformed bacteria were plated onto a M9CA-thiamine-ampicillin agar plate supplemented with guanine as the only source of purine base. The plate with *T. foetus* cDNA transformed SØ609 produced two colonies after 3 days, while the negative control (Bluescript alone) produced none, and the positive control (full-length *S. mansoni* HGPRTase cDNA in pBluescript, pBSmc2") produced five colonies. The two colonies resulting from the transformation with the *T. foetus* cDNA library contained an insert of approximately 500 bp. One colony, containing the plasmid designated pTfc1, was selected for further characterization.

Characterization of pTfc1

To generate cell extracts for enzyme assays, M9CA-thiamine-guanine-ampicillin media was inoculated with SØ609/pTfc1, the positive control cells (SØ609/pBSmc2") the negative control cells (SØ609/pBluescript). The cell extract from bacteria containing pTfc1 demonstrated PRTase activities for hypoxanthine, guanine and xanthine (see Fig. 1.3). The negative control cells showed no PRTase activitites for the three purines, whereas the SØ609 cells transformed with the pBSmc2" demonstrated HPRTase and GPRTase activities but not XPRTase activity.

Under stringent conditions the 496 bp EcoRI fragment from pTfc1 hybridized to specific DNA fragments on a blot of restriction endonuclease digests of

T. foetus genomic DNA (Fig. 1.4). Each digest produces only one fragment which hybridizes to the probe. The double digests suggest that HindIII, PstI and XbaI flank the genomic DNA encoding the HGXPRTase (see Fig. 1.5 for restriction map). The Southern blot of partially digested genomic DNA using various dilutions of EcoRI shows only two species, 23 kb or 0.8 kb, which hybridize to the probe (Fig. 1.6). This indicates that the gene encoding the HGXPRTase is most likely a single copy gene. Hybridization of a Northern blot of *T. foetus* poly (A^+) RNA with the same probe (Fig. 1.7) indicates that the mRNA encoding the *T. foetus* HGXPRTase exists as a single species. The size of the mRNA is estimated to be 700-800 bp.

The sequence of the 536 bpTfc1 has been determined and is shown in Fig. 1.8 (nucleotides no. 14-550). The coding region of this cDNA predicts a protein with a molecular weight of 20.5 kD, which is smaller than what is reported for the purified HGXPRTase of *T. foetus*, 24 kD (Beck and Wang, 1993) suggesting that pTfc1 is not a full-length clone, even though its translational product has HGXPRTase activities.

Isolation and characterization of the full-length T. foetus genomic clone

The 496 bp EcoRI fragment of pTfc1 was used to screen a genomic library of *T. foetus* constructed in λEMBL3 phage. Purification of the λEMBL phage clone was carried through three successive screenings with the probe. The phage DNA was digested with HindIII/PstI, producing a 1.4 Kb fragment, which was cloned into Bluescript, and designated as pTfg1. The DNA sequence was determined for both strands of pTfg1. As shown in Fig. 1.8, pTfg1 encodes an open reading frame of 549 bp which were identical with the 536 bp of pTfc1 plus 13 bp at the 5' end not found in the cDNA clone. The coding region of pTfg1 has an AT content of 58.5%, and predicts a protein with a molecular weight of 21.1 kDa, which is

still lower than the 24 kDa estimated from SDS-PAGE (Beck and Wang, 1993). Primer extension with a synthetic primer, hybriziding to nucleotides no. 19-48 in Fig. 1.8, generated a cDNA fragment with an estimated size of 114 bp (Fig. 1.9). The results suggest that the poly (A^+) transcript of the cloned gene should begin 66 nucleotides upstream from the proposed start ATG shown in Fig. 1.8. This upstream region contains nonsense codons at positions -32, -37, -46 and -51 and no other initiation codon in the proposed reading frame (Fig. 1.8), thus suggesting that the proposed start ATG is correct. The simple banding pattern of the genomic Southern blot, and comparison of the cDNA sequence with the genomic sequence also indicates that the cloned gene does not contain any introns.

Sequence Alignment

The amino acid sequence deduced from the full-length genomic clone is aligned with the sequences of human HGPRTase (Jolly, *et al.*, 1983), *S. mansoni* HGPRTase (Craig, *et al.*, 1988), *Plasmodium falciparum* HGXPRTase (King and Melton, 1987), *Toxoplasma gondii* (Roos, 1994; Vasanthakumar, *et al.*, 1994), *Trypanosoma brucei* (Allen and Ullman, 1993), *Trypanosoma cruzi* (Allen and Ullman, 1994), *Leishmania donovani* (Allen, *et al.*, 1993), *Crithidia fasciculata* (Ullman, 1994) and *Vibrio harveyi* HGPRTase (Showalter and Silverman, 1990), and shown in Fig. 1.10. The degree of amino acid sequence identity relative to the *T. foetus* sequence is 25.1%, 23.5%, 21.3%, 23.0%, 25.1%, 27.3%, 25.1%, 26.2% and 36.1%, respectively. The degree of amino acid sequence similarity relative to the *T. foetus* sequence when chemically similar amino acid substitutions are taken into account is 48.6%, 45.9%, 44.3%, 46.4%, 46.4%, 50.3%, 50.8%, 50.8% and 60.1%, respectively. The *T. foetus* sequence is the smallest of the published eukaryotic sequences encoding an HGPRTase, and it is only two amino acids longer than the sequence encoding the *V. harveyi* HGPRTase (Showalter and Silverman, 1990).

Alignment of the amino acid sequence deduced from the full-length genomic clone with the sequences of *E. coli* XGPRTase (Pratt and Subramani, 1983), *V. harveyi* HGPRTase and *Lactococcus lactis* HGPRTase (Nilsson and Lauridsen, 1992) is shown in Fig. 1.11 . The degree of amino acid sequence identity is 19.1%, 35% and 40.4%, respectively, and the degree of amino acid sequence similarity relative to the *T. foetus* sequence when chemically similar amino acid substitution are taken into account are 36.1%, 54.6% and 64.5%, respectively.

DISCUSSION

Using functional complementation, we have isolated and sequenced a cDNA clone, pTfc1, coding for a major portion of the HGXPRTase of *T. foetus*. Subsequently, using pTfc1 as a probe, we have isolated the full-length, intronless gene encoding the enzyme. This is the first phosphoribosyltranferase gene to be cloned by complementation. Since our attempts to isolate this gene with other methods have failed, this successful approach demonstrates that complementation may be useful for isolating genes encoding enzymes of metabolic pathways that may not be well conserved at the nucleic acid level.

As an artifact of the library construction, the partial cDNA clone, pTfc1, expressed HGXPRTase activities in SØ609 in the form of a fusion protein with the 41 amino acids from β-galactosidase and the EcoRI/NotI adaptor at the amino terminus. This fusion protein is apparently an active HGXPRTase, suggesting that the N-terminal portion of the molecule is not important for activity. Three pieces of evidence support our assertion that we have cloned the cDNA encoding the *T. foetus* HGXPRTase. First, the plasmid pTfc1 encodes a protein which exhibits PRTase activities for hypoxanthine, guanine and xanthine, and when used to transform the *E. coli* mutant, SØ609, it allows SØ609 to grow on minimal medium supplemented with guanine. Second, under stringent

conditions a fragment of pTfc1 hybridizes to *T. foetus* DNA and not to λ phage DNA, indicating that the cDNA is from *T. foetus*. Finally, although the overall similarity of the deduced *T. foetus* HGXPRTase sequence to those of the other PRTases is low, the 15 amino acid region located at positions 138-152 (Fig. 1.10) demonstrates a 60-80% identity and 87-100% similarity with the putative PRPP binding sites in the other HGPRTases (Hershey and Taylor, 1986). These are to be expected since all the enzymes recognize PRPP as a substrate.

Comparison of residues corresponding to 129-VLIVEDIIDTGK-140 of the human HGPRTase, which are involved in PRPP-binding (Eads, *et al.*, 1994), show 41.7-91.7% identity and 91.7-100% similarity (Fig. 1.10 and Fig. 1.11). This agrees with the region hypothesized by Hershey and Taylor (Hershey and Taylor, 1986) to play a role in PRPP-binding. Residues in other HGPRTases corresponding to the flexible loop of the human HGPRTase, which is hypothesized to be important for PRPP and PP_i binding and to move during catalysis (Eads, *et al.*, 1994), have 10-70% identity and 20-80% similarity with the *T. foetus* sequence (Fig.1.10 and Fig. 1.11). Hershey and Tayler (Hershey and Taylor, 1986) predicted that the putative purine binding site was located between residues 65-104 (numbering for the human sequence); however, crystallographic studies of the human HGPRTase (Eads, *et al.*, 1994) indicate that structural elements found at the carboxy-terminus, such as Lys-165, Val-187 and Asp 193, give rise to purine base binding and specificity. Lys-165 in the human HGPRTase which hydrogen bonds with the exocyclic guanine oxygen at C6 is conserved in all HGPRTases, HGXPRTases and XGPRTases. Val-187 in the human enzyme which hydrogen bonds with the exocyclic guanine oxygen at C6 and the exocyclic amine group at C2 is conserved in all species except for *T. foetus*, *T. gondii*, and *E. coli* . Asp-193 in the human HGPRTase also forms hydrogen bonds to the exocyclic amine

group at C2, and like Lys-165, the corresponding residue appears to be conserved in all species.

Eads *et al.* (Eads, *et al.*, 1994) hypothesize that the human enzyme may have a greater affinity for hypoxanthine over xanthine because xanthine has an exocyclic oxygen at C2 which may prevent formation of hydrogen bonds with the main chain oxygens of Val-187 and Asp-193; whereas, hypoxanthine having no substituent at the C2 position may be less sterically hindered and even allow a water molecule to occupy the O2 pocket. However, alignment of HGPRTases, HGXPRTases and XGPRTase show that an aspartic acid occupies the analogous position to the human Asp-193 in all these enzymes; thus, this residue may be involved in purine binding but it may not have a role in determining purine specificity. In all HGPRTases a valine occupies the equivalent position of Val-187 in the human enzyme; however, the enzymes from *T. gondii* and *T. foetus*, which are HGXPRTases, have an isoleucine in the equivalent position, and the *E. coli* enzyme, which is an XGPRTase, has a tryptophan in the equivalent position. The *P. falciparum* enzyme, also an HGXPRTase, has a valine at the position analogous to Val-187 in the human enzyme, but the malarial enzyme has a 100-fold higher K_m value for xanthine than for hypoxanthine and guanine (Queen, *et al.*, 1988) which may make it more similar to the HGPRTases than to the *T. gondii* and *T. foetus* HGXPRTases, which have K_m values two- and ten-fold higher than those for hypoxanthine and guanine, respectively (Beck and Wang, 1993; Maion and Chamberland, 1992). Site-directed mutational studies may aid in determining whether these residues do play a role in determining purine base specificity.

The high degree of amino acid sequence identity and similarity between the *T. foetus* sequence and the prokaryote enzyme sequences (Fig. 1.11) is not surprising since *T. foetus* is one of the earlier eukaryotes (Viscogliosi, *et al.*, 1993).

Again there is a high degree of conservation in the residues involved in PRPP-binding, the flexible, catalytic loop and the three residues mentioned above that play a role in purine base binding.

The open reading frame in the full-length genomic clone, pTfg1, for the HGXPRTase of *T. foetus* predicts a protein with a molecular mass of 21.1 kDa. This is smaller than the 24 kDa reported for the purified HGXPRTase of *T. foetus* (Beck and Wang, 1993). But there are several indications that the origin of translation of the HGXPRTase is the one predicted in Fig. 1.8. First, there is no other ATG codon present in the same translation frame for at least 300 bp upstream from the proposed translation initiation site. Second, there are three in-frame termination codons within 160 bp upstream from the predicted ATG translation start site. Third, there is only one ATG within the 66 nucleotide region of the poly(A^+) transcript preceding the proposed initiation codon, and it is followed immediately by an in-frame termination codon. Finally, the C, A and A at positions -4, -3 and +4 conform to the consensus sequence for eukaryotic initiation sites described by Kozak (Kozak, 1984).

Comparison of the *T. foetus* HGXPRTase and inosine monophosphate dehydrogenase (IMPDH) (Beck, *et al.*, 1994) genes reveals that 5' and 3' untranslated regions of these two genes are AT-rich. Examination of the 5' untranslated region revealed sequences which resemble TATA-like boxes located 84 (TCTAA) and 161 (TATAA) nucleotides upstream from the start methionine. Both of these TATA-like motifs are preceded by CAAT motifs at positions -110 and -186, respectively. Hexanucleotide sequences which may act as polyadenylation signals in several eukaryotic mRNAs (Birnstiel, *et al.*, 1985) were not found in the 3' untranslated region of the *T. foetus* HGXPRTase gene. Among the trichomonads, only the genes in *Trichomonas vaginalis* have had their regulatory sequences examined (Johnson, *et al.*, 1990). Johnson and co-workers

(Johnson, *et al.*, 1990) identified possible regulatory sequences for the *T. vaginalis* ferrodoxin gene. At the 5' end, there is a TATA-like motif (TATAAA) at -97, and at the 3' end, the sequences AATAAA and YGTGTTYY could function as polyadenylation signals (Johnson, *et al.*, 1990). The *T. vaginalis* succinyl-CoA synthetase beta subunit gene (Lahti, *et al.*, 1992) has the AATAAA sequence but not the YGTGTTYY sequence at its 3' end. Examination of the sequences of the 5' and 3' untranslated regions of the *T. foetus* HGXPRTase and IMPDH (Beck, *et al.*, 1994) genes and the *T. vaginalis* ferredoxin, succinyl-CoA synthetase beta subunit (Lahti, *et al.*, 1992) and beta-tubulin (GenBank accession number L05468) genes does not reveal any consensus sequences governing transcription. More genes from the *Trichomonadidae* family will have to be analyzed before any conclusions can be made regarding transcription regulatory sequences in these organisms.

The availability of the gene encoding the *T. foetus* HGXPRTase will allow us to express the *T. foetus* HGXPRTase in its apparent native form. Having a ready supply of the recombinant enzyme will enable us to carry out 1) detailed kinetic analyses of the enzyme, 2) crystallographic studies, allowing the elucidation of its 3-dimensional structure and 3) studies of the active site of the enzyme, leading to the discovery of the residues involved in catalysis and purine base specificity.

Figure 1.3. Assay for enzyme activity in SØ609/pTfc1.

LaneA, SØ609/pBSmc2" with [^{14}C]guanine as substrate.
Lane B, SØ609/pBluescript with [^{14}C]guanine as substrate.
Lane C, SØ609/pTfc1 with [^{14}C]hypoxanthine as substrate.
Lane D, SØ609/pTfc1 with [^{14}C]guanine as substrate.
Lane E, SØ609/pTfc1 with [^{14}C]xanthine as substrate.
Products [^{14}C]GMP, [^{14}C]IMP and [^{14}C]XMP remain at the origin, and purine bases migrate away from the origin.

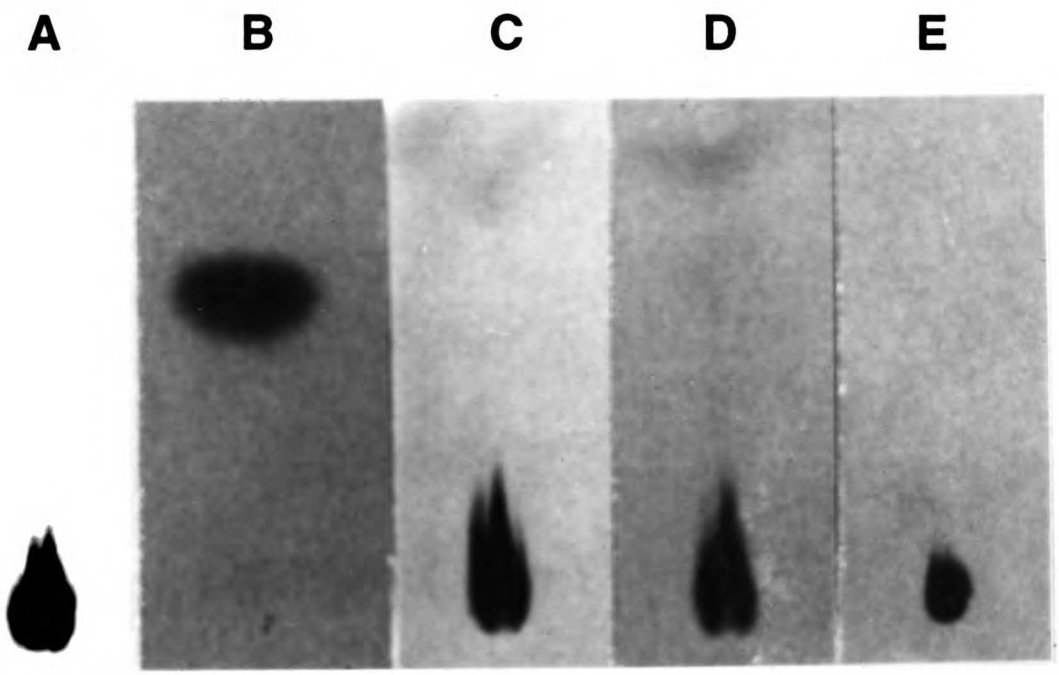
A
B
C
D
E

Figure 1.4. Genomic southern blot analysis of *T. foetus* DNA

Genomic DNA prepared from *T. foetus* strain KV_1 was digested to completion with various restriction endonucleases (as labeled in the figure), fractionated on a 0.8% agarose gel, transferred to a Nytran filter and probed with the 496-bp EcoRI cDNA fragment of pTfc1.

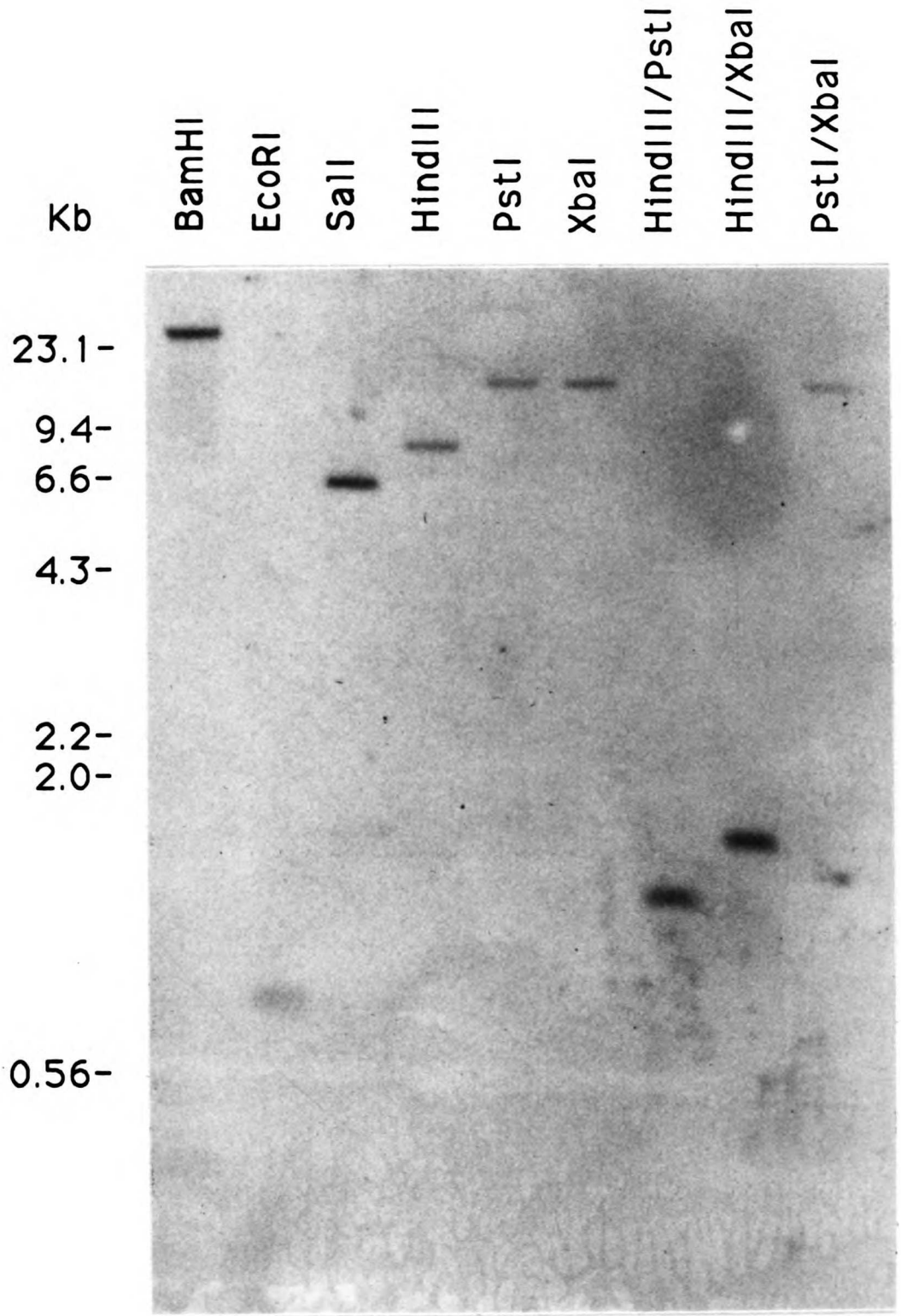
Kb
BamHI
EcoRI
SalI
HindIII
PstI
XbaI
HindIII/PstI
HindIII/XbaI
PstI/XbaI
23.1-
9.4-
6.6-
4.3-
2.2-
2.0-
0.56-

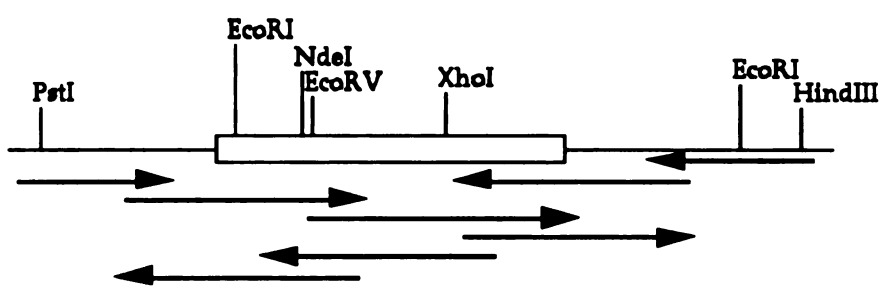

Figure 1.5. Restriction map and sequencing strategy for pTfg1.

The solid black line represents the genomic clone, pTfg1 (1427 bp), obtained by screening a genomic library with pTfc1. The box represents the region encoding the putative *T. foetus* HGXPRTase gene. The arrows below the map show length and direction of sequences read. Distances are not drawn to scale.

Figure 1.6. Genomic southern blot analysis of *T. foetus* DNA digested with various dilutions of *Eco*RI.

Genomic DNA prepared from *T. foetus* strain KV_1 was digested for 10 min with various concentrations of EcoRI (as labeled above each lane), fractionated on a 0.8% agarose gel, transferred to a Nytran filter and probed with a 419-bp fragment (see Fig. 1.8).

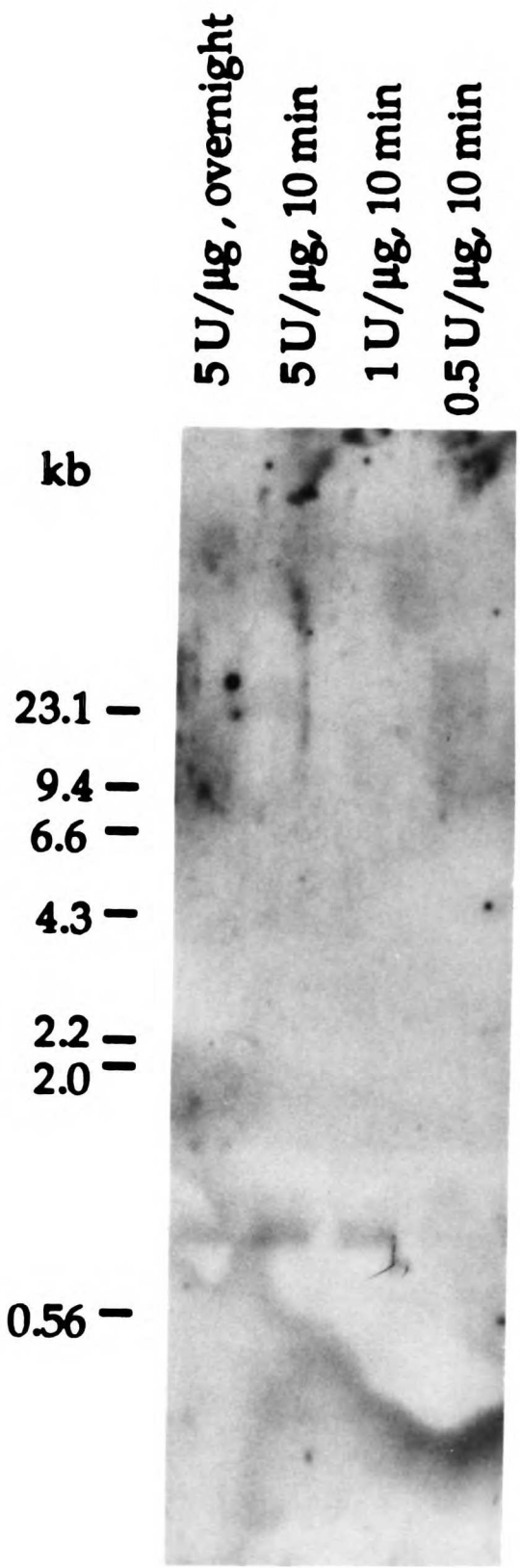
5 U/µg, overnight
5 U/µg, 10 min
1 U/µg, 10 min
0.5 U/µg, 10 min
kb
23.1
9.4
6.6
4.3
2.2
2.0
0.56

Figure 1.7. Northern blot analysis of *T. foetus* poly(A^+) RNA.

Poly (A^+) RNA prepared from *T. foetus* strain KV_1 was fractionated on a MOPS-formaldehyde-agarose gel, transferred to a nitrocellulose filter and probed with the 496-bp *Eco*RI cDNA fragment from pTfc1.

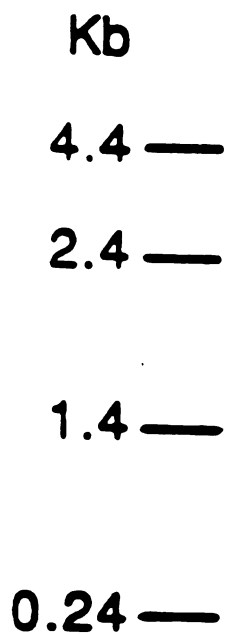
Kb
4.4
2.4
1.4
0.24

Figure 1.8. Nucleotide sequence of the HGXPRTase gene of *T. foetus* and deduced amino acid sequence of the coding region.

Underlined sequence represents the 496-bp cDNA fragment used to screen a genomic library of *T. foetus*. Boxed sequence represents the 536-bp cDNA clone, pTfc1. Single underline marks the stop codons upstream from the assumed initating ATG codon at position 1. ↓ shows where the transcript starts. Bold letters indicate potential TATA boxes, and double underline marks possible CAT boxes.

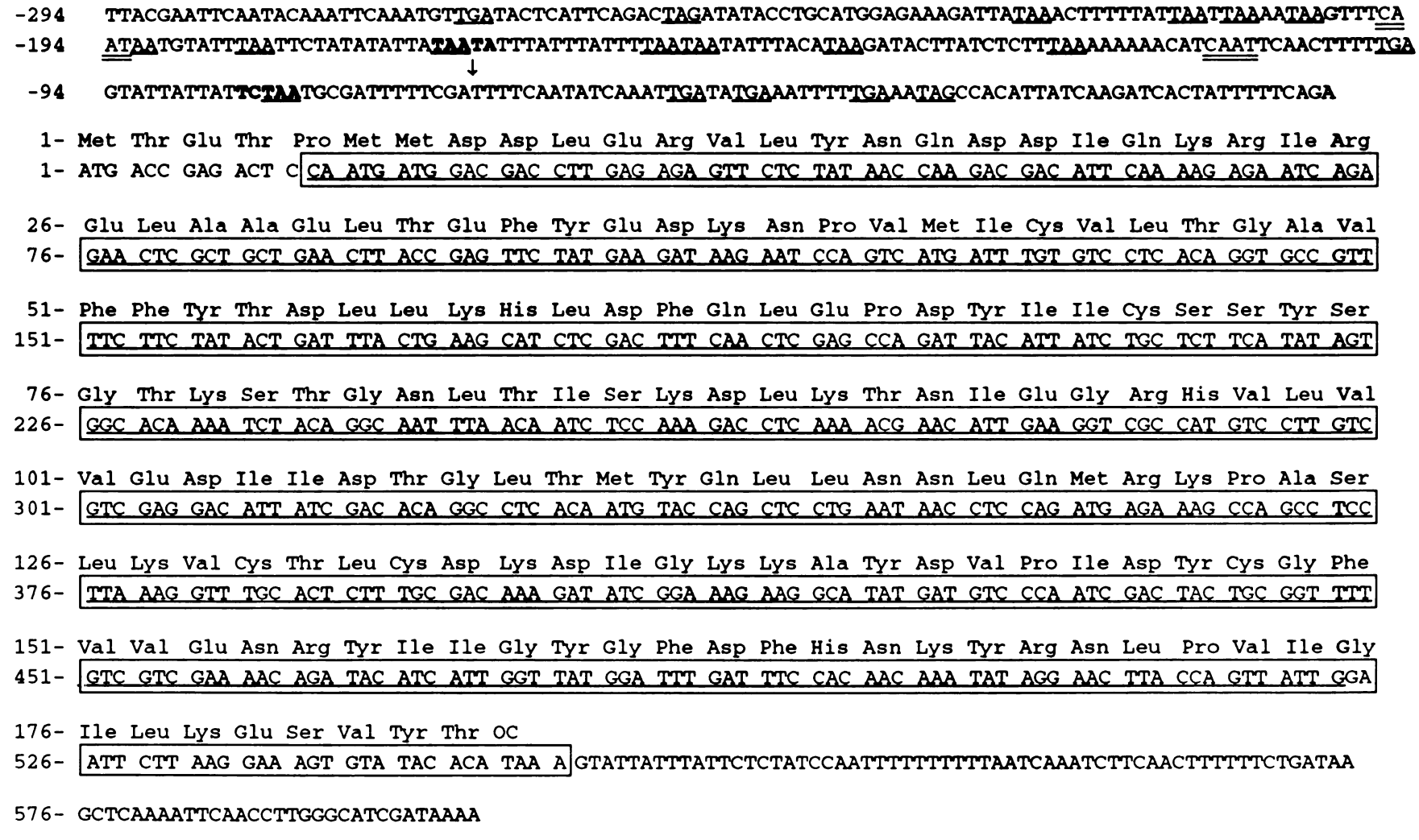
-294 TTACGAATTCAATACAAATTCAAATGTTGATACTCATTCAGACTAGATATACCTGCATGGAGAAAGATTATAAACTTTTTATTAATTAAAATAAGTTTCA
-194 ATAATGTATTTAATTCTATATATTATAATATTTATTTATTTTAATAATATTTACATAAGATACTTATCTCTTTAAAAAAAACATCAATTCAACTTTTTGA
-94 GTATTATTATTCTAATGCGATTTTTCGATTTTCAATATCAAATTGATATGAAATTTTTGAAATAGCCACATTATCAAGATCACTATTTTTCAGA
1- Met Thr Glu Thr Pro Met Met Asp Asp Leu Glu Arg Val Leu Tyr Asn Gln Asp Asp Ile Gln Lys Arg Ile Arg
1- ATG ACC GAG ACT CCA ATG ATG GAC GAC CTT GAG AGA GTT CTC TAT AAC CAA GAC GAC ATT CAA AAG AGA ATC AGA
26- Glu Leu Ala Ala Glu Leu Thr Glu Phe Tyr Glu Asp Lys Asn Pro Val Met Ile Cys Val Leu Thr Gly Ala Val
76- GAA CTC GCT GCT GAA CTT ACC GAG TTC TAT GAA GAT AAG AAT CCA GTC ATG ATT TGT GTC CTC ACA GGT GCC GTT
51- Phe Phe Tyr Thr Asp Leu Leu Lys His Leu Asp Phe Gln Leu Glu Pro Asp Tyr Ile Ile Cys Ser Ser Tyr Ser
151- TTC TTC TAT ACT GAT TTA CTG AAG CAT CTC GAC TTT CAA CTC GAG CCA GAT TAC ATT ATC TGC TCT TCA TAT AGT
76- Gly Thr Lys Ser Thr Gly Asn Leu Thr Ile Ser Lys Asp Leu Lys Thr Asn Ile Glu Gly Arg His Val Leu Val
226- GGC ACA AAA TCT ACA GGC AAT TTA ACA ATC TCC AAA GAC CTC AAA ACG AAC ATT GAA GGT CGC CAT GTC CTT GTC
101- Val Glu Asp Ile Ile Asp Thr Gly Leu Thr Met Tyr Gln Leu Leu Asn Asn Leu Gln Met Arg Lys Pro Ala Ser
301- GTC GAG GAC ATT ATC GAC ACA GGC CTC ACA ATG TAC CAG CTC CTG AAT AAC CTC CAG ATG AGA AAG CCA GCC TCC
126- Leu Lys Val Cys Thr Leu Cys Asp Lys Asp Ile Gly Lys Lys Ala Tyr Asp Val Pro Ile Asp Tyr Cys Gly Phe
376- TTA AAG GTT TGC ACT CTT TGC GAC AAA GAT ATC GGA AAG AAG GCA TAT GAT GTC CCA ATC GAC TAC TGC GGT TTT
151- Val Val Glu Asn Arg Tyr Ile Ile Gly Tyr Gly Phe Asp Phe His Asn Lys Tyr Arg Asn Leu Pro Val Ile Gly
451- GTC GTC GAA AAC AGA TAC ATC ATT GGT TAT GGA TTT GAT TTC CAC AAC AAA TAT AGG AAC TTA CCA GTT ATT GGA
176- Ile Leu Lys Glu Ser Val Tyr Thr OC
526- ATT CTT AAG GAA AGT GTA TAC ACA TAA AGTATTATTTATTCTCTATCCAATTTTTTTTTTAATCAAATCTTCAACTTTTTTCTGATAA
576- GCTCAAAATTCAACCTTGGGCATCGATAAAA

Figure 1.9. Primer extension of *T. foetus* poly(A^+) RNA with a 30-mer designed within the *T. foetus* HGXPRTase gene.

Panel A shows the dideoxy sequencing reaction of the genomic clone using the 30-mer used for the primer extension reaction. Panel B shows the primer extension reaction which was carried out at 37°C for two hours using the MMLV reverse transcriptase.

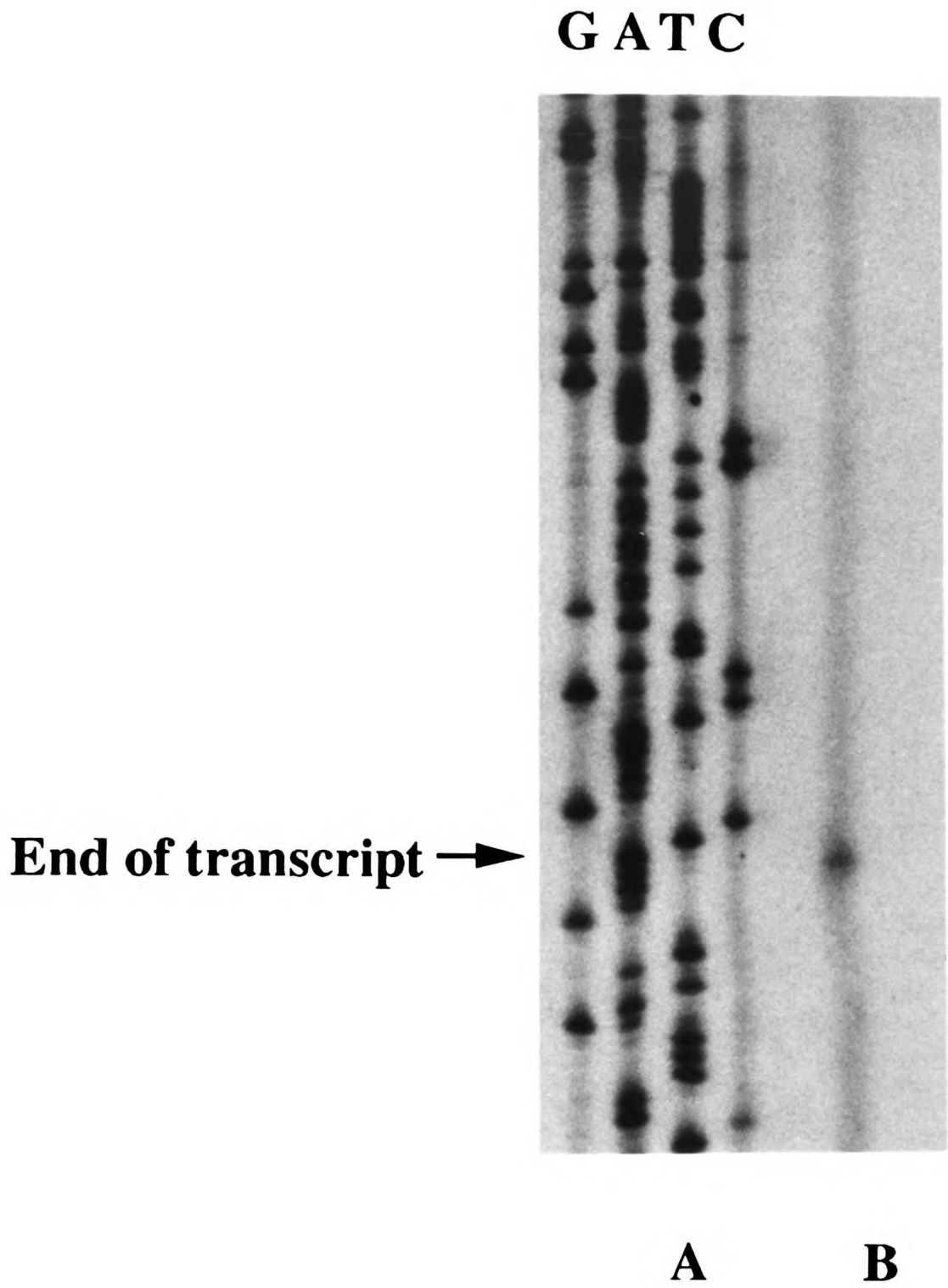
G A T C
End of transcript
A
B

Figure 1.10. Alignment of the deduced amino acid sequence of HGXPRTase of *T. foetus* with the amino acid sequences for HS: human (Jolly, *et al.*, 1983), SM; *S. mansoni* (Craig, *et al.*, 1988), PF; *P. falciparum* (King and Melton, 1987), TG; *T. gondii* (Roos, 1994; Vasanthakumar, *et al.*, 1994), TB; *T. brucei* (Allen and Ullman, 1993), TC; *T. cruzi* (Allen and Ullman, 1994), LD; *L. donovani* (Allen, *et al.*, 1993), CF; *C. fasciculata* (Ullman, 1994) and VH; *V. harveyi* (Showalter and Silverman, 1990).

Shading in red represents amino acids identical to the deduced *T. foetus* sequence, and light red represents chemically similar amino acids to the deduced *T foetus* sequence. Regions in blue represent the residues involved in PRPP-binding and the flexible catalytic loop (dark blue=identical and light blue=similar). Residues shaded in yellow represent amino acids involved in purine base binding and specificity (dark yellow=identical and light yellow=similar). Numbering in the text used for sequence comparisons refers to the *P. falciparum* sequence, unless otherwise noted in the text.

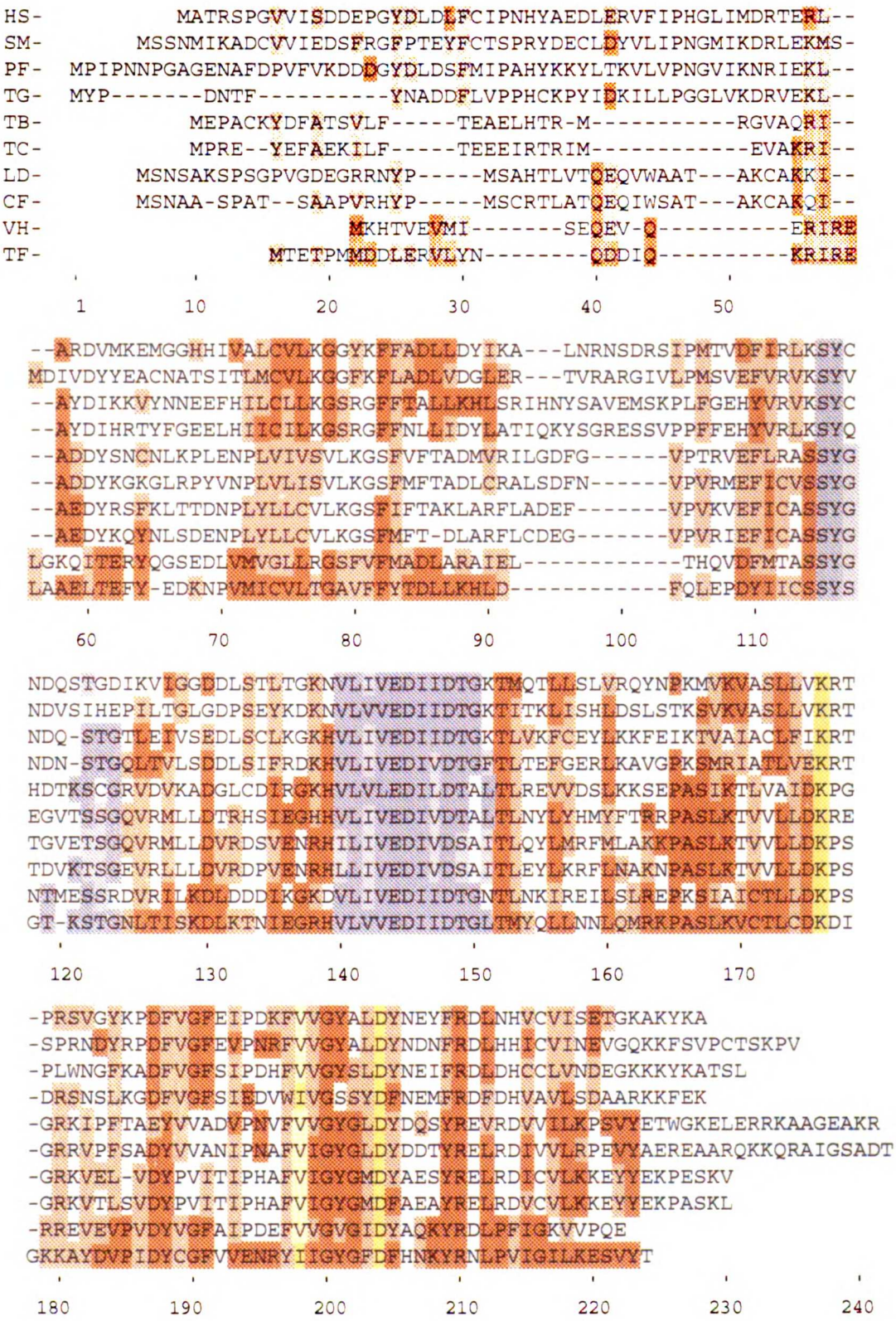
HS-
SM-
PF-
TG-
TB-
TC-
LD-
CF-
VH-
TF-
1
10
20
30
40
50
60
70
80
90
100
110
120
130
140
150
160
170
180
190
200
210
220
230
240

Figure 1.11. Alignment of the deduced amino acid sequence of HGXPRTase of *T. foetus* with the amino acid sequences for EC; *E. coli* (Pratt and Subramani, 1983), VH; *V. harveyi* (Showalter and Silverman, 1990) and LL; *L. lactis* (Nilsson and Lauridsen, 1992).

Shading in red represents amino acids identical to the deduced *T. foetus* sequence, and light red represents chemically similar amino acids to the deduced *T foetus* sequence. Regions in blue represent the residues involved in PRPP-binding and the flexible catalytic loop (dark blue=identical and light blue=similar). Residues shaded in yellow represent amino acids involved in purine base binding and specificity (dark yellow=identical and light yellow=similar). Residues shaded in dark purple represent identical residues and light purple represent chemically similar residues between the prokaryotic sequences.

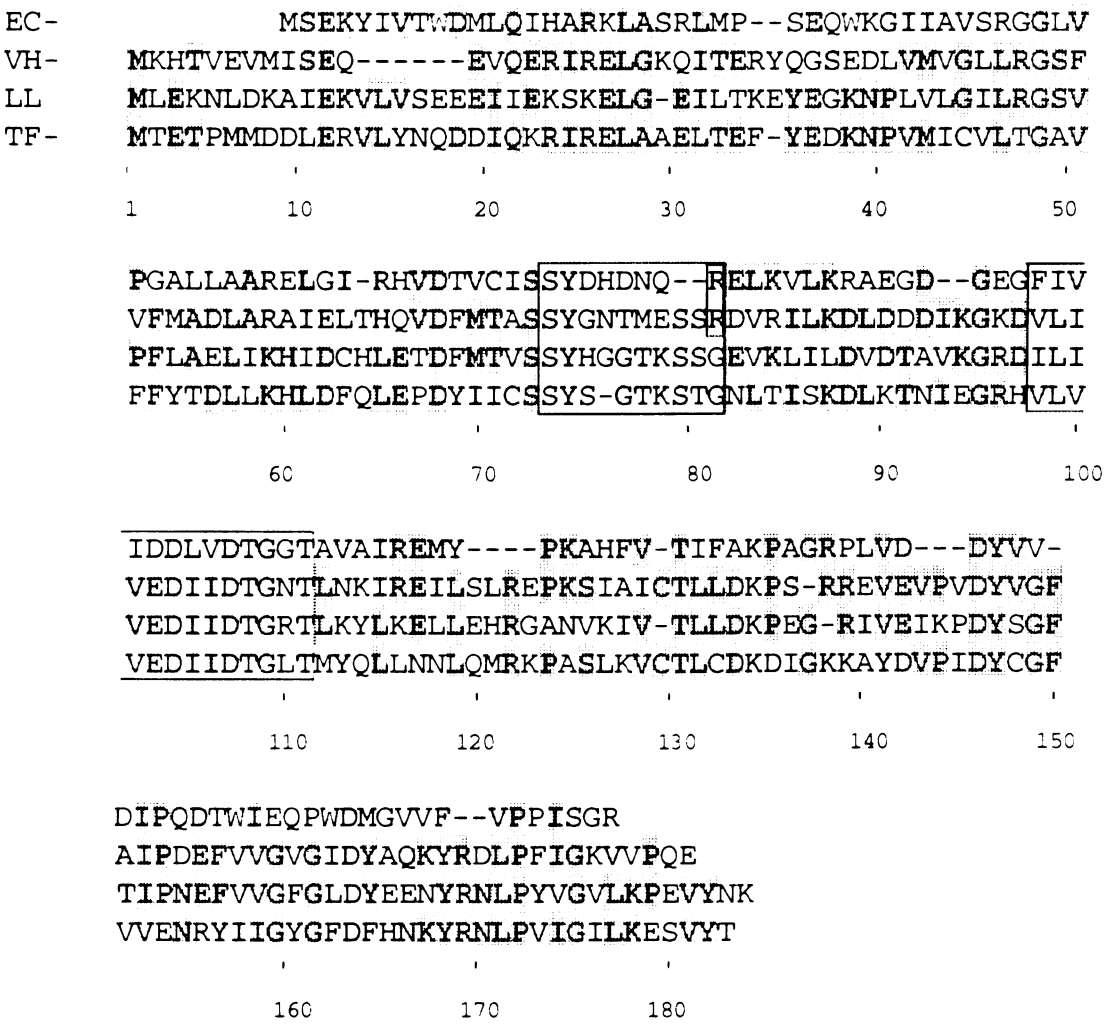
EC- MSEKYIVTWDMLQIHARKLASRLMP--SEQWKGIIAVSRGGLV
VH- MKHTVEVMISEQ------EVQERIRELGKQITERYQGSEDLVMVGLLRGSF
LL MLEKNLDKAIEKVLVSEEEIIEKSKELG-EILTKEYEGKNPLVLGILRGSV
TF- MTETPMMDDLERVLYNQDDIQKRIRELAAELTEF-YEDKNPVMICVLTGAV
1 10 20 30 40 50
PGALLAARELGI-RHVDTVCISSYDHDNQ--RELKVLKRAEGD--GEGFIV
VFMADLARAIELTHQVDFMTASSYGNTMESSRDVRILKDLDDDIKGKDVLI
PFLAELIKHIDCHLETDFMTVSSYHGGTKSSGEVKLILDVDTAVKGRDILI
FFYTDLLKHLDFQLEPDYIICSSYS-GTKSTGNLTISKDLKTNIEGRHVLV
60 70 80 90 100
IDDLVDTGGTAVAIREMY----PKAHFV-TIFAKPAGRPLVD---DYVV-
VEDIIDTGNTLNKIREILSLREPKSIAICTLLDKPS-RREVEVPVDYVGF
VEDIIDTGRTLKYLKELLEHRGANVKIV-TLLDKPEG-RIVEIKPDYSGF
VEDIIDTGLTMYQLLNNLQMRKPASLKVCTLCDKDIGKKAYDVPIDYCGF
110 120 130 140 150
DIPQDTWIEQPWDMGVVF--VPPISGR
AIPDEFVVGVGIDYAQKYRDLPFIGKVVPQE
TIPNEFVVGFGLDYEENYRNLPYVGVLKPEVYNK
VVENRYIIGYGFDFHNKYRNLPVIGILKESVYT
160 170 180

CHAPTER 2: EXPRESSION, PURIFICATION AND CHARACTERIZATION OF THE RECOMBINANT *TRITRICHOMONAS FOETUS* HYPOXANTHINE-GUANINE-XANTHINE PHOSPHORIBOSYLTRANSFERASE

INTRODUCTION

Earlier work from this laboratory (Beck and Wang, 1993) has demonstrated that purification of the native *T. foetus* HGXPRTase yields approximately 0.8 mg of active enzyme from 2 liters of mid-logarithmic culture of the parasite. In order to obtain enough enzyme to start kinetic and structural studies, about 40 liters of the cultured parasite would be needed. It would be more cost and labor effective to clone the gene encoding the enzyme into an expression system which could produce the recombinant enzyme in native form at much higher levels.

Many prokaryotic systems have been explored for expression of HGPRTases; for example, the HGXPRTase of *Plasmodium falciparum* has been expressed in both *E. coli* and *Salmonella typhimurium* using the temperature-inducible λ bacteriophage P_L-P_R promoter (Shahabuddin and Scaife, 1990), and the human HGPRTase has been expressed in *E. coli* using the IPTG inducible bacteriophage T7 promoter (Free, *et al.*, 1990; Eads, *et al.*, 1994). These systems have expressed the recombinant enzymes, but in some instances the majority of the enzyme was inactive (Shahabuddin and Scaife, 1990), or insoluble (Free, *et al.*, 1990). The most successful method used to express HGPRTases has been with the pBAce vector and an *E. coli* mutant, SØ606, which is unable to salvage purine bases other than adenine (Craig, *et al.*, 1991; Craig, *et al.*, 1992; Allen and Ullman, 1993; Allen and Ullman, 1994; Eakin, *et al.*, 1995). With pBAce, expression of the recombinant protein is regulated by an *E. coli* alkaline phosphatase promoter on the expression plasmid.

While the native *T. foetus* HGXPRTase has been estimated to have a molecular mass of 24 kDa from both SDS-PAGE and gel filtration chromatography (Beck and Wang, 1993), the size of the protein is 21.1 kDa based on the predicted amino acid sequence translated from the cloned full-length gene (Chin and Wang, 1994). This difference in the estimated and calculated molecular mass may be due to the inherent inaccuracies in determining protein sizes from polyacrylamide gel electrophoresis and gel filtration (Laue and Rhodes, 1990). Expression of the recombinant *T. foetus* HGXPRTase from the full-length gene will help resolve this discrepancy.

MATERIAL AND METHODS

Materials

The *E. coli* strain used for gene expression, SØ606 (F^- *ara, Δpro-gpt-lac, thi, hpt, rec*A1), was obtained from Dr. P. Nygaard (University Institute of Biological Chemistry B, Copenhagen, Denmark). The pBAce expression vector was obtained from Dr. Sydney Craig (University of California, San Francisco, CA) (Craig, *et al.*, 1991). The partially purified native *T. foetus* HGXPRTase was obtained from Dr. Joanne Beck (University of California, San Francisco, CA). [8-^{3}H]GMP (20 mCi/mmole) was purchased from ICN (Costa Mesa, CA). All restriction endonucleases were obtained from New England Biolabs (Beverly, MA) or Gibco/BRL (Gaithersburg, MD). Bacto-tryptone, bacto-agar and vitamin-free Casamino acids were from Difco (Detroit, MI), and Bacto-yeast extract from Becton Dickinson and Co. (Cockeysville, MD). All the other chemicals were purchased from Sigma Chemical Co. (St Louis, MO), and were of the highest purity available.

Expression plasmid construction and gene expression

Polymerase chain reactions (PCR) were used with a pair of designed primers to generate a fragment of DNA from the genomic clone with an added 5' NdeI site and a 3' PstI site. The product was first subcloned into the plasmid, pCR1000 (In Vitrogen, San Diego, CA), and then digested with PstI, partially digested with NdeI and ligated into the NdeI/PstI cleaved expression plasmid, pBAce (Craig, *et al.*, 1991). The resulting construct was named pBTfprt (see Fig. 2.1).

E. coli strain SØ606 was made competent (Hanahan, 1983), transformed with the expression plasmid, and plated onto LB-ampicillin agar plates. Colonies from the LB-ampicillin plates were each used to inoculate the induction medium (MOPS salt supplemented with 11 mM glucose, 1.5 μM thiamine, 148 mM adenine, 75 μg/ml ampicillin, 0.2% vitamin free Casamino acids and 0.1 mM equimolar mixture of Na_2HPO_4 and NaH_2PO_4) (Craig, *et al.*, 1991) and incubated at 37°C with aeration for approximately 16 h. Dimethyl sulfoxide was added to a final concentration of 8% in 1 ml aliquots of the SØ606 possessing pBTfprt culture, which were then stored at -70°C as frozen stocks. Cell extracts used for 12% SDS-PAGE analysis (Laemmli, 1970) (see Appendix D) and enzyme assays were prepared by pelleting the bacteria cells from 3 ml of the culture, resuspending in 100 μl TE buffer containing 0.9 mM PRPP and 3 mg/ml lysozyme, incubating at 37°C for 15 min and freeze-thawing three times to lyse the cells. Cell debris was removed by microcentrifugation. The intensities of protein bands in the stained gel were determined using a LKB 2202 Ultroscan Laser Densitometer.

Purification of the enzyme

Fifty microliters of a mid-logarithmic culture of SØ606/pBTfprt was used to inoculate 500 ml of the induction medium in a 2 L flask. The resulting culture

was incubated at 37°C with aeration for approximately 16 h. The cells were pelleted and resuspended in 10 ml of lysis buffer (25 mM Tris-HCl, pH 7.2, 10 mM $MgCl_2$, 1 mM DTT, 1 mM PRPP, 1 mM PMSF, 1 μg/ml leupeptin and 1 μg/ml pepstatin) and lysed by sonication. Nucleic acids were precipitated with protamine sulfate at a ratio of 1:20 (w/w, protamine sulfate/total protein), and the pellets were removed by centrifugation at 5000g for 10 min. As described by Beck and Wang (Beck and Wang, 1993), ammonium sulfate was added to the supernatant to 45% saturation, incubated on ice for one hour and centrifuged at 10,000xg for 20 min. More ammonium sulfate was then added to the supernatant, to 75% saturation. The suspension was incubated on ice for 1 h and then centrifuged at 10,000xg for 20 min. The protein pellet was resuspended in Buffer A (50 mM Bis-Tris, pH 6.8, 6 mM $MgCl_2$ and 1 mM DTT) and desalted over a 9.1 ml Sephadex G-25 M column (Pharmacia LKB, Uppsala, Sweden). Twenty milliliters of the desalted sample were loaded onto a Mono Q column (Pharmacia LKB, Uppsala, Sweden), equilibrated with Buffer A, and eluted with a non-linear gradient of 0-0.5 M KCl at a rate of 3 ml/min. PRPP was added to each of the collected fractions to a final concentration of 1 mM, and the fractions were assayed for HPRTase activity. Those fractions containing the activity were pooled, dialyzed overnight at 4°C in 100 volumes of Buffer A, and applied to a Mono P column (Pharmacia LKB, Uppsala, Sweden), equilibrated with Buffer A, and eluted with 7.5% Polybuffer 74-HCl, pH 4.0 containing 6 mM $MgCl_2$ and 1 mM DTT at a flow rate of 0.8 ml/min. The pH of each fraction was adjusted to approximately 7 using 1 M Tris-HCl, pH 8.5. Fractions were assayed for HPRTase activity and analyzed by SDS-PAGE. To determine the pI of the purified enzyme, the pH of each fraction collected from the mono P column was measured directly with a Fisher Accumet pH meter.

Enzyme assay

Five microliters of the sample of purified enzyme were added to 20 µl of a reaction mixture of 0.3 M Tris-HCl pH 7.8, 18 mM $MgCl_2$, 0.5 mM PRPP containing either 17.5 µM ^{14}C-hypoxanthine (57.0 mCi/mmole), 18.2 µM ^{14}C-guanine (55.0 mCi/mmole), or 17 µM ^{14}C-xanthine (59.0 mCi/mmole). The reaction mixture was incubated at 37°C for 5 min, and the reaction stopped with 1 mM hypoxanthine and 1 mM IMP. Twenty microliters of the reaction mixture was spotted on a PEI cellulose sheet, and the chromatogram was developed with 5 mM NH_4Ac pH 4.5, dried and exposed to X-ray film (Yuan, *et al.*, 1990). Determination of the pH optimum for the enzyme employed the same assay method with the following changes: 0.3 M sodium acetate was used as the buffer system for pH 4, 4.5, 5 and 5.5, 0.3 M Bis-Tris was used as the buffer system for pH 6, 6.4 and 6.8 and 0.3 M Tris-HCl was used as the buffer system for pH 7, 7.2, 7.4, 7.6, 7.8, 8, 8.5 and 9.

Gel filtration

A Superose 6 FPLC column (Pharmacia LKB, Uppsala, Sweden) was equilibrated with Buffer A (50 mM Bis-Tris, pH 6.8, 6 mM $MgCl_2$ and 1 mM DTT), and 100 µg each of blue dextran (2000 kDa), bovine serum albumin (67 kDa), ovalbumin (44 kDa), chymotrypsinogen (25.66 kDa) and RNase A (13.7 kDa) were applied to the column as molecular weight calibration standards along with approximately 100 µg of the purified enzyme. The proteins were eluted at a flow rate of 0.4 ml/min and 1 ml fractions were collected and assayed for HPRTase activity.

Preparation of samples for mass spectrometry

The purified enzyme was dialyzed against double deionized water and dried on a Savant or lyophilyzer. The samples were then submitted to mass

spectrometry analysis which was provided by the Mass Spectrometry Facility at the University of California, San Francisco, and by David King at HHMI, Department of Molecular and Cell Biology at the University of California, Berkeley.

Enzyme labeling by [8-^{3}H]-GMP dialdehyde

[8-^{3}H]-GMP dialdehyde was synthesized from [8-^{3}H] GMP (20 mCi/mmole) as follows (Gutensohn and Huber, 1975, Yuan, *et al.*, 1992): 10 µl of 0.5 nM [8-^{3}H] GMP were mixed with 2 µl of 1 mM $NaIO_4$ in 100 mM of phosphate buffer, pH 7 and incubated at room temperature for 1 h. The excess periodate was depleted by addition of 1 µl of 10 mM ethylene glycol. The oxidized [8-^{3}H] GMP was allowed to react with the protein at 4°C for 16 h. The reaction mixtures were then each mixed with SDS-sample buffer, boiled for 5 min and loaded on a 12% polyacrylamide gel. After electrophoresis, the gel was soaked in Fluoro-Hance (RPI, Mount Prospect, Ill) for 30 min, dried and exposed to X-ray film.

RESULTS

Expression of the T. foetus HGXPRTase in E. coli

The expression of pBTfprt in the soluble fraction of transformed SØ606 is demonstrated by a prominent protein band at approximately 24 kDa on a Coomassie blue-stained SDS-PAGE gel (Fig. 2.2). Whereas, cell lysates of the negative control, SØ606/pBAce, lacked a prominent band of the same size. The recombinant HGXPRTase appears to constitute at least 50% of the total cellular protein of the transformed *E. coli* by densitometer scanning of the total proteins on an SDS-PAGE gel. Partially purified cell extracts of SØ606/pBTfprt demonstrated specific activities for HPRTase, GPRTase and XPRTase at 965 nmol min^{-1} (mg protein)$^{-1}$, 952 nmol min^{-1} (mg protein)$^{-1}$ and 909 nmol min^{-1} (mg protein)$^{-1}$, respectively.

Purification of the recombinant T. foetus HGXPRTase

HGXPRTase was purified to at least 95% homogeneity from bacterial cells expressing the product of the pBTfprt construct following a modified version of the protocol used by Beck and Wang (Beck and Wang, 1993). The elution profile from the mono Q column is shown in Figure 2.4, and the enzyme activity is associated with the largest eluted protein peak (data not shown). A typical protocol of enzyme purification is summarized in Table 2.1, and the SDS-PAGE analysis of the purification is shown in Fig. 2.3. The yield from this enzyme preparation was 7.6 mg of purified recombinant HGXPRTase per liter of *E. coli* culture, the specific activity for HPRTase was 3685 nmol min^{-1} (mg protein)$^{-1}$, the fold of purification was 4.3, and 66.2% of the enzyme was recovered. Later enzyme preparations yielded between 20 to 60 mg of purified recombinant HGXPRTase per liter of *E. coli* culture (data not shown). This difference in yield is affected by the efficiency of bacterial cell breakage. The mono P column was added to the original protocol to provide an additional purification step and to concentrate the sample.

Characterization of the recombinant T. foetus HGXPRTase

The isoelectric point of the recombinant enzyme was determined by measuring the pH of the fractions collected from the mono P column with a pH meter. The plot of pH versus fraction number is shown in Fig. 2.5, and the pI was determined to be 4.8. This is the average of the values determined for fractions 30 and 31 which both demonstrated HGXPRTase activity. This value is identical to the pI calculated from the amino acid sequence. The pH optimum of the recombinant enzyme is 6.6 for HPRTase activity, 6.8 for GPRTase activity and 6.6 for XPRTase activity (data not shown). The recombinant enzyme retains 50% of its activity over a pH range of 5.5 to 8.0.

The apparent molecular weight of the recombinant HGXPRTase was measured by gel filtration on a Superose 6 column and found to be 24 kDa (Fig. 2.6). Like the native enzyme, the recombinant enzyme, also elutes from the gel filtration column as a monomer while fully retaining its activity. The molecular mass of the recombinant enzyme was determined on three separate occasions using mass spectrometry. The first determination was carried out on a laser desorption mass spectrometer and gave a broad, weak signal at a molecular mass of 21519 (data not shown). The second and third determinations were carried out using electrospray ionization mass spectrometry and gave molecular masses for two species in the sample; the first species had a molecular mass of 21093.91 and 21091.04 and the second species had a molecular mass of 20963.77 and 20960.5 (data not shown). This second species is most likely the recombinant *T. foetus* HGXPRTase without the formylmethionine residue at the amino terminus. Thus, the data from mass spectrometry agree with the molecular mass calculated from the protein sequence, whereas the same protein exhibited a higher mass of 24 kDa in SDS-PAGE and gel filtration.

SDS-PAGE analysis of an extract of SØ606/pBTfprt and a partially purified native enzyme both labeled with oxidized [8-^{3}H] GMP showed that this method has labeled only one protein species in each sample. The two radiolabeled bands have a similar molecular massof 24 kDa (Fig. 2.7).

DISCUSSION

The pBAce vector (Craig, *et al.*, 1991) has been used successfully to express high levels of HGPRTasesfrom many origins; such as the human (Craig, *et al.*, 1992), *S. mansoni* (Craig, *et al.*, 1991), *P. falciparum* (Eakin, *et al.*, 1995), *T. brucei* (Allen and Ullman, 1993) and *T. cruzi* (Allen and Ullman, 1994) HGPRTases. Levels of 30-45 mg of the recombinant *S. mansoni* HGPRTase/liter of culture

(Craig, *et al.*, 1991), 100 mg of the recombinant *T. brucei* HGPRTase/liter of culture (Allen and Ullman, 1993) have been obtained. The recombinant *T. cruzi* HGPRTase makes up approximately 70% of the total cellular protein (Allen and Ullman, 1994). The recombinant *T. foetus* HGXPRTase makes up at least 50% of the total cellular protein when it is expressed in transformed *E. coli*. This is 500-fold over the native enzyme, from its original source, which composes approximately less than 0.1% of the parasite's total cellular protein (Beck and Wang, 1993). The average yield from one liter of bacterial cells is approximately 20 mg of purified recombinant *T. foetus* HGXPRTase. Higher yields are obtained with higher percentages of bacterial cell breakage.

In addition to providing large amounts of purified *T. foetus* HGXPRTase, this expression system also produces an active enzyme with no apparent differences from the native enzyme. Some properties of the recombinant *T. foetus* HGXPRTase are compared to those of the native enzyme in Table 2.2. The molecular weight (24 kDa), as determined by SDS-PAGE and gel filtration, for both the native and recombinant enzyme is identical. The specific activities of the two enzymes for hypoxanthine, guanine and xanthine are similar, and the pH range for maximal enzyme activity is similar suggesting that the catalytic function of the two proteins are similar. The pI values for the two proteins are similar, though not identical, with the pI of the recombinant enzyme being more acidic than the pI of the native enzyme. The difference in the pI values may be due to experimental errors in determining the pI, or it may indicate that the native enzyme purified from the parasite may undergo post-translational modification, such as glycosylation.

It is interesting to note that the pI values of two forms of HGPRTase purified from bovine brain are 7.85 and 8.10 (Paulus, *et al.*, 1980). These values are very unusual because all the pI values of HGPRTases from mammalian sources have

been in the acidic range (Olsen and Milman, 1977; Gutensohn, *et al.*, 1976; Olsen and Milman, 1974). The enzymes isolated from bovine brain are also more basic proteins than the parasitic enzyme. The difference in substrate specificity and isoelectric characteristics of the bovine and tritrichomonal enzyme may aid in design of a specific inhibitor for the parasitic enzyme.

Periodate-oxidized GMP specifically labels the active site (Gutensohn and Huber, 1975; Kanaaneh, *et al.*, 1994). The guanosine 2',3'-dialdehyde-5'-phosphate forms a covalent bond with an amino acid residue near the nucleotide binding site of the HGPRTases (Kanaaneh, *et al.*, 1994). Labeling an extract of SØ606/pBTfprt and partially purified native *T. foetus* HGXPRTase with periodate-oxidized [8-^{3}H] GMP demonstrate that the label is specific since a single species, each approximately 24 kDa, is labeled in each sample.

There appears to be no difference in the calculated and experimentally determined molecular mass of the recombinant enzyme, since the calculated mass is 21089.699 and the experimentally determined values are 21093.91 and 21091.04. The second species seen on mass spectrometry with values of 20963.77 and 20960.5 could be the enzyme without the formylmethionine residue at the amino terminus, since the N-formylmethionine residue is normally removed from proteins expressed in prokaryotes by the successive action of a deformylase (Adams, 1968) and a methionyl-aminopeptidase (Takeda and Webster, 1968; Ben-Bassat, *et al.*, 1987; Miller, *et al.*, 1987). The high level of expression of HGXPRTase could saturate one or both of these enzymes, and the recombinant HGXPRTase expressed in *E. coli* would be isolated as a mixture, with and without the N-formylmethionine. Results from protein sequencing the N-terminus (data not shown) also agree with the mass spectrometry results. The first molecular mass determination by laser desorption mass spectrometer may have a large error associated it since the signal was broad and weak. The

accuracy of the apparent molecular weight determined by SDS-PAGE and gel filtration chromatography both depend on the assumption that the unknown protein resembles the protein standards (Laue and Rhodes, 1990). The protein standards used were compact spherical proteins. The shape of the human HGPRTase is not spherical, since the regions of the enzyme which make-up the nucleotide (GMP) binding cleft form a concave surface. Based on the HGPRTase alignments in Chapter 1, the shape of the *T. foetus* enzyme should be similar to that of the human enzyme. Thus, the difference between the true molecular mass and the apparent molecular weight as determined by SDS-PAGE or gel filtration could be postulated to occur because the shape of the folded enzyme causes it to behave as if it was a larger protein.

The high expression of recombinant *T. foetus* HGXPRTase in its apparent native form will allow the purification of large quantities of active enzyme. This will enable us to further characterize the enzyme with both kinetic and structural studies. Information gleaned from these studies could be used for the structure-based drug design of inhibitors for the treatment of bovine urogenital trichomoniasis.

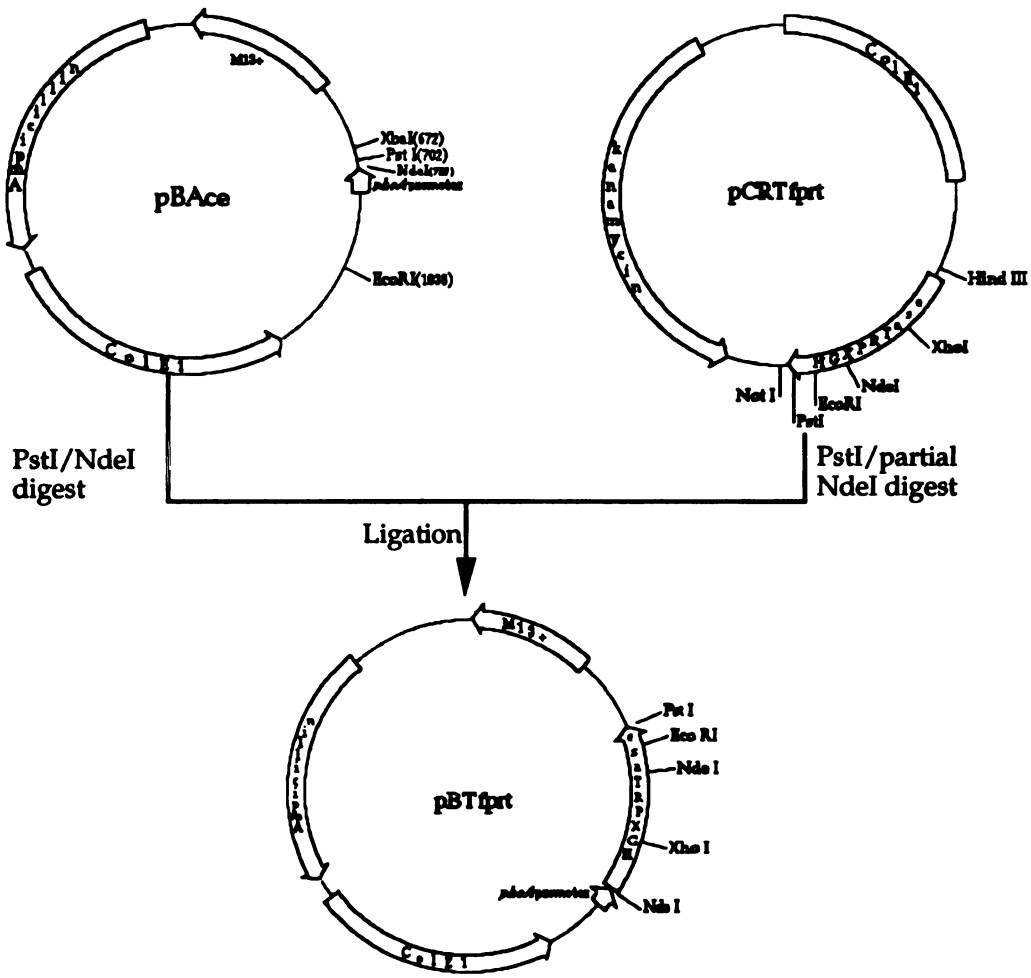

Figure 2.1. Construction of the expression plasmid pBTfprt.

Using the polymerase chain reaction (PCR) a 608 bp fragment of pTfg1 encoding the *T. foetus* HGXPRTase was amplified. The oligonucleotide primers used added a 5' NdeI site and a 3' PstI site. The PCR-amplified product was first subcloned into the plasmid pCR1000 (In Vitrogen, San Diego, CA), and the resulting plasmid, pCRTfprt, was digested with PstI and partially digested with NdeI. This NdeI/PstI fragment was then ligated into pBAce which had been digested with PstI and NdeI to generate pBTfprt.

Figure 2.2. SDS-PAGE of whole cell extracts of (A) SØ606/pBTfprt and (B) SØ606/pBAce.

The gel was stained with Coomaisie blue. Sizes of molecular weight markers (in kDa) are indicated to the left of the gel.

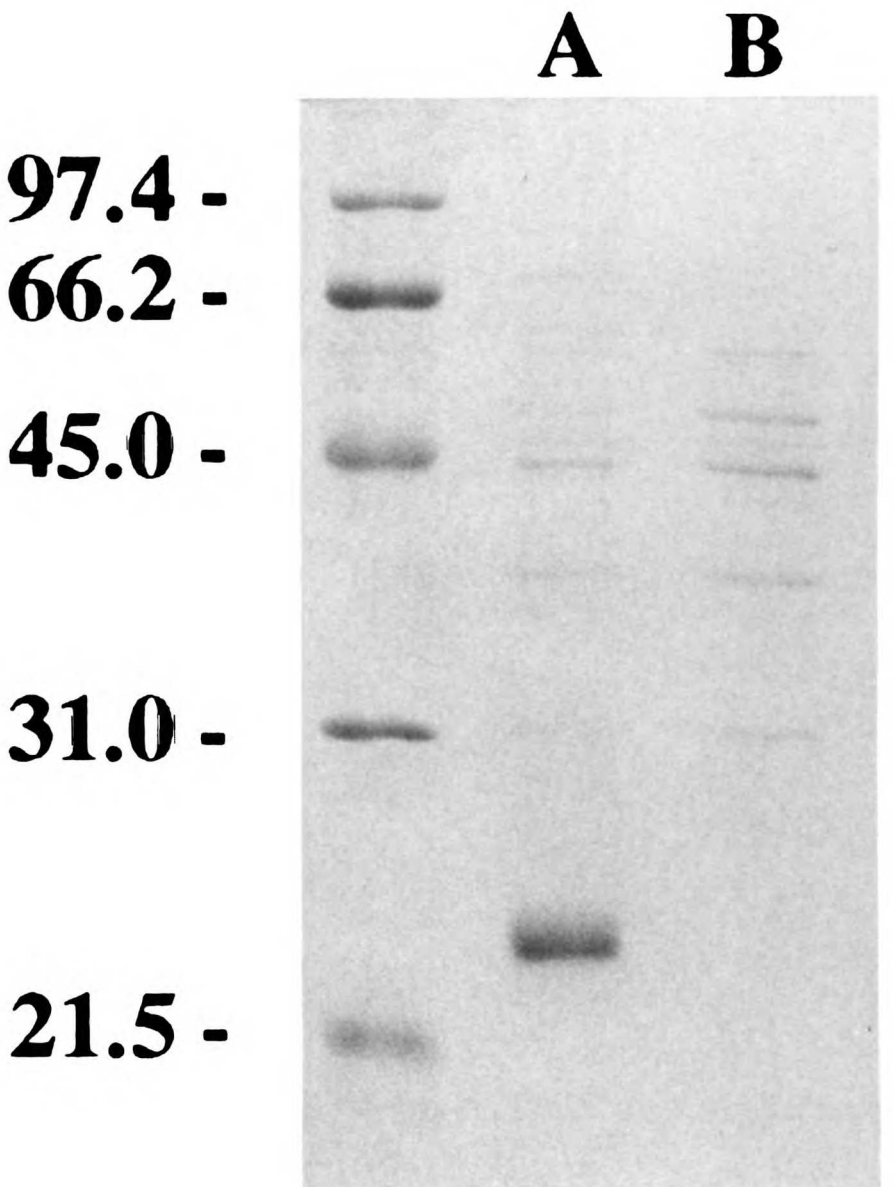
A
B
97.4 -
66.2 -
45.0 -
31.0 -
21.5 -

Figure 2.3. SDS-PAGE gel of the Purification of Recombinant *T. foetus* HGXPRTase.

Lane A. Cell lysate of SØ606/pBTfprt
Lane B. Supernatant after protamine sulfate precipitation.
Lane C. Supernatant after a 45% ammonium sulfate precipitation.
Lane D. Pellet after a 75% ammonium sulfate precipitation.
Lane E. Fraction with HGXPRTase activity after elution from an HPLC mono Q column.
Lane F. Fraction with HGXPRTase activity after elution from an HPLC mono P column.
Sizes of molecular weight markers in kilodaltons are indicated to the left of the gel.

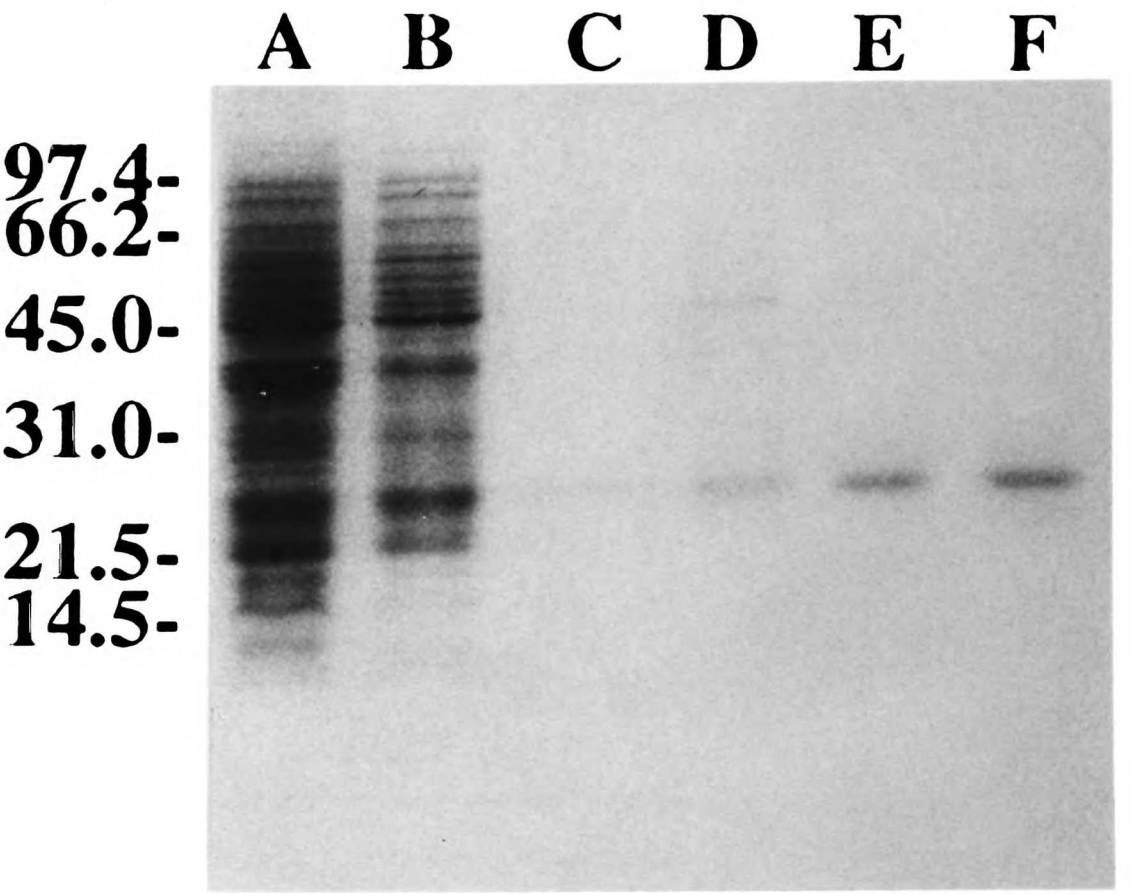
A
B
C
D
E
F
97.4-
66.2-
45.0-
31.0-
21.5-
14.5-

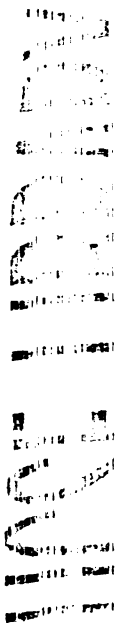

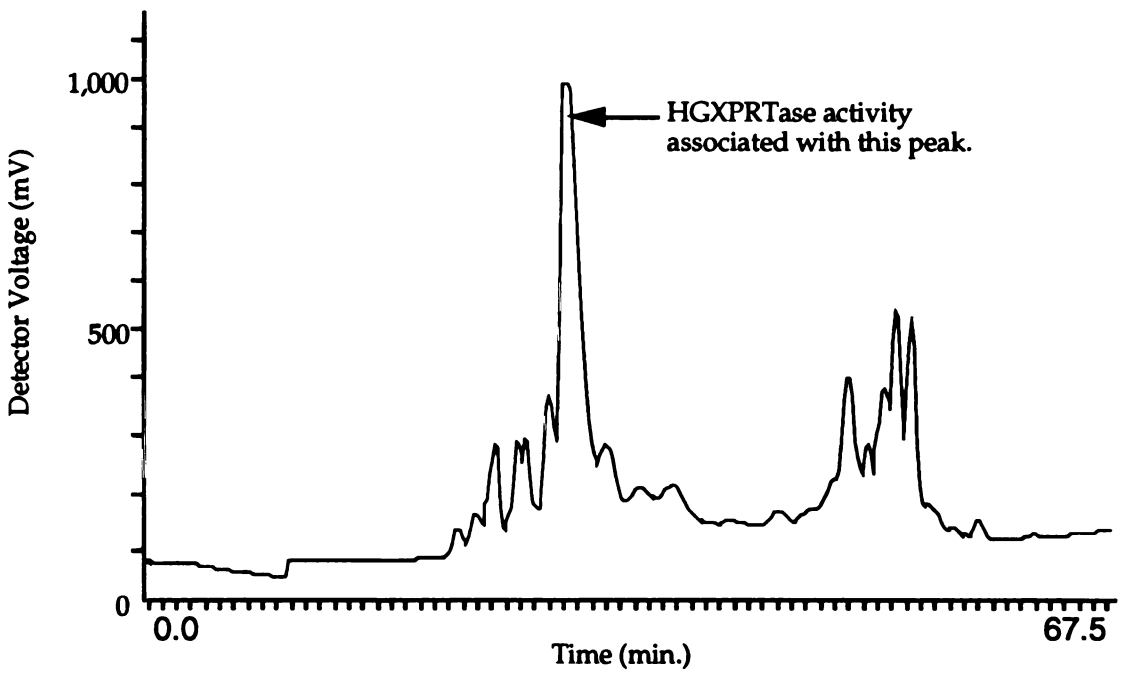

Figure 2.4. Chromatogram of protein eluted from an HPLC mono Q column.

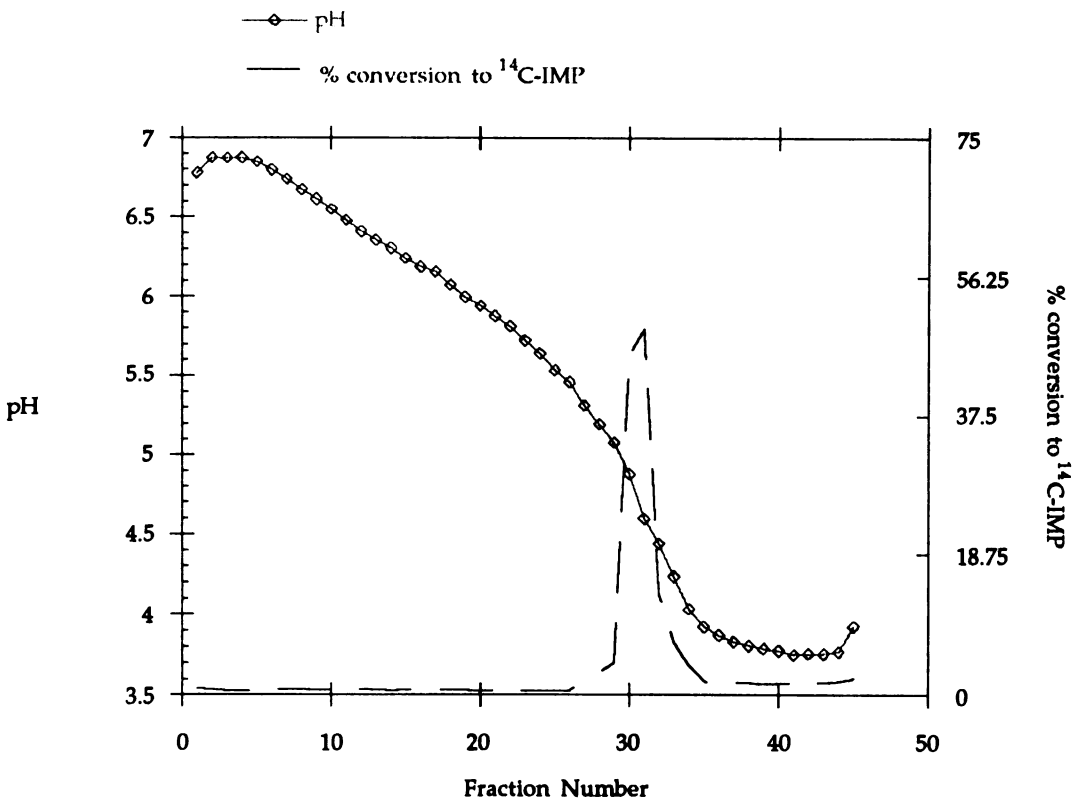

Figure 2.5. Determination of the pI for recombinant *T. foetus* HGXPRTase.

Recombinant *T. foetus* HGXPRTase was applied to a Mono P isoelectric chromatofocusing column at a flow rate of 0.8 ml/min. Fractions collected every minute were assayed for HPRTase activity, and the pH of each fraction was measured directly on a Fisher Accumet pH meter.

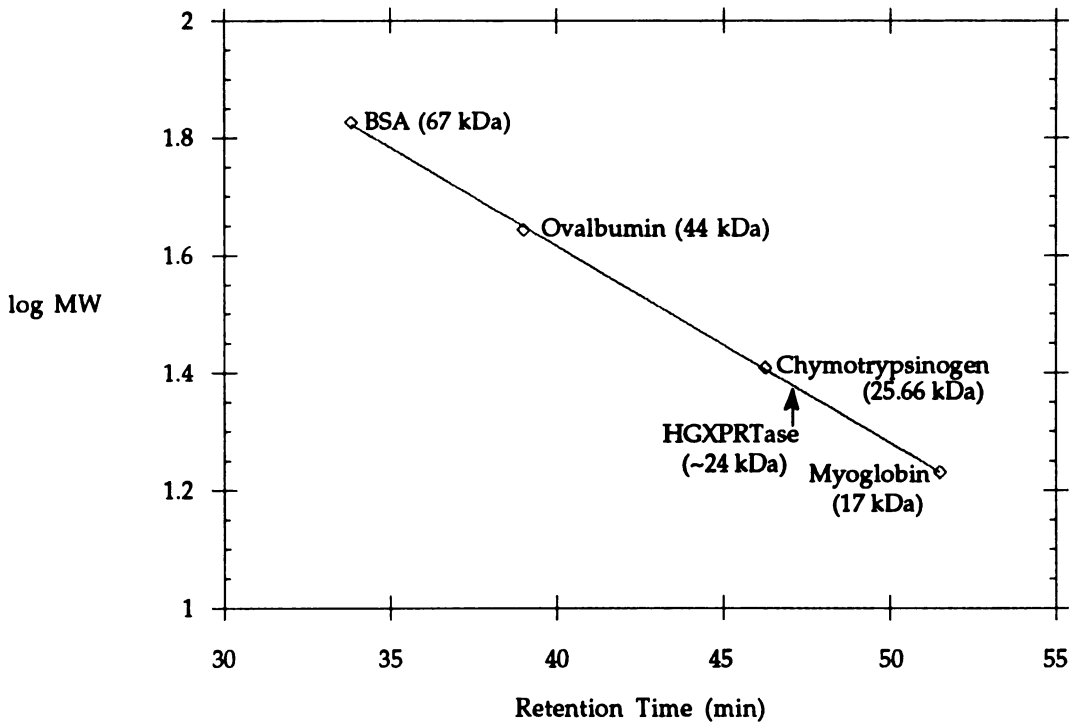

Figure 2.6. Molecular weight determination of the recombinant *T. foetus* HGXPRTase.

Purified HGXPRTase was mixed with molecular weight standards and applied to a Superose 6 gel filtration column at a flow rate of 0.4 ml/min. Fractions collected every minute were assayed for HPRTase activity. The elution time of the molecular weight standards was plotted versus the molecular weight of the standards, and the elution time of the peak HPRTase activity was compared to that of the protein standards.

Figure 2.7. SDS-PAGE of native *T. foetus* HGXPRTase and whole cell extract of SØ606 with pBTfprt labeled with oxidized [8-^{3}H] GMP.

Oxidized [8-^{3}H] GMP was synthesized, and samples were labeled as described in Materials and Methods.
Lane A. SØ606 with pBTfprt.
Lane B. Native *T. foetus* HGXPRTase.
Sizes of molecular weight markers are indicated to the left of the gel.

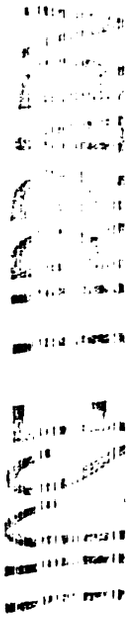

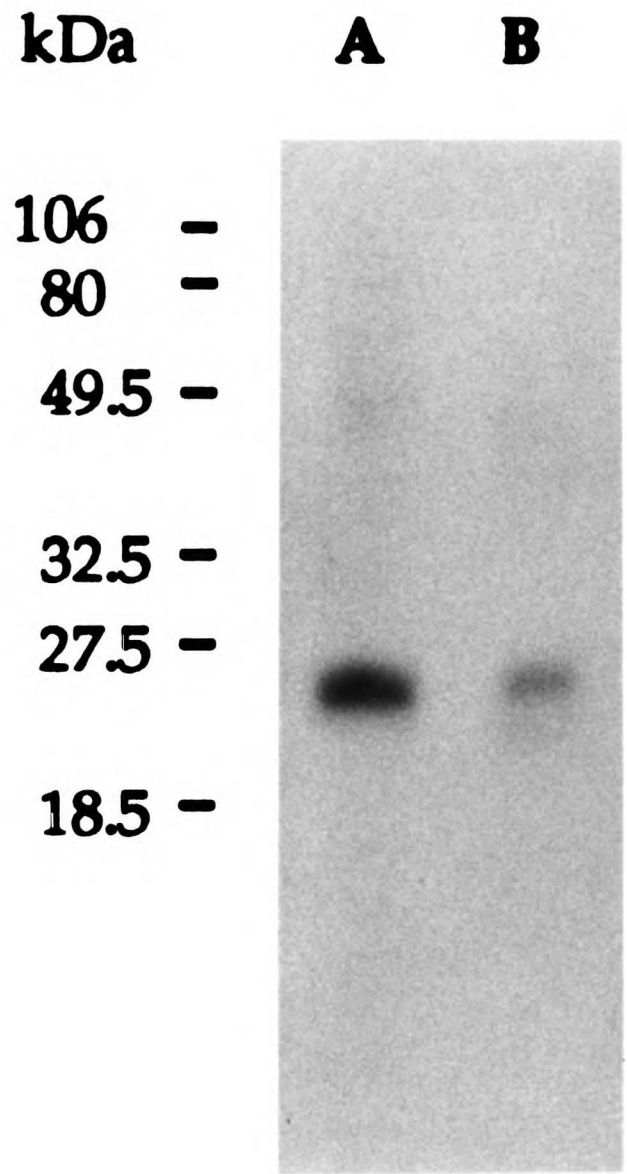
kDa
A
B
106
80
49.5
32.5
27.5
18.5

Table 2.1. Purification of the recombinant HGXPRTase.

Steps	Volume	[Protein]	Total protein	Total activity HPRT	Specific activity HPRT	Purification HPRT	Yield HPRT
	ml	*mg/ml*	*mg*	*nmol/min*	*nmol/min-mg*	*Fold*	%
Cell lysate	30	3.35	100	85,100	851	1	100
Protamine sulfate precipitation	30	2.74	82.2	141,795	1725	2	167
45% $(NH_4)_2SO_4$	40	0.4	16	11,232	702	0.82	13.2
75% $(NH_4)_2SO_4$	17.5	2.95	51	82,314	1614	1.9	96.7
Mono Q	27	1.19	32.1	112,607	3508	4.1	132
Mono P	10	1.53	15.3	56,380	3685	4.3	66.2

Table 2.2. Comparison of Recombinant and Native *T. foetus* HGXPRTase

	Recombinant	Native
Molecular weight (kDa)	24	24
Isoelectric point	4.8	5.5
Specific activity nmol IMP/min-mg	2856	2294
Specific activity nmol GMP/min-mg	2496	2179
Specific activity nmol XMP/min-mg	1567	1399

CHAPTER 3: STEADY-STATE KINETICS OF THE RECOMBINANT HYPOXANTHINE-GUANINE-XANTHINE PHOSPHORIBOSYLTRANSFERASE OF *TRITRICHOMONAS FOETUS*

INTRODUCTION

Hypoxanthine-guanine phosphoribosyltransferase (HGPRTase; EC 2.4.2.8) catalyzes the transfer of the phosphoribosyl moiety from α-D-5-phosphoribosyl-1-pyrophosphate to the imidazole N-9 of a purine base (either hypoxanthine, guanine or xanthine) to form a purine nucleotide (either IMP, GMP or XMP) and pyrophosphate (Fig. 3.1). This reaction occurs with an anomeric inversion of the ribosyl C1.

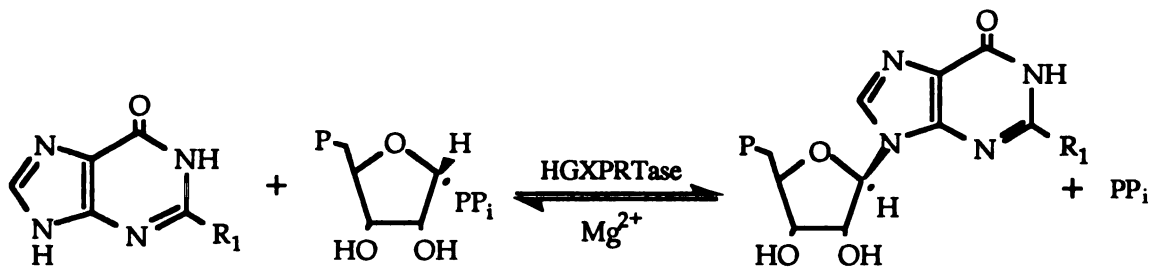

Figure 3.1. Reaction catalyzed by the HGXPRTase of *Tritrichomonas foetus*.

hypoxanthine: R_1 = -H, guanine: R_1 = $-NH_2$, xanthine: R_1 = =O

HGPRTase plays a role in purine metabolism and belongs to a class of approximately ten phosphoribosyltransferases (PRTases) which catalyze similar reactions involving a nitrogenous base, a divalent metal ion and PRPP (Musick, 1981). The mechanism of a few of the PRTase-catalyzed reactions have been studied, but the mechanism for a majority of these reactions remains unknown. No single kinetic mechanism can be used to define PRTase-catalyzed reactions, but two mechanisms have been observed. Studies of the human APRTase (Srivastava and Beutler, 1971; Thomas, *et al.*, 1973), *E. coli* APRTase (Hochstadt,

1978), yeast OPRTase (Victor, *et al.*, 1979) and the yeast UPRTase (Natalini, *et al.*, 1979) indicate that these enzymes follow a ping-pong kinetic mechanism, which involves an enzyme-ribosylphosphate intermediate. However, a sequential mechanism, which requires both substrates to bind to the enzyme prior to the release of any product, appears to be favored by many PRTases (Ali and Sloan, 1982; Bhatia, *et al.*, 1990; Giacomello and Salerno, 1978; Musick, 1981; Yuan, *et al.*, 1992) with ordered and random binding of substrates or release of products being observed.

The HGXPRTase of *T. foetus* has been proposed as a possible target for the design of chemotherapeutic agents against this parasite (Beck and Wang, 1993; Chin and Wang, 1994; Wang, *et al.*, 1983). Kinetic analyses of both the parasitic HGXPRTase and the host HGPRTase are necessary to elucidate any differences in the catalytic mechanism that may exist and may be exploited to design specific inhibitors to the parasitic enzyme. The cDNA encoding the HGXPRTase of *T. foetus* has been expressed in *Escherichia coli* (Chin and Wang, 1994), allowing large quantities of the enzyme to be available for kinetic studies with hypoxanthine, guanine and xanthine and also product inhibition studies in both the forward and reverse reactions. The model postulated from these studies is an ordered bi-bi mechanism where the first substrate bound is Mg_2PRPP and the last product released is the purine nucleotide.

MATERIALS AND METHODS

Materials

All reagents, including hypoxanthine, guanine, xanthine, IMP, GMP, XMP, pyrophosphate and the tetrasodium salt of PRPP, were purchased from Sigma Chemical Co. (St. Louis, MO), and of the highest purity available. Xanthine

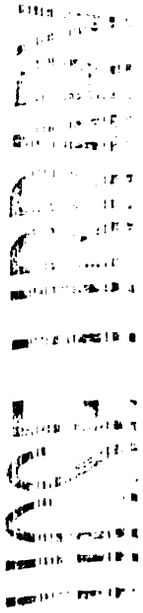

oxidase (20 U/ml) was from Boehringer Mannheim (Indianapolis, IN), and the guanase (0.85 U/ml) was from Sigma Chemical Co. (St. Louis, MO).

Enzyme purification

T. foetus HGXPRTase was purified as described in Chapter 2. After elution from the Mono P column, the HGXPRTase-containing fractions were pooled, dialyzed against storage buffer (50 mM Bis-Tris, pH 6.8, 6 mM $MgCl_2$ and 1 mM DTT) and stored in small aliquots at -80°C.

Enzyme assay

Kinetic data were collected using a Gilford Response 2 spectrophotometer (Ciba-Corning Geigy, Medfield, MA) equipped with a kinetics accessory. The formation of IMP and GMP were followed spectrophotometrically at 245 and 257.5 nm, respectively (Hill, 1970). The formation of XMP was followed spectrophotometrically at 247 nm, which is the wavelength where the difference in absorbance between XMP and xanthine is the largest. All measurements were carried out in 100 mM Tris-HCl, pH 7.0 and 12 mM $MgCl_2$ at 37°C. Under these conditions, the change in extinction coefficient for the formation of IMP from hypoxanthine, GMP from guanine and XMP from xanthine were 1250, 6410 and 5440 M^{-1} cm^{-1}, respectively. The final volume of the assay mixture, containing various amounts of substrates, was 350 µl.

IMP pyrophosphorolysis was monitored spectrophotometrically as described by Giacomello and Salerno (Giacomello and Salerno, 1978) and Yuan *et al.* (Yuan, *et al.*, 1992). The formation of hypoxanthine was monitored indirectly by the continuous spectrophotometric assay of uric acid production in the presence of 0.02 U/ml xanthine oxidase. The reaction was initiated by the addition of the purified HGXPRTase, and the formation of uric acid was monitored at 293 nm. A molar extinction coefficient of 12,000 M^{-1} cm^{-1} was used for uric acid at 293 nm

(Kalckar, 1947). XMP pyrophosphorolysis was also followed by the continuous spectrophotometric assay of uric acid formation from xanthine in the presence of 0.02 U/ml xanthine oxidase. The formation of guanine from GMP was determined by observing uric acid formation in the presence of both guanase (0.01 U/ml) and xanthine oxidase (0.02 U/ml). Again, all measurements were carried out in 100 mM Tris-HCl, pH 7.0, and 12 mM $MgCl_2$ at 37°C. Data are averaged from five independent determinations.

In determining the initial velocities for the forward reaction, the concentration of hypoxanthine varied between 2-30 μM; the concentration of guanine varied between 1-30 μM; the concentration of xanthine varied between 5-200 μM; and the concentration of Mg_2PRPP ranged between 20-1000 μM. In the reverse reactions, the concentration of MgIMP varied from 1-100 μM; the concentration of MgGMP varied from 75-1000 μM; the concentration of MgXMP varied from 5-150 μM; and the concentration of $MgPP_i$ ranged from 100-2000 μM.

Work by Salerno and Giacomello (Salerno and Giacomello, 1981) have demonstrated that the actual substrates of HGPRTase are the dimagnesium salt of PRPP (Mg_2PRPP) and monomagnesium complexes of IMP, GMP, XMP and PP_i (MgIMP, MgGMP, MgXMP, and $MgPP_i$, respectively). Assuming that hypoxanthine, guanine and xanthine do not form Mg^{2+} complexes, the concentrations of Mg_2PRPP, MgIMP, MgGMP, MgXMP, and $MgPP_i$ used in data analysis were calculated as described previously (Giacomello and Salerno, 1978; Salerno and Giacomello, 1981; Yuan, *et al.*, 1992).

Data analysis

Initial rate data were fitted to equations 1-3 using kinetics software from BioMetallics, Inc. (K•CAT) and IntelliKinetics (KinetAsyst) with Gauss-Newton analysis.

For competitive inhibition

$$v = V_{max}S \ / \ [K_m (1 + I/K_{is}) + S \ ] \qquad (1)$$

For noncompetitive inhibition

$$v = V_{max}S \ / \ [K_m (1 + I/K_{is}) + S (1 + I/K_{ii})] \qquad (2)$$

For uncompetitive inhibition

$$v = V_{max}S \ / \ [K_m + S (1 + I/K_{ii})] \qquad (3)$$

The best fits were determined by the relative fit error and errors in the constants. The nomenclature is that of Cleland (Cleland, 1963): v, initial velocity; V_{max}, maximum velocity; S, substrate concentration; K_m, apparent Michaelis constant; K_{is} and K_{ii}, slope and intercept inhibition constants, respectively; I, inhibitor concentration.

RESULTS AND DISCUSSION

Purification of the recombinant *T. foetus* HGXPRTase has been reported in Chapter 2. The purified enzyme appears to be stable at -80°C for at least six months.

The steady-state kinetics of synthesis and pyrophosphorolysis of IMP, GMP and XMP and the product inhibitions of these reactions were analyzed to determine the order of substrate binding and product release. Initial rates of these reactions were proportional to enzyme concentration, and substrate inhibition was not observed under these conditions (data not shown).

Steady-state kinetics

The first step in elucidating the mechanism of a multiple substrate enzyme-catalyzed reaction is the use of initial velocity experiments to determine if the reaction proceeds by a ping pong or a sequential mechanism. An enzyme follows a ping pong mechanism if a product is released between the addition of

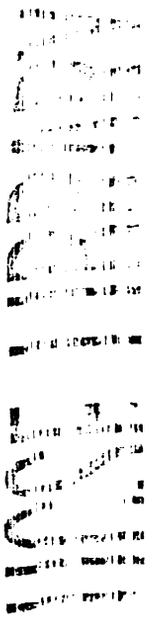

two substrates (Segel, 1975), and the scheme is shown below using Cleland's notation.

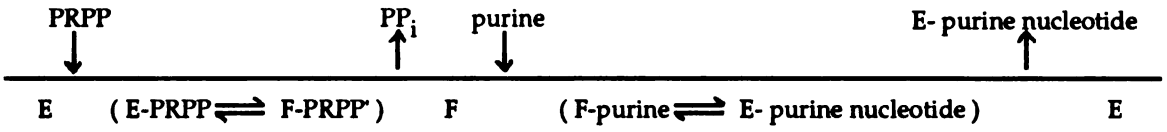

Scheme 1

In this mechanism the enzyme exists in two stable forms unassociated with substrates or products, E, F. Double-reciprocal plots obtained for an enzyme-catalyzed reaction which follows a ping pong mechanism are characterized by the patterns of parallel lines. Examples of PRTases following a ping pong mechanism include the human APRTase (Srivastava and Beutler, 1971; Thomas, *et al.*, 1973), yeast OPRTase (Victor, *et al.*, 1979) and yeast UPRTase (Natalini, *et al.*, 1979). If, instead, an enzyme follows a sequential mechanism, all substrates must bind to the enzyme, forming a ternary complex, prior to any product release (Segel, 1975) (see schemes 2 and 3).

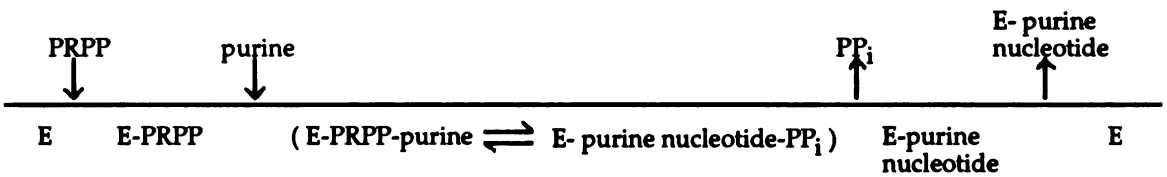

Scheme 2

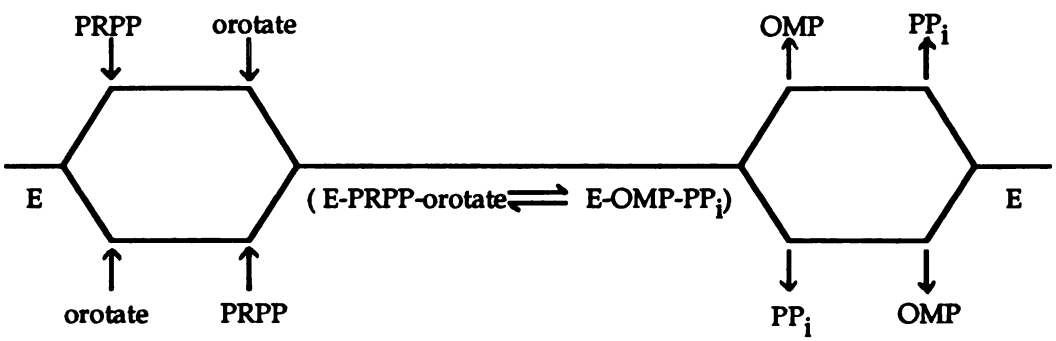

Scheme 3

In these mechanisms the enzyme exists in only one stable form, E. Characteristic double-reciprocal plots observed for an enzyme-catalyzed reaction following a

sequential mechanism are the pattern of lines converging to the left of the 1/V axis. Examples of PRTases following a sequential mechanism include the schistosomal HGPRTase (Yuan, *et al.*, 1992), the yeast HGPRTase (Ali and Sloan, 1982), the human HGPRTase (Giacomello and Salerno, 1978) and the *Salmonella typhimurium* OPRTase (Bhatia, *et al.*, 1990).

Double-reciprocal plots of initial velocity versus the concentration of one substrate at a series of fixed concentration of the other, for both forward (Figs. 3.2-3.4) and reverse reactions (Figs. 3.5-3.7) of the *T. foetus* HGXPRTase, give a family of converging straight lines (Figs. 3.2-3.13). Plots of the data for the forward reactions show lines intersecting below the 1/[S] axis, which would be characteristic of either a ping-pong or a sequential mechanism (Figs. 3.2-3.4). However, the plots of the data for the reverse reactions clearly indicate a sequential mechanism since these plots also show intersecting lines, with the point of intersection occurring above the 1/[S] axis for most of the plots (Figs. 3.5-3.7).

Using the method of Ainsworth (Ainsworth, 1977), the Michaelis constant (K_m) and dissociation constant (K_S) for the substrates and products were calculated from secondary plots of the initial velocity experiments and are listed in Table 3.1. The results indicate that the *T. foetus* HGXPRTase favors hypoxanthine and guanine over xanthine, with the former two equally favored as substrates. This is consistent with earlier results of Beck and Wang (Beck and Wang, 1993). The enzyme may not bind xanthine as well as hypoxanthine and guanine as indicated by the K_m values for hypoxanthine, guanine and xanthine, which are 1.0 ± 0.3 μM, 1.8 ± 0.1 μM and 31.2 ± 4.9 μM, respectively. The Vmax values are 22.2, 6.9 and 20.5 μmol/min-mg protein for hypoxanthine, guanine and xanthine, respectively.

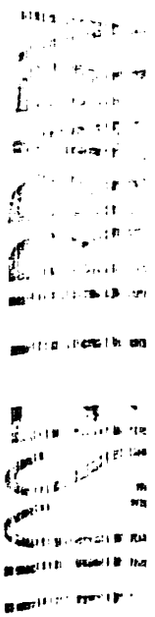

Comparison of the K_m values obtained for the *T. foetus* enzyme with the K_m values of other HGPRTases is shown in Table 3.2. The values for the K_m of $MgPP_i$ for the schistosomal and human enzymes are of the same order of magnitude as their K_m values for Mg_2PRPP (Giacomello and Salerno, 1978; Yuan, *et al.*, 1992). However, the values of the K_m of $MgPP_i$ for the *T. foetus* HGXPRTase (500 μM, 422.5 μM and 5070 μM) are at least ten-fold larger than the K_m values for Mg_2PRPP (43.5 μM, 55.6 μM and 111.1 μM). Thus, it appears that $MgPP_i$ may not bind as well to the *T. foetus* enzyme as compared to the purine bases or to Mg_2PRPP. Since PP_i serves as a high energy compound in *T. foetus*, the weak binding of $MgPP_i$ to HGXPRTase would allow PP_i to be available for reactions that are coupled to the consumption of a high energy compound, such as the glycolytic reaction, mediated by PP_i-dependent phosphofructokinase (Mertens, *et al.*, 1989; Müller, 1992). One can speculate that this preference for binding substrates of the forward reaction is necessary to ensure that the purine salvaging activities of the enzyme are optimal, since HGXPRTase is the only purine salvaging enzyme in *T. foetus* (Wang, *et al.*, 1983). Consistent with this finding is the observation that the K_m value of MgGMP, is approximately 100-fold larger than the K_m value of guanine. Again, one could speculate that this would ensure that the forward reaction of the enzyme to be favorable. However, since the value of the K_m for MgIMP is of the same magnitude as the K_m for hypoxanthine, the K_m value for MgGMP needs to be reconfirmed before any conclusions can be made.

Product inhibition

Cleland has formulated a set of rules for predicting the type of inhibition a compound exerts on an enzymatic reaction as a function of a given substrate (Cleland, 1977). The rules are as follows: An inhibitor is competitive if it binds reversibly to the same enzyme form (or different forms connected by a series of

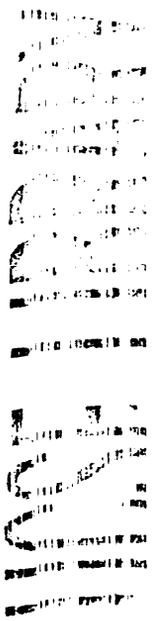

reversible steps) that binds the variable substrate. In this case, the inhibitor only affects the slope of a double reciprocal plot. An inhibitor is uncompetitive, if it binds to an enzyme that is different from the form that binds the variable substrate. In this case, the inhibitor only affects the 1/V axis intercept of a double reciprocal plot. An inhibitor is noncompetitive if its binding affects the binding of the variable substrate, but it does not necessarily bind the same site in the enzyme as the substrate. In this case, the inhibitor affects both the slope and the 1/V axis intercept of a double reciprocal plot.

In order to identify whether the sequential mechanism is ordered or random, product inhibition was analyzed for the phosphoribosyltransferase and the pyrophosphorolysis reactions. $MgPP_i$ was noncompetitive with respect to both hypoxanthine (Fig. 3.8a) and Mg_2PRPP (Fig. 3.8b), while MgIMP, the second product, is noncompetitive with respect to hypoxanthine (Fig. 3.9a) but competitive with respect to Mg_2PRPP (Fig. 3.9b). Likewise, $MgPP_i$ is noncompetitive with respect to both guanine (Fig. 3.11a) and Mg_2PRPP (Fig. 3.11b), while MgGMP, the second product is, noncompetitive with respect to guanine (Fig. 3.12a) but competitive with respect to Mg_2PRPP (Fig. 3.12b). Product inhibition studies of XMP synthesis and XMP pyrophosphorolysis were not measurable due to the insolubility of $MgPP_i$ at high concentrations. However, in agreement with the previous results, MgXMP is noncompetitive with respect to xanthine (Fig. 3.13a), but competitive with respect to Mg_2PRPP (Fig. 3.13b). Results of product inhibition studies of the pyrophosphorolysis reaction agree with the product inhibition studies of the phosphoribosyltransferase reaction. Mg_2PRPP is competitive with respect to MgIMP (Fig. 3.10a) and MgXMP (Fig. 3.14a), but noncompetitive with respect to $MgPP_i$ (Fig. 3.10b and Fig. 3.14b). The product inhibition patterns, K_{ii} and K_{is} values are listed in Table 3.3. Product inhibition studies of the GMP

pyrophosphorolysis reaction could not be measured due to a contamination of the guanase with 5'-nucleotidase and purine nucleotide phosphorylase (data not shown). Product inhibition studies of the pyrophosphorolysis reaction using hypoxanthine, guanine and xanthine could not be examined due to the presence of xanthine oxidase and guanase activities. Product inhibition studies with saturating concentrations of the substrates were hampered by the insolubilities of the bases and the high UV absorbance of these compounds at the wavelengths used to monitor the reactions.

The results of the product inhibition studies of the *T. foetus* HGXPRTase indicate that the Mg-complexed purine nucleotides are competitive with respect to Mg_2PRPP, and when the reaction is reversed, Mg_2PRPP is competitive with respect to the Mg-complexed purine nucleotides. All other product inhibition patterns were noncompetitive. Thus, Mg_2PRPP and the Mg-complexed purine nucleotides bind to the same enzyme form; consequently, the minimum kinetic model that describes the experimental data is an ordered bi-bi mechanism. Since the only times that the same form of the enzyme exists is prior to binding the first substrate and after release of the last product, Mg_2PRPP must bind the enzyme first and the Mg-complexed purine nucleotides must be released last. Scheme 4 shows the proposed mechanism for the *T. foetus* HGXPRTase.

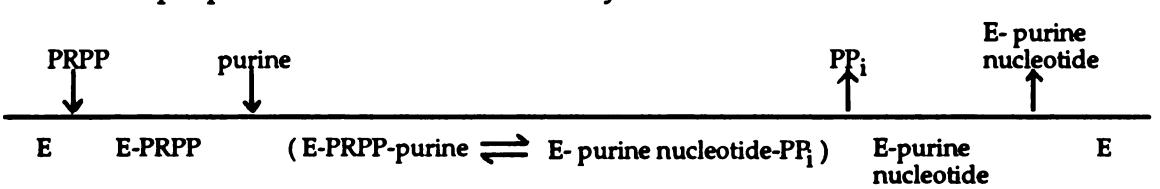

Scheme 4

The kinetic mechanism of a few PRTases have been presented (see scheme 1, 2 and 3). The product inhibition patterns of a few of them are presented in Table 3.4. Both the yeast and *S. mansoni* HGPRTase appear to follow an ordered bi-bi mechanism (Ali and Sloan, 1982; Yuan, *et al.*, 1992). Flow dialysis experiments of

the yeast HGPRTase identified the E-PRPP complex, but no enzyme complexes with the purine bases were detected (Ali and Sloan, 1982) which supports the ordered bi-bi model. The only mammalian HGPRTase that has undergone extensive kinetic analyses is the human enzyme which has an ordered bi rapid equilibrium random bi mechanism (scheme 5). This model is supported by the initial rate measurements of the forward and reverse reactions (Giacomello and Salerno, 1978), product inhibition and isotope exchange studies (Henderson, *et al.*, 1968).

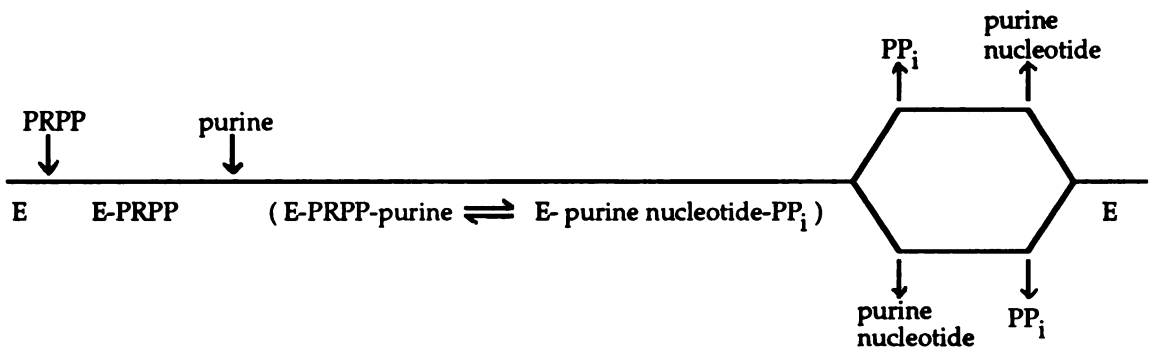

Scheme 5

Thus, the difference between the *T. foetus* HGXPRTase and the human HGPRTase kinetic mechanisms lies in the release of the products. Discrete binary complexes of the *T. foetus* HGXPRTase with PRPP or purine nucleotides must exist, and it should be possible to design inhibitors which bind specifically to either of these forms. Inhibitors which only bind to the E-purine nucleotide forms should have higher specificity for the *T. foetus* HGXPRTase than for an enzyme which follows a mechanism of random product release, such as the human enzyme. Substrate recognition is also a factor which can aid in inhibitor design, since the *T. foetus* HGXPRTase uses xanthine, as well as hypoxanthine and guanine. Inhibitors based on the structure of xanthine or XMP would selectively bind to the *T. foetus* enzyme rather than to the mammalian enzymes. Further work will be needed to confirm the results for the *T. foetus* HGXPRTase,

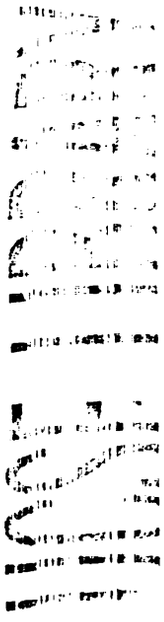

Table 3.1: Kinetic Constants for the *T. foetus* HGXPRTase

	K_m (μM)	K_S (μM)
(A) HPRTase		
Mg_2PRPP	43.5 ± 15.1	59.9 ± 29.2
hypoxanthine	1.0 ± 0.3	5.8 ± 1.6
$MgPP_i$	500.0 ± 33.0	2500 ± 400
MgIMP	1.1 ± 0.4	5.4 ± 0.9
(B) GPRTase		
Mg_2PRPP	55.6 ± 6.2	22.3 ± 4.1
guanine	1.8 ± 0.1	1.5 ± 0.2
$MgPP_i$	303.9 ± 62.5	1700 ± 1300
MgGMP	199 ± 352	624 ± 147
(C) XPRTase		
Mg_2PRPP	111.1 ± 25	23.5 ± 9.9
xanthine	31.2 ± 4.9	9.8 ± 2.4
$MgPP_i$	5070 ± 190	5100 ± 200
MgXMP	52.6 ± 16.6	30.9 ± 2.1

Table 3.2. Comparison of K_m values for HGPRTases

Forward Reaction

	K_m(hypoxanthine)	K_m (guanine)	K_m (xanthine)	K_m (Mg_2PRPP)
T. foetus	1.0 ± 0.3 μM	1.8 ± 0.1 μM	31.2 ± 4.9 μM	(H) 43.5 ± 15.1 μM (G) 55.6 ± 6.2 μM (X) 111.1 ± 24.7 μM
Human (Giacomello and Salerno, 1978)	7.7 ± 0.4 μM	----------	----------	(H) 66 ± 2.0 μM
S. mansoni (Yuan, *et al.*, 1992)	5.4 ± 0.2 μM	3.0 ± 0.2 μM	----------	(H) 9.3 ± 1.1 μM (G) 18.2 ± 1.3 μM
**P. falciparum* (Queen, *et al.*, 1988)	0.46 ± 0.007 μM	0.3 ± 0.07 μM	29 ± 7.7 μM	(H) 20.7 ± 6.3 μM (G) 21.4 ± 8.1 μM (X) 13.3 ± 6.1 μM
**T. gondi* (Maion and Chamberland, 1992)	8.8 μM	19.1 μM	21.2 μM	----------
**T. brucei* (Allen and Ullman, 1993)	2.3 μM	4.8 μM	----------	----------
**T. cruzi* (Allen and Ullman, 1994)	6.4 ± 0.3 μM	9.9 ± 0.29 μM	----------	----------

Reverse Reaction

	K_m (MgIMP)	K_m (MgGMP)	K_m (MgXMP)	K_m ($MgPP_i$)
T. foetus	1.1 ± 0.4 μM	199 ± 352 μM	52.6 ± 16.6 μM	(MgIMP) 500 ± 33 μM (MgGMP) 303.9 ± 62.5 μM (MgXMP) 5070 ± 190 μM
Human (Giacomello and Salerno, 1978)	5.8 ± 0.2 μM	----------	----------	(MgIMP) 39 ± 6 μM
S. mansoni (Yuan, *et al.*, 1992)	5.7 ± 0.4 μM	8.4 ± 0.8 μM	----------	(MgIMP) 22.7 ± 0.5 μM (MgGMP) 25.6 ± 1.3 μM

* = $K_{m'}$ apparent not true K_m values.

Table 3.3. Product Inhibition of *T. foetus* HGXPRTase

inhibitor	varied substrate	fixed substrate (μM)	pattern type	Kii	Kis
(A) HPRTase					
$MgPP_i$	Mg_2PRPP	hypoxanthine (20)	NC	13.2 ± 26.9 mM	1.7 ± 0.3 mM
$MgPP_i$	hypoxanthine	Mg_2PRPP (1000)	NC	89.3 ± 70 μM	22.5 ± 8.4 μM
MgIMP	Mg_2PRPP	hypoxanthine (20)	C	------	7.6 ± 0.8 μM
MgIMP	hypoxanthine	Mg_2PRPP (1000)	NC	149.8 ± 46.5 μM	23.2 ± 1.5 μM
Mg_2PRPP	$MgPP_i$	MgIMP (10)	NC	171.5 ± 121.8 μM	165.6 ± 71.1 μM
Mg_2PRPP	MgIMP	Mg PP_i (1500)	C	------	3.3 ± 0.4 μM
hypoxanthine	$MgPP_i$	MgIMP	-------	------	------
hypoxanthine	MgIMP	$MgPP_i$	-------	------	------
(B) XPRTase					
$MgPP_i$	Mg_2PRPP	xanthine (250)	-------	------	------
$MgPP_i$	xanthine	Mg_2PRPP (1000)	-------	------	------
MgXMP	Mg_2PRPP	xanthine (250)	C	------	39.2 ± 2.8 μM
MgXMP	xanthine	Mg_2PRPP (1000)	NC	162.6 ± 61.1 μM	571.4 ± 828.2 μM
Mg_2PRPP	$MgPP_i$	MgXMP (600)	NC	125.6 ± 23.8 μM	294.5 ± 118.3 μM
Mg_2PRPP	MgXMP	$MgPP_i$	C	------	9.4 ± 0.8 μM
xanthine	$MgPP_i$	MgXMP	-------	------	------
xanthine	MgXMP	$MgPP_i$	-------	------	------
(C) GPRTase					
$MgPP_i$	Mg_2PRPP	guanine (50)	NC	1.2 ± 0.2 mM	0.9 ± 0.5 mM
$MgPP_i$	guanine	Mg_2PRPP (1000)	NC	2.0 ± 0.3 mM	6.2 ± 9.0 mM
MgGMP	Mg_2PRPP	guanine (50)	C	------	4.53 ± 0.5 μM
MgGMP	guanine	Mg_2PRPP (1000)	NC	40.9 ± 14.3 μM	283.2 ± 701 μM

Table 3.4. Product Inhibition Patterns.

Inhibitor	Substrate	Inhibition Type
S. typhimurium OPRTase (Bhatia, *et al.*, 1990)		
OMP	PRPP	C
OMP	orotate	C
PP_i	PRPP	C
PP_i	orotate	NC
orotate	PPi	NC
orotate	OMP	C
PRPP	PP_i	C
PRPP	OMP	C
Human HGPRTase (Giacomello and Salerno, 1978)		
MgIMP	Mg_2PRPP	C
MgIMP	hypoxanthine	NC
$MgPP_i$	Mg_2PRPP	C
$MgPP_i$	hypoxanthine	NC
Mg_2PRPP	$MgPP_i$	C
Mg_2PRPP	MgIMP	C
hypoxanthine	$MgPP_i$	----------
hypoxanthine	$MgPP_i$	----------
S. mansoni HGPRTase (Yuan, *et al.*, 1992)		
MgIMP	Mg_2PRPP	C
MgIMP	hypoxanthine	NC
$MgPP_i$	Mg_2PRPP	NC
$MgPP_i$	hypoxanthine	NC
Mg_2PRPP	$MgPP_i$	NC
Mg_2PRPP	MgIMP	C
hypoxanthine	$MgPP_i$	----------
hypoxanthine	$MgPP_i$	----------

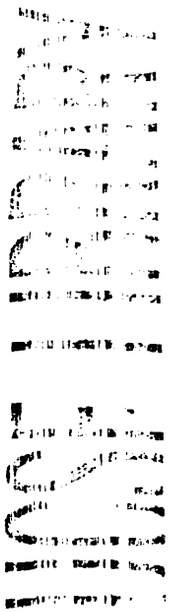

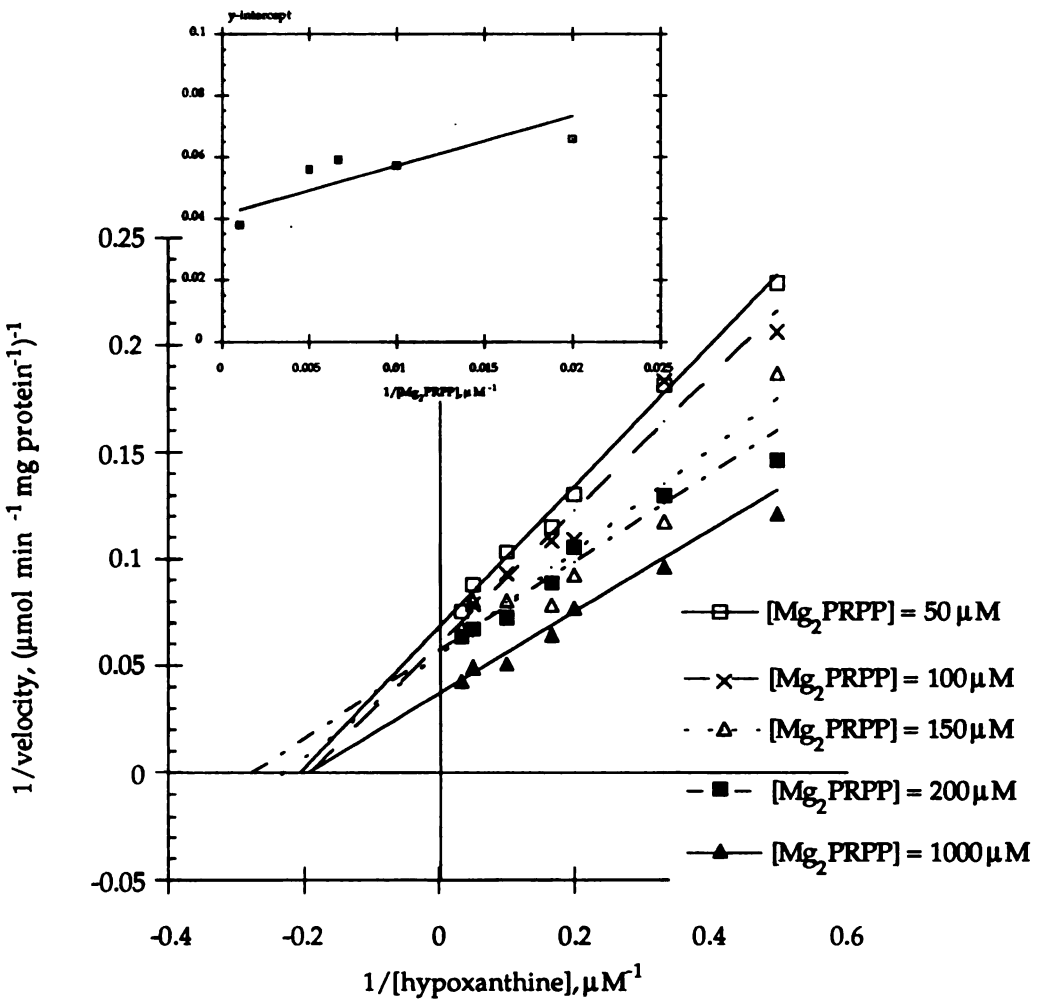

Figure 3.2a. Initial velocity pattern for the forward reaction with hypoxanthine as the variable substrate (2-30 μM) at different fixed concentrations of Mg_2PRPP (50-1000 μM). All conditions were as described under Materials and Methods. (Inset) Replot of $1/V_{max,\,app}$ (or y-intercept) with respect to 1/[Mg2PRPP].

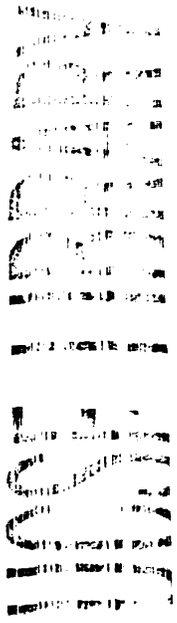

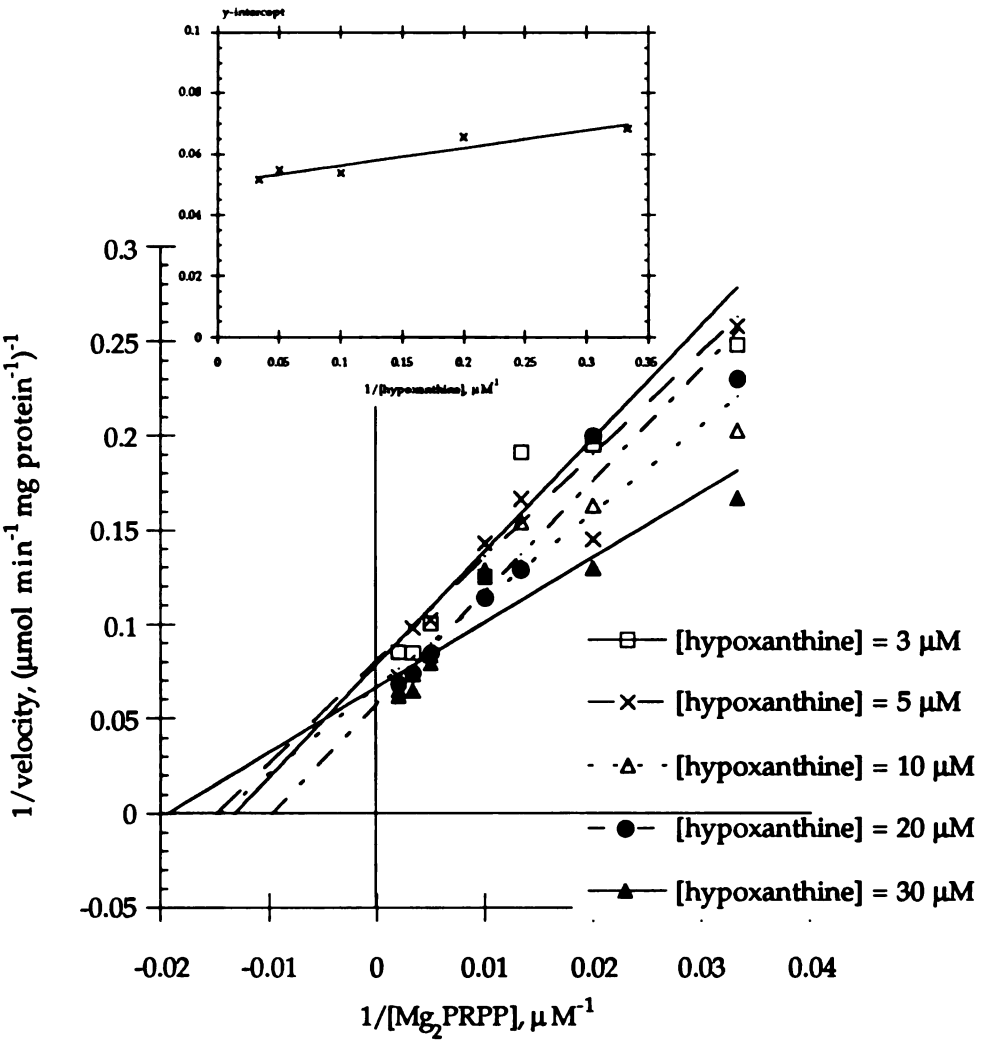

Figure 3.2b. Initial velocity pattern for the forward reaction with Mg_2PRPP as the variable substrate (30-500 μM) at different fixed concentrations of hypoxanthine (3-30 μM). All conditions were as described under Materials and Methods. (Inset) Replot of $1/V_{max,\ app}$ (or y-intercept) with respect to 1/[hypoxanthine].

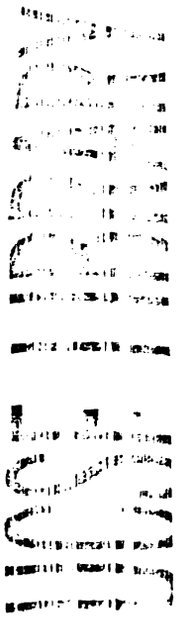

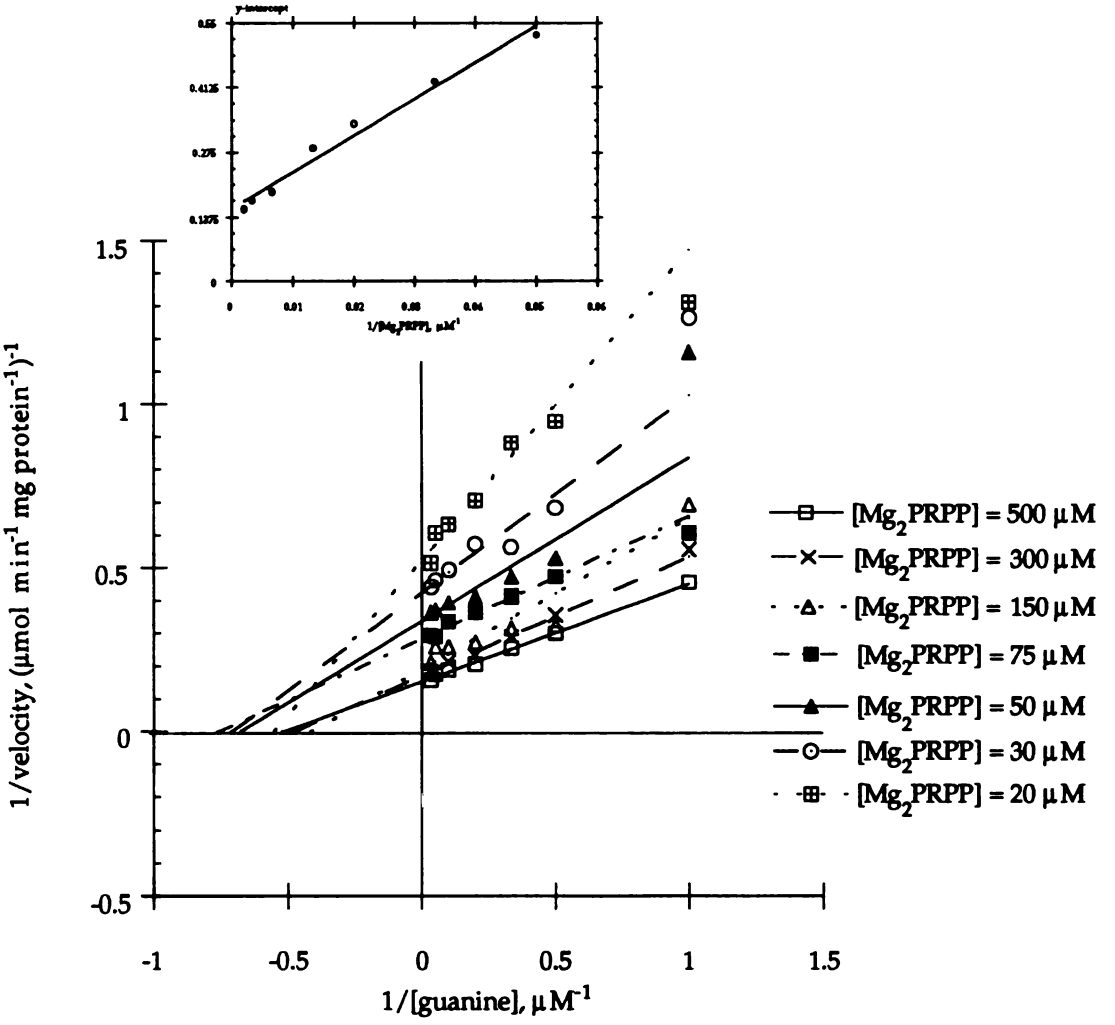

Figure 3.3a. Initial velocity pattern for the forward reaction with guanine as the variable substrate (1-30 μM) at different fixed concentrations of Mg_2PRPP (20-500 μM). All conditions were as described under Materials and Methods. (Inset) Replot of $1/V_{max,\,app}$ (or y-intercept) with respect to 1/[Mg2PRPP].

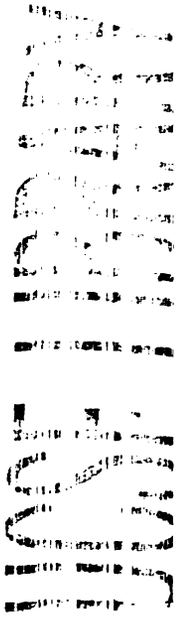

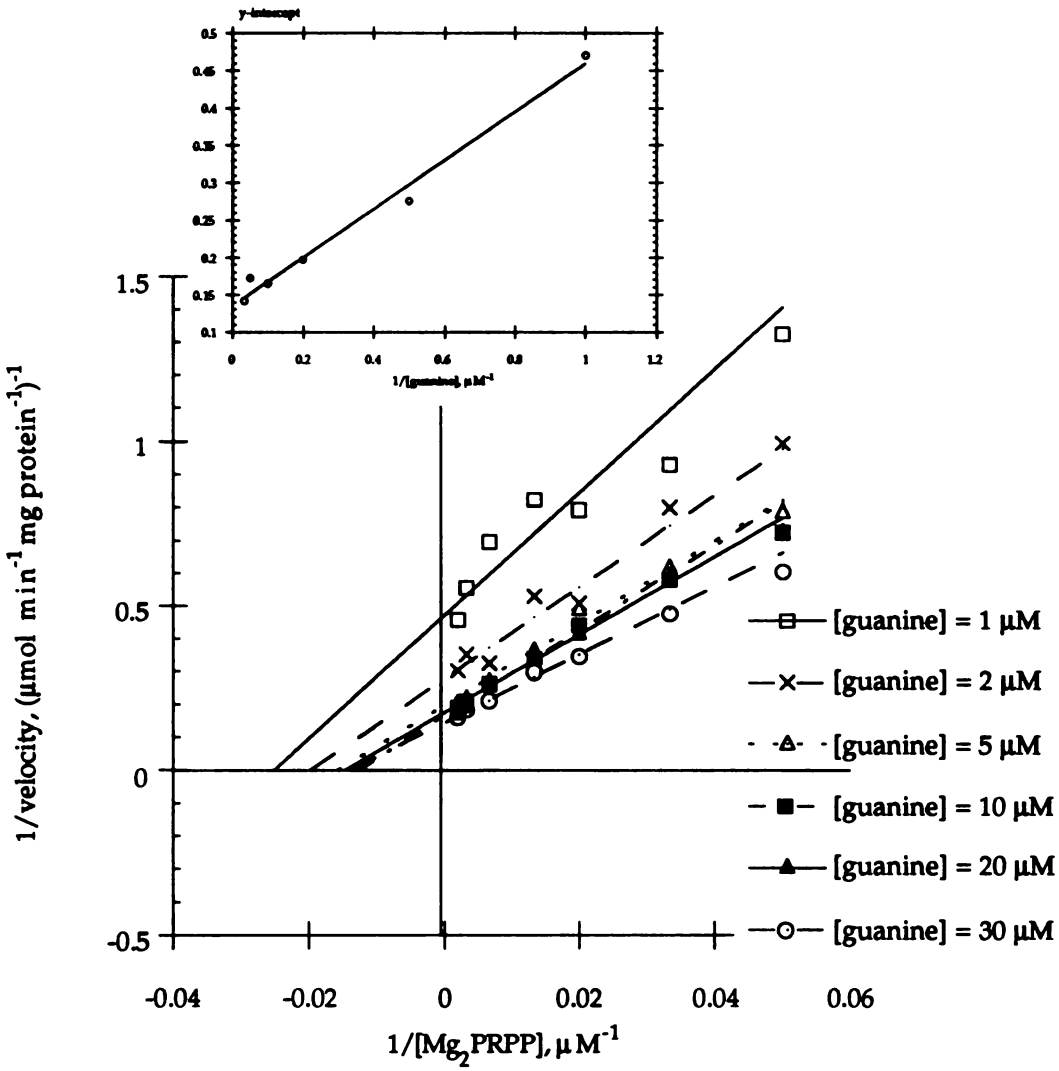

Figure 3.3b. Initial velocity pattern for the forward reaction with Mg_2PRPP as the variable substrate (20-500 μM) at different fixed concentrations of guanine (1-30 μM). All conditions were as described under Materials and Methods. (Inset) Replot of $1/V_{max,\,app}$ (or y-intercept) with respect to 1/[guanine].

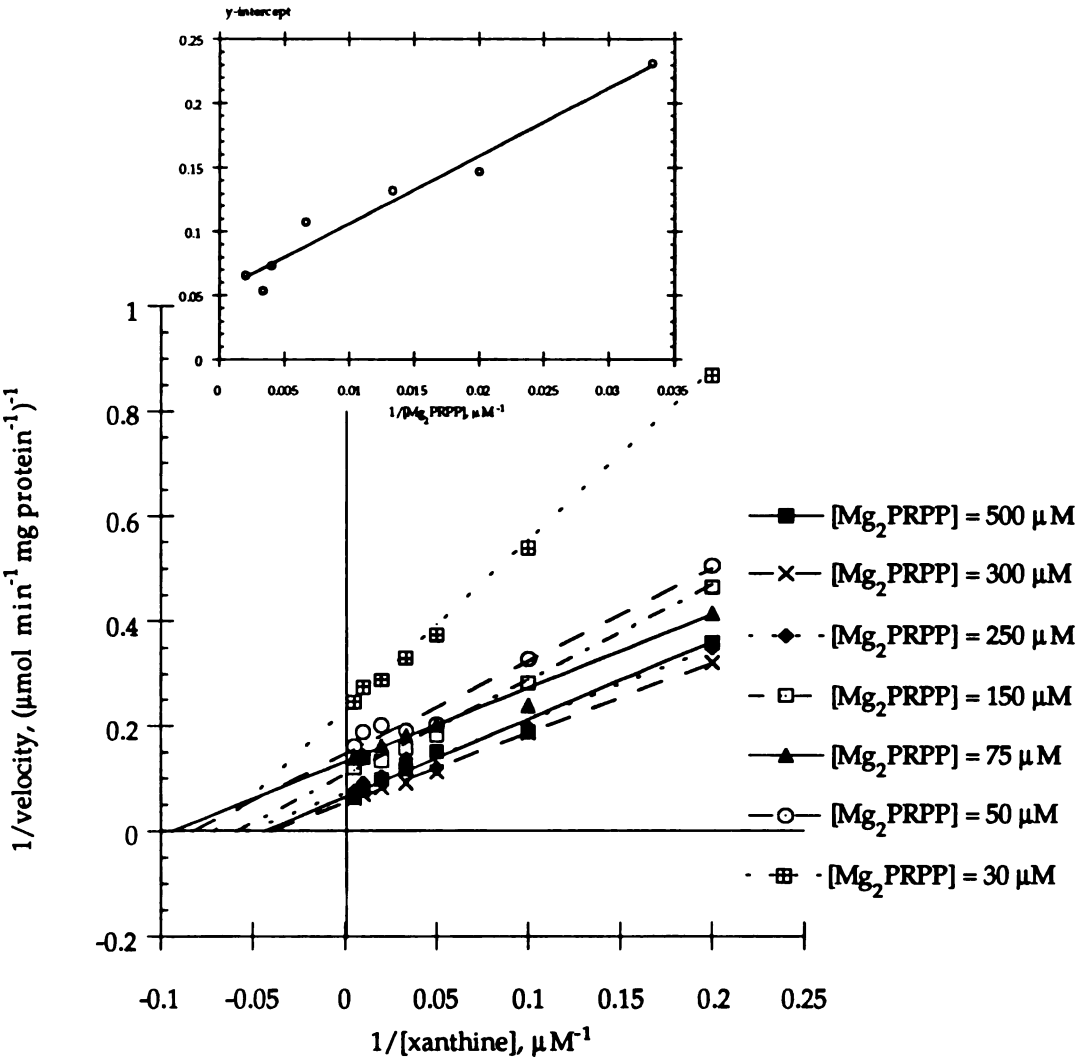

Figure 3.4a. Initial velocity pattern for the forward reaction with xanthine as the variable substrate (5-200 μM) at different fixed concentrations of Mg_2PRPP (30-500 μM). All conditions were as described under Materials and Methods. (Inset) Replot of $1/V_{max, app}$ (or y-intercept) with respect to 1/[Mg2PRPP].

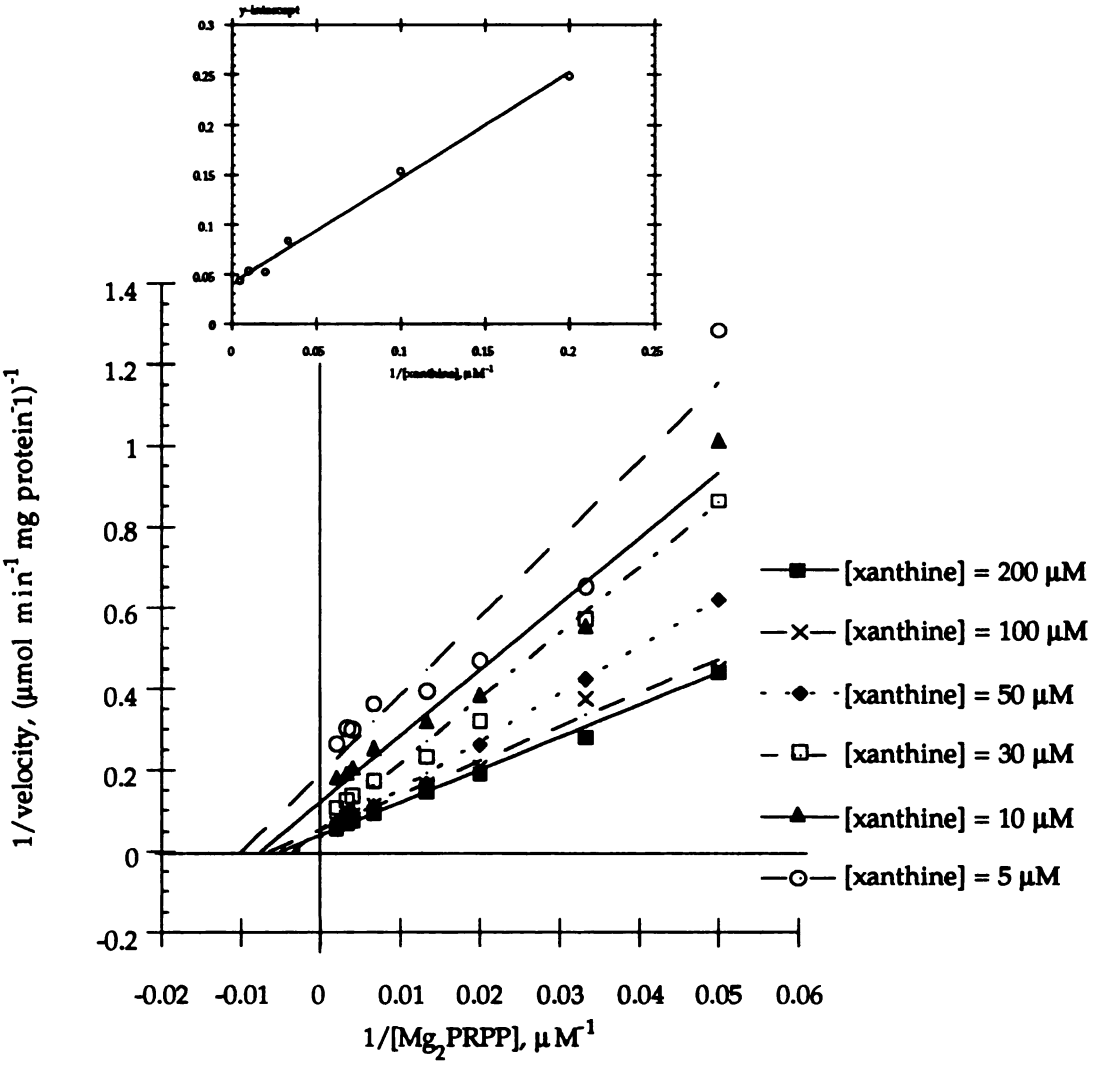

Figure 3.4b. Initial velocity pattern for the forward reaction with Mg_2PRPP as the variable substrate (20-500 µM) at different fixed concentrations of xanthine (5-200 µM). All conditions were as described under Materials and Methods. (Inset) Replot of $1/V_{max,\,app}$ (or y-intercept) with respect to 1/[xanthine].

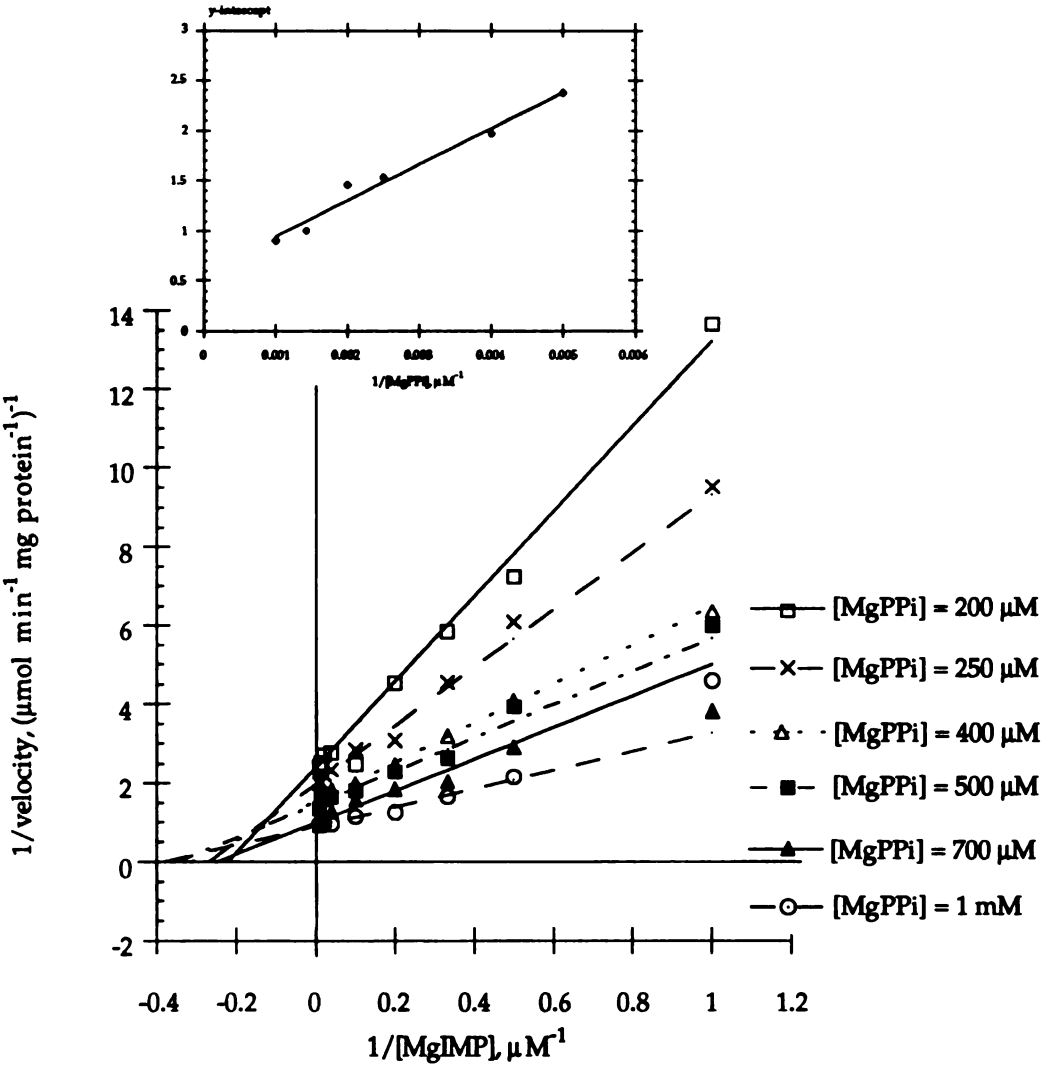

Figure 3.5a. Initial velocity pattern for the reverse reaction with MgIMP as the variable substrate (1-100 μM) at different fixed concentrations of $MgPP_i$ (200-1000 μM). All conditions were as described under Materials and Methods. (Inset) Replot of $1/V_{max,\,app}$ (or y-intercept) with respect to 1/[MgPPi].

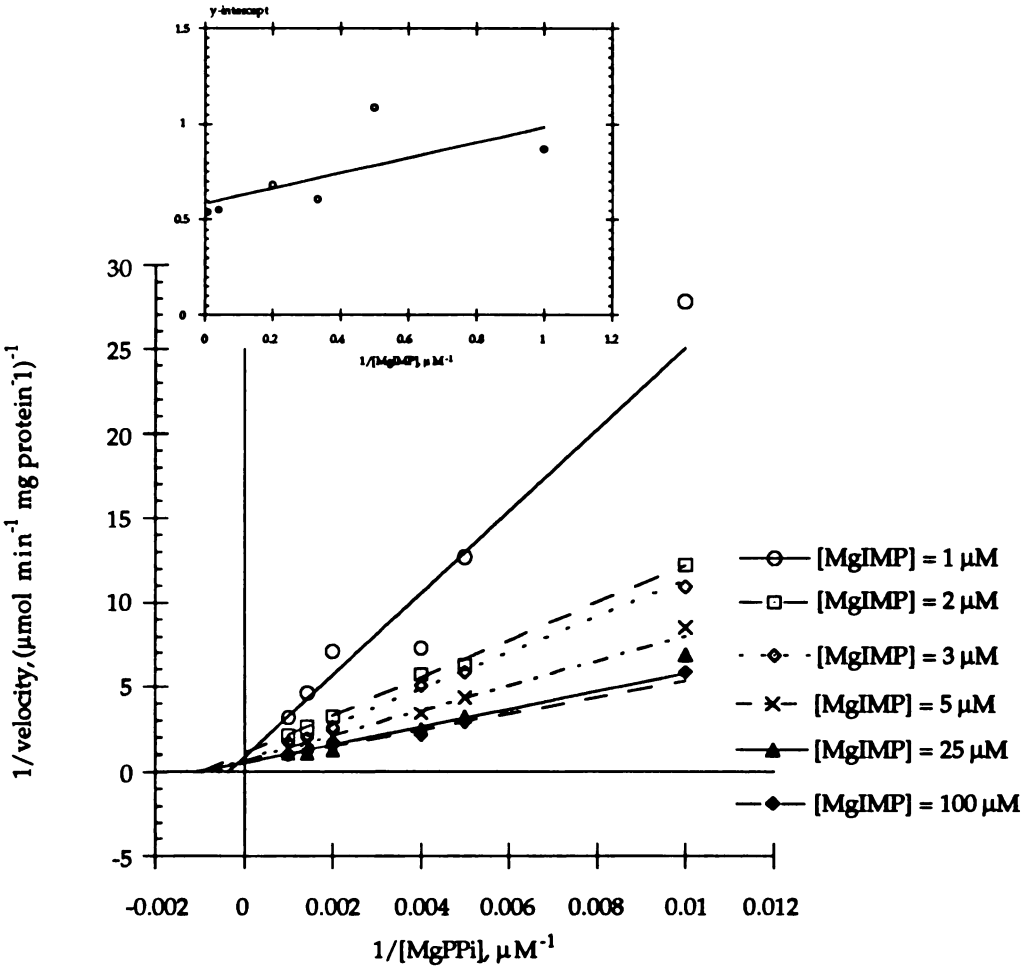

Figure 3.5b. Initial velocity pattern for the reverse reaction with $MgPP_i$ as the variable substrate (100-1000 μM) at different fixed concentrations of MgIMP (2-100 μM). All conditions were as described under Materials and Methods. (Inset) Replot of $1/V_{max,\,app}$ (or y-intercept) with respect to 1/[MgIMP].

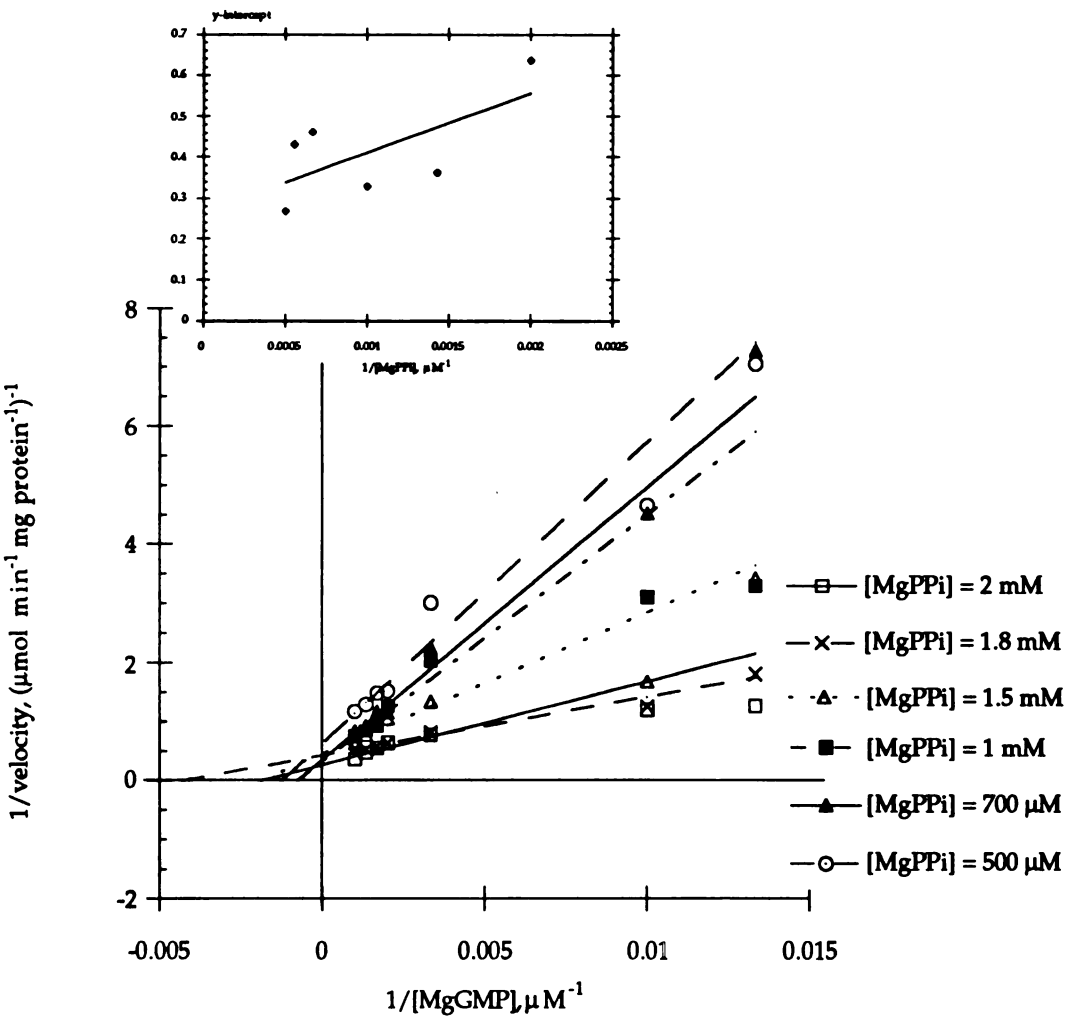

Figure 3.6a. Initial velocity pattern for the reverse reaction with MgGMP as the variable substrate (75-1000 μM) at different fixed concentrations of $MgPP_i$ (500-2000 μM). All conditions were as described under Materials and Methods. (Inset) Replot of $1/V_{max,\,app}$ (or y-intercept) with respect to 1/[MgPPi].

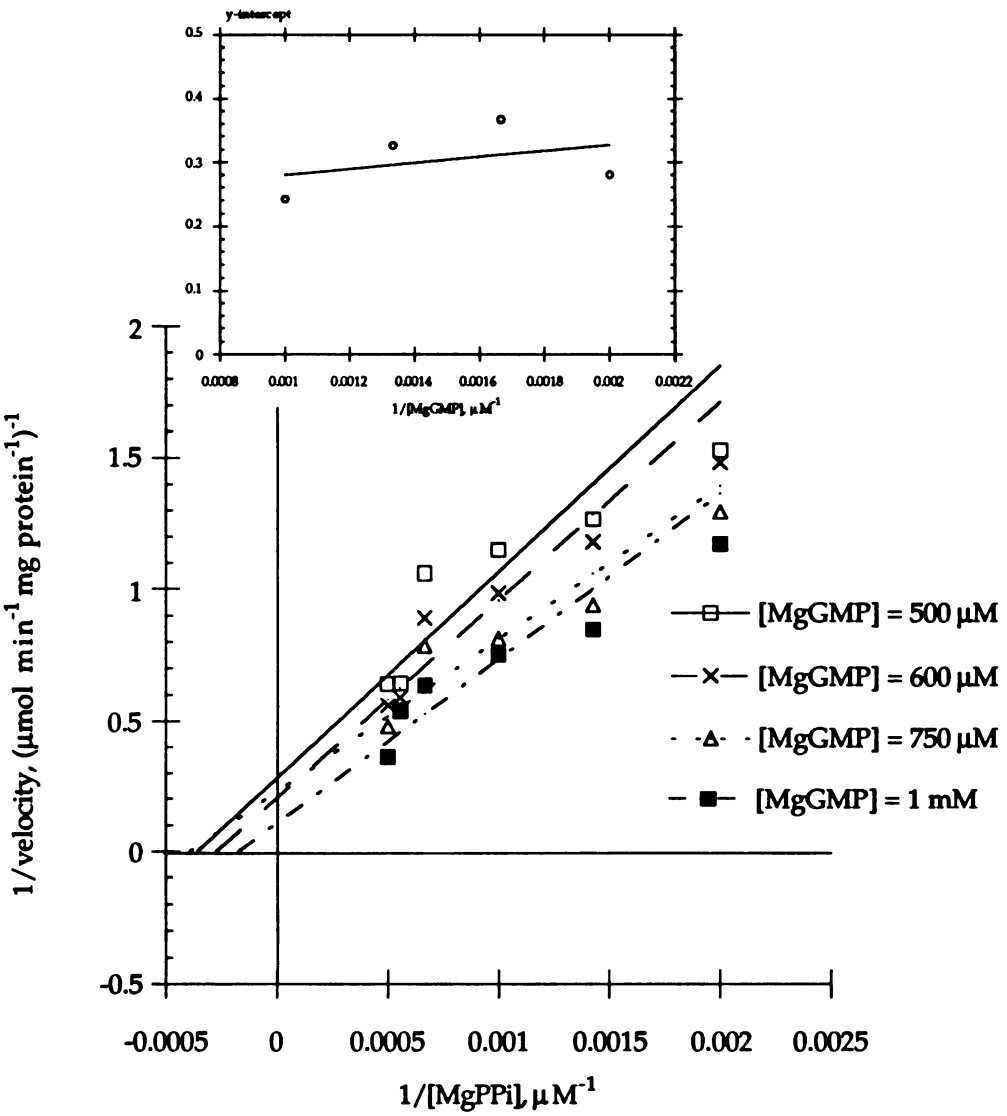

Figure 3.6b. Initial velocity pattern for the reverse reaction with $MgPP_i$ as the variable substrate (500-2000 μM) at different fixed concentrations of MgGMP (500-1000 μM). All conditions were as described under Materials and Methods. (Inset) Replot of $1/V_{max,\,app}$ (or y-intercept) with respect to 1/[MgGMP].

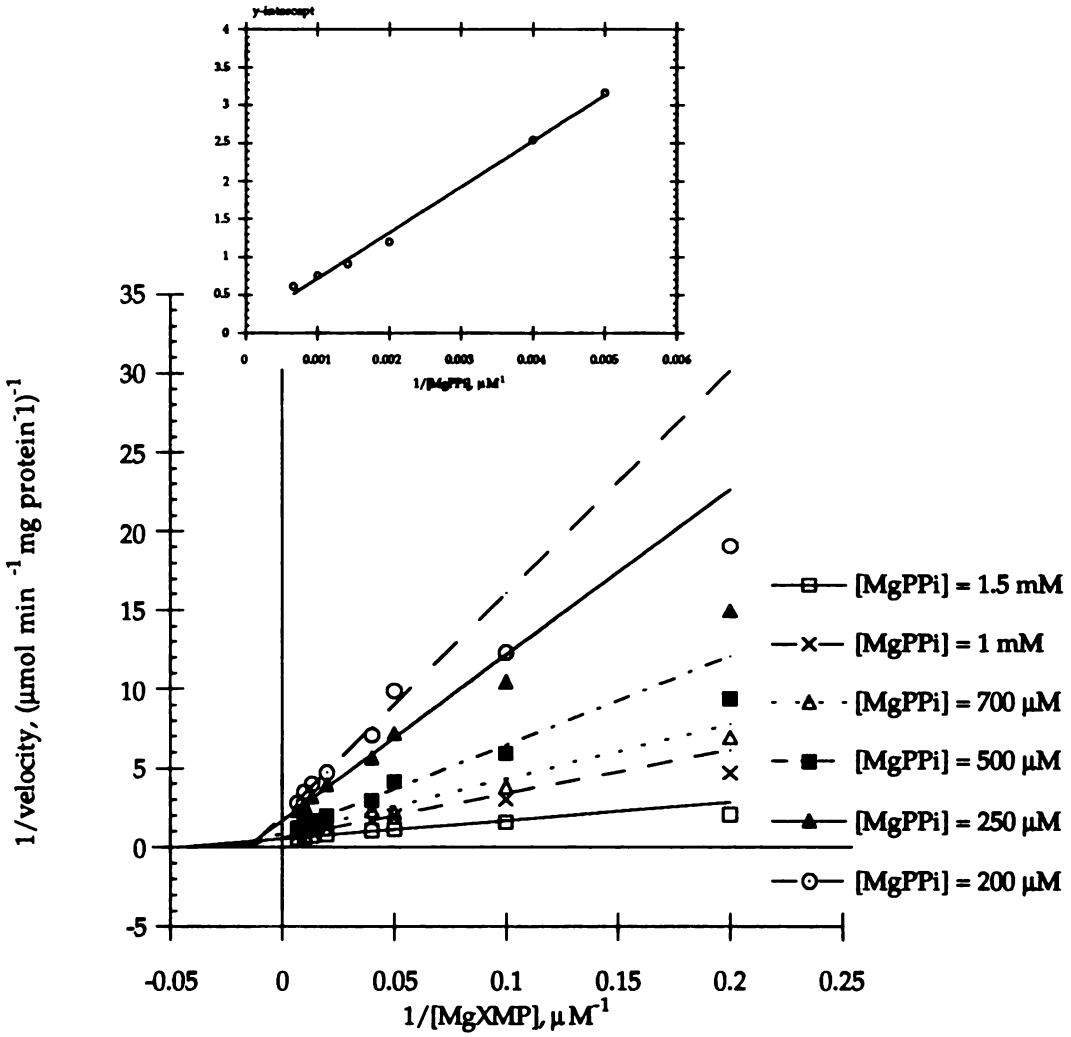

Figure 3.7a. Initial velocity pattern for the reverse reaction with MgXMP as the variable substrate (5-150 µM) at different fixed concentrations of $MgPP_i$ (200-1500 µM). All conditions were as described under Materials and Methods. (Inset) Replot of $1/V_{max,\,app}$ (or y-intercept) with respect to 1/[MgPPi].

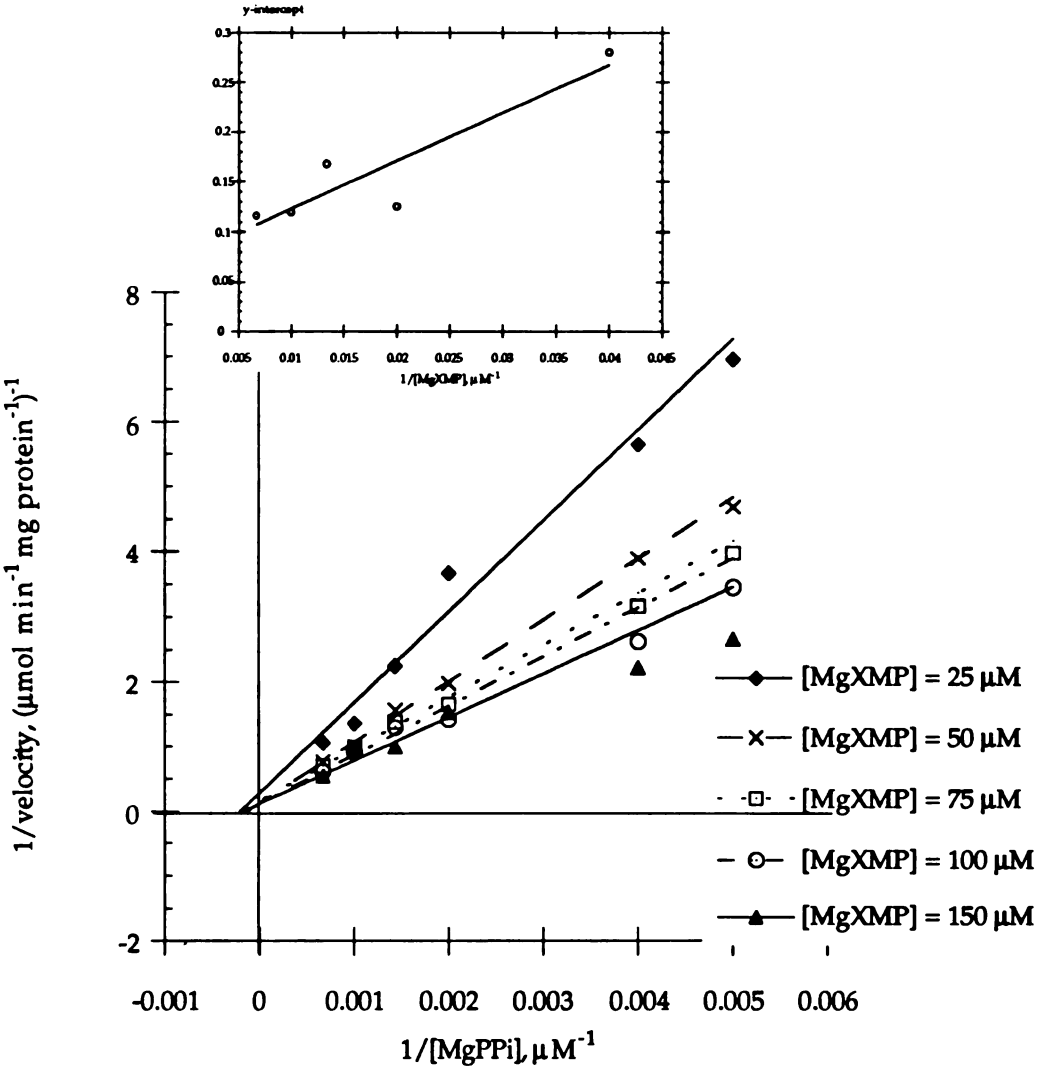

Figure 3.7b. Initial velocity pattern for the reverse reaction with $MgPP_i$ as the variable substrate (200-1500 μM) at different fixed concentrations of MgXMP (25-1500 μM). All conditions were as described under Materials and Methods. (Inset) Replot of $1/V_{max,\,app}$ (or y-intercept) with respect to 1/[MgXMP].

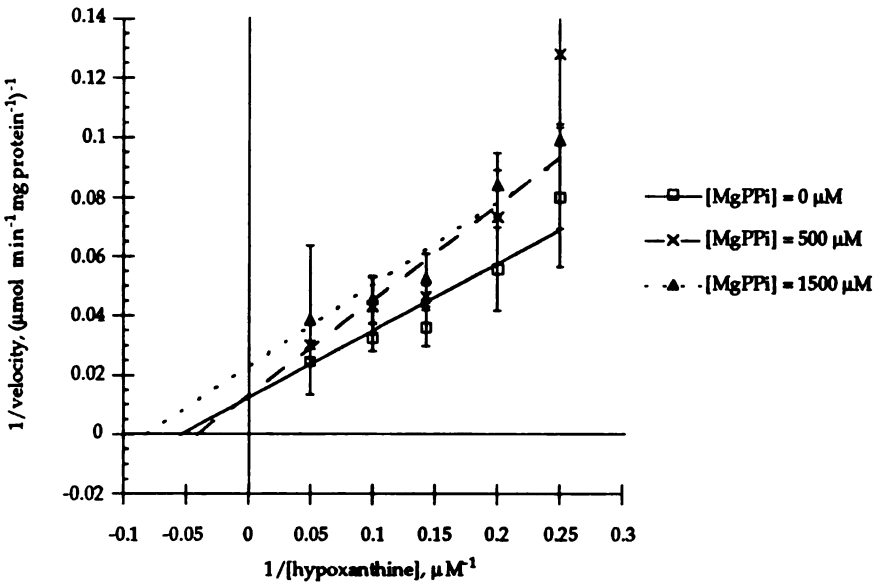

Figure 3.8a. Product inhibition by $MgPP_i$ on the reaction: hypoxanthine + $Mg_2PRPP \rightarrow MgIMP + MgPP_i$, with hypoxanthine as the variable substrate and with the concentration of Mg_2PRPP held constant at 1000 μM. All conditions were as described under Materials and Methods.

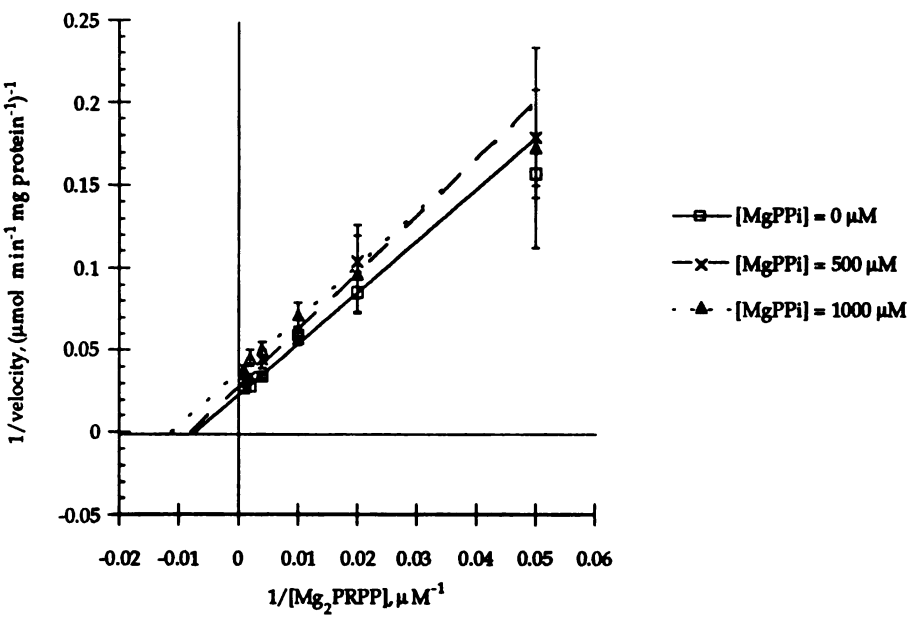

Figure 3.8b. Product inhibition by $MgPP_i$ on the reaction: hypoxanthine + $Mg_2PRPP \rightarrow MgIMP + MgPP_i$, with Mg_2PRPP as the variable substrate and with the concentration of hypoxanthine held constant at 20 μM. All conditions were as described under Materials and Methods.

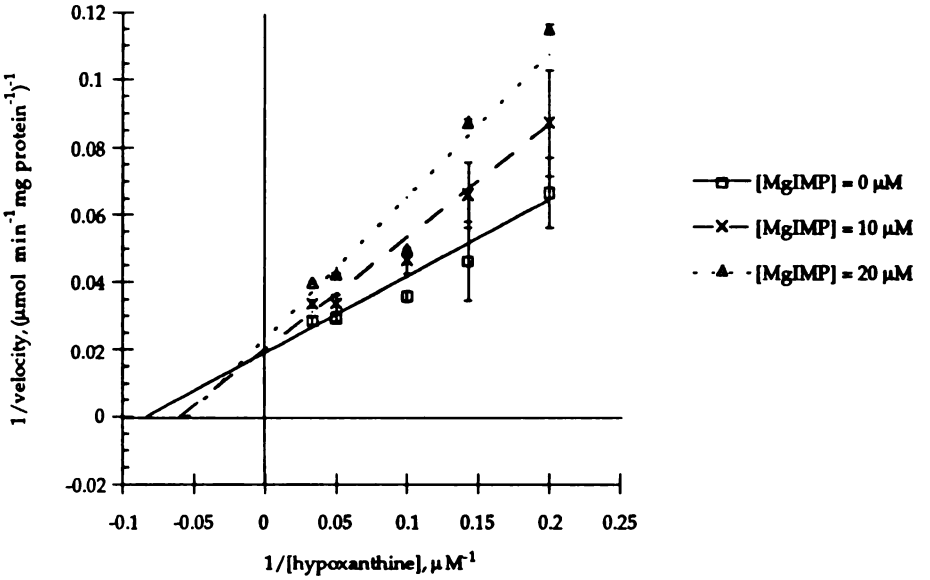

Figure 3.9a. Product inhibition by MgIMP on the reaction: hypoxanthine + $Mg_2PRPP \rightarrow$ MgIMP + $MgPP_i$, with hypoxanthine as the variable substrate and with the concentration of Mg_2PRPP held constant at 1000 μM. All conditions were as described under Materials and Methods.

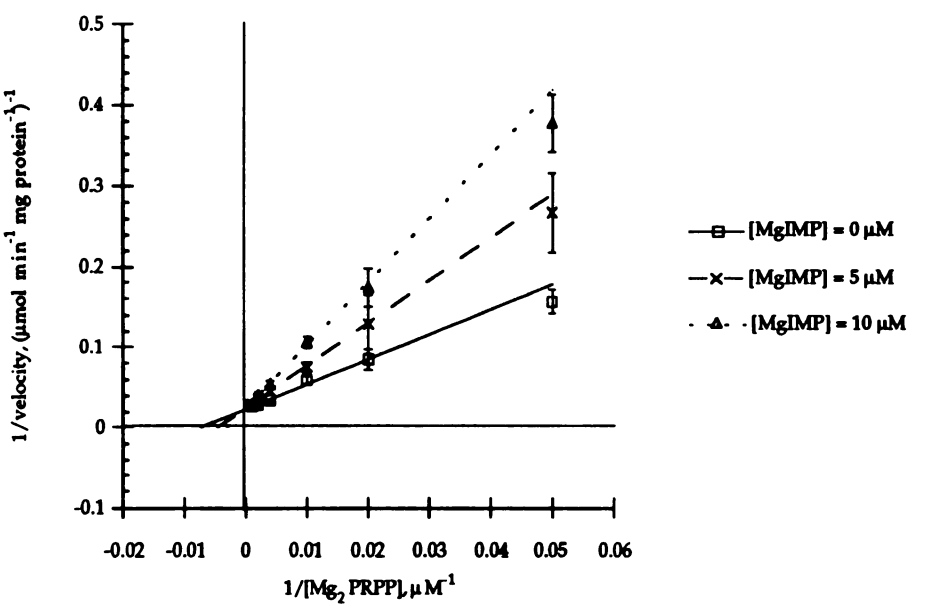

Figure 3.9b. Product inhibition by MgIMP on the reaction: hypoxanthine + $Mg_2PRPP \rightarrow$ MgIMP + $MgPP_i$, with Mg_2PRPP as the variable substrate and with the concentration of hypoxanthine held constant at 20 μM. All conditions were as described under Materials and Methods.

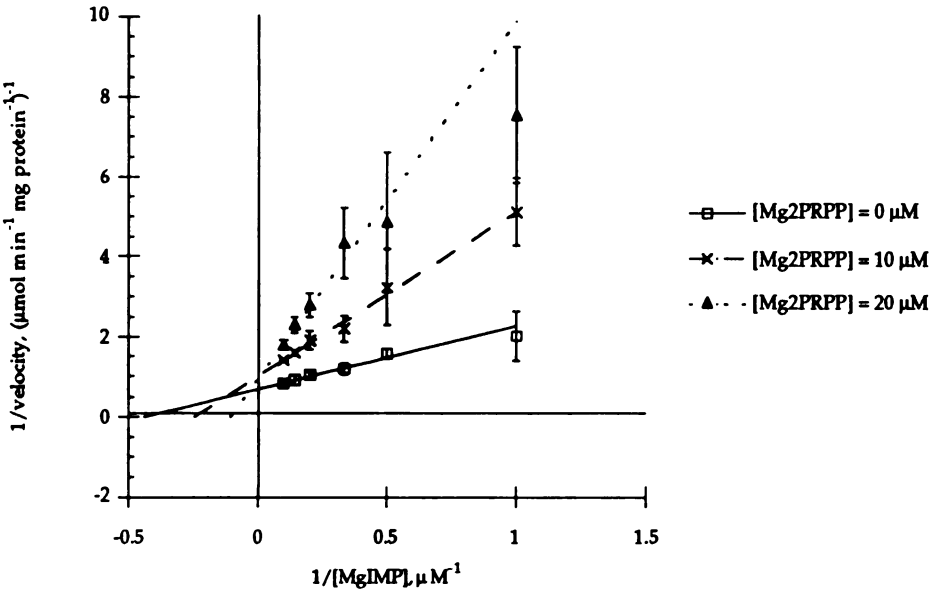

Figure 3.10a. Product inhibition by Mg_2PRPP on the reaction: MgIMP + $MgPP_i$ → hypoxanthine + Mg_2PRPP, with MgIMP as the variable substrate and with the concentration of $MgPP_i$ held constant at 1.5 mM. All conditions were as described under Materials and Methods.

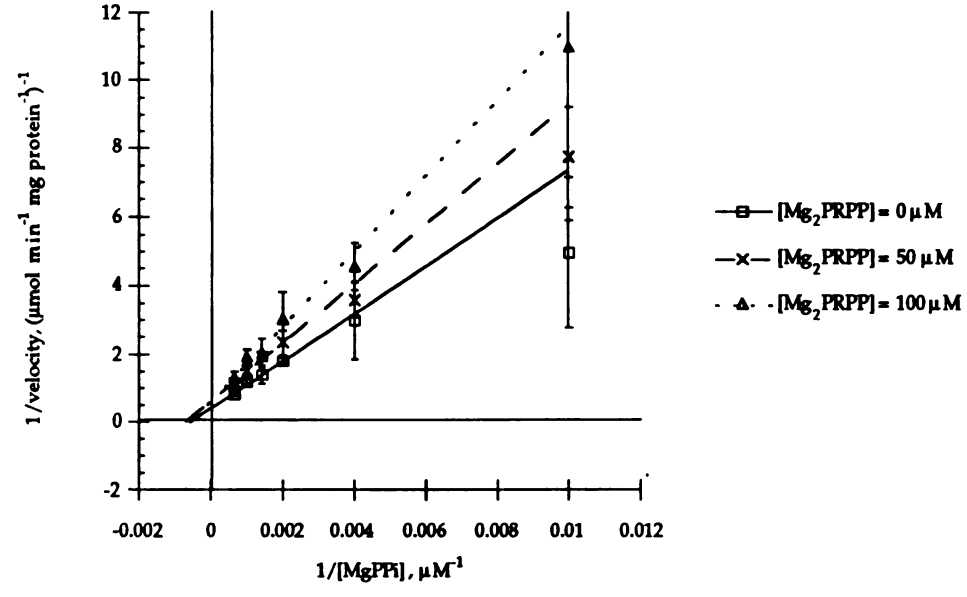

Figure 3.10b. Product inhibition by Mg_2PRPP on the reaction: MgIMP + $MgPP_i$ → hypoxanthine + Mg_2PRPP, with $MgPP_i$ as the variable substrate and with the concentration of MgIMP held constant at 10 µM. All conditions were as described under Materials and Methods.

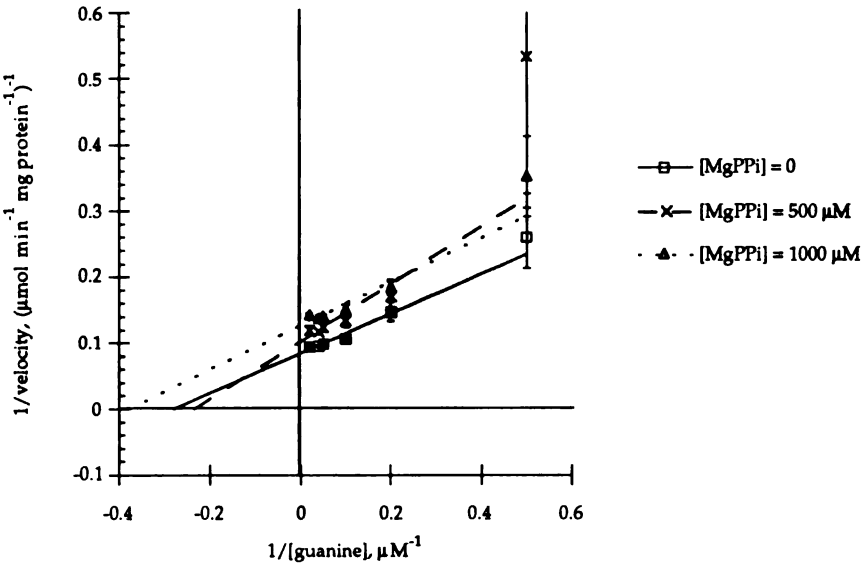

Figure 3.11a. Product inhibition by $MgPP_i$ on the reaction: guanine + Mg_2PRPP → MgGMP + $MgPP_i$, with guanine as the variable substrate and with the concentration of Mg_2PRPP held constant at 1000 µM. All conditions were as described under Materials and Methods.

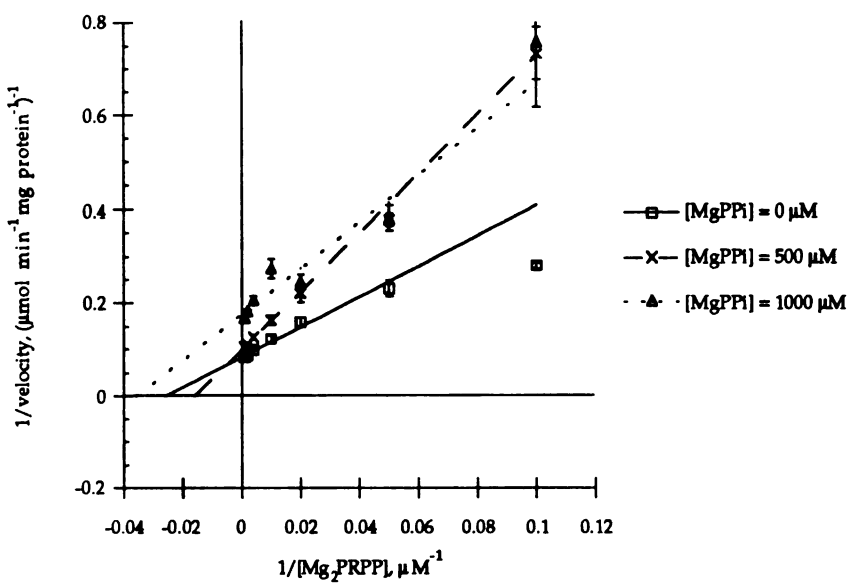

Figure 3.11b. Product inhibition by $MgPP_i$ on the reaction: guanine + Mg_2PRPP → MgGMP + $MgPP_i$, with Mg_2PRPP as the variable substrate and with the concentration of guanine held constant at 50 µM. All conditions were as described under Materials and Methods.

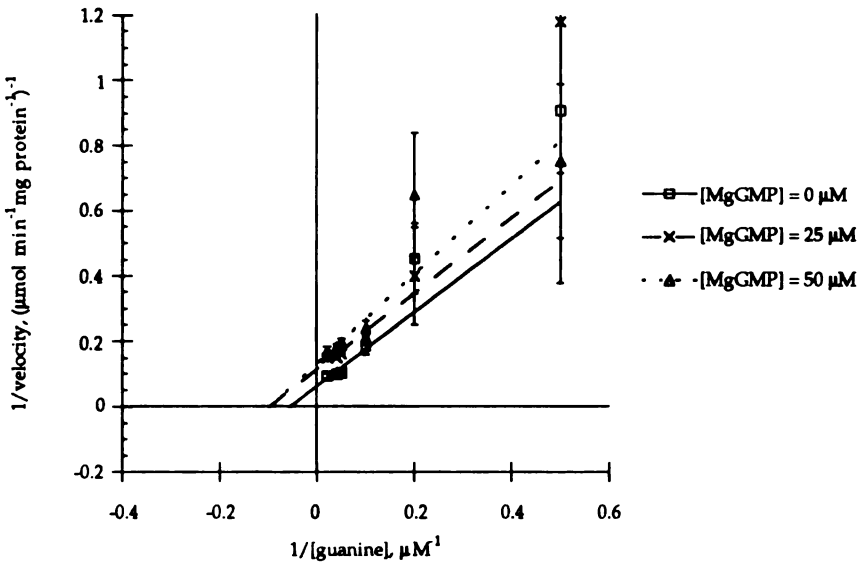

Figure 3.12a. Product inhibition by MgGMP on the reaction: guanine + $Mg_2PRPP \rightarrow MgGMP + MgPP_i$, with guanine as the variable substrate and with the concentration of Mg_2PRPP held constant at 1000 µM. All conditions were as described under Materials and Methods.

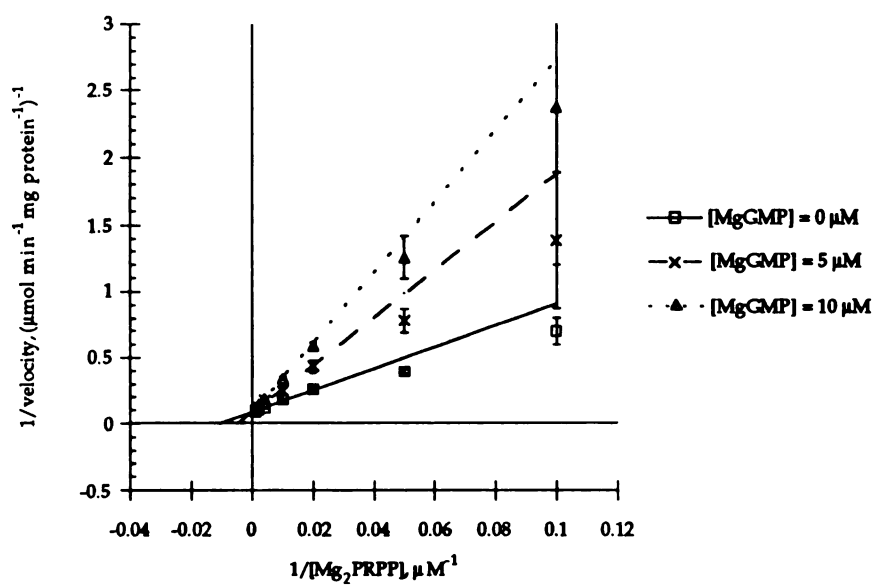

Figure 3.12b. Product inhibition by MgGMP on the reaction: guanine + $Mg_2PRPP \rightarrow MgGMP + MgPP_i$, with Mg_2PRPP as the variable substrate and with the concentration of guanine held constant at 50 µM. All conditions were as described under Materials and Methods.

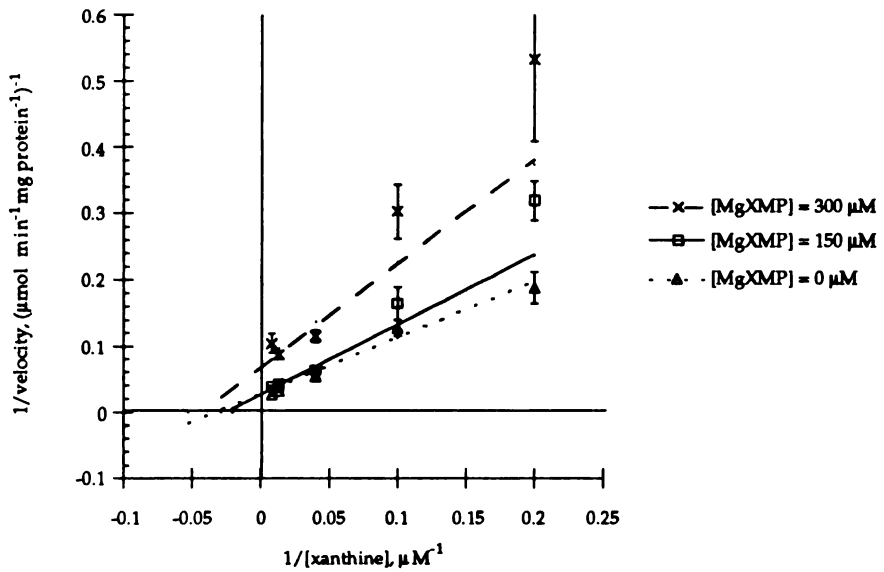

Figure 3.13a. Product inhibition by MgXMP on the reaction: xanthine + $Mg_2PRPP \rightarrow MgXMP + MgPP_i$, with xanthine as the variable substrate and with the concentration of Mg_2PRPP held constant at 1000 µM. All conditions were as described under Materials and Methods.

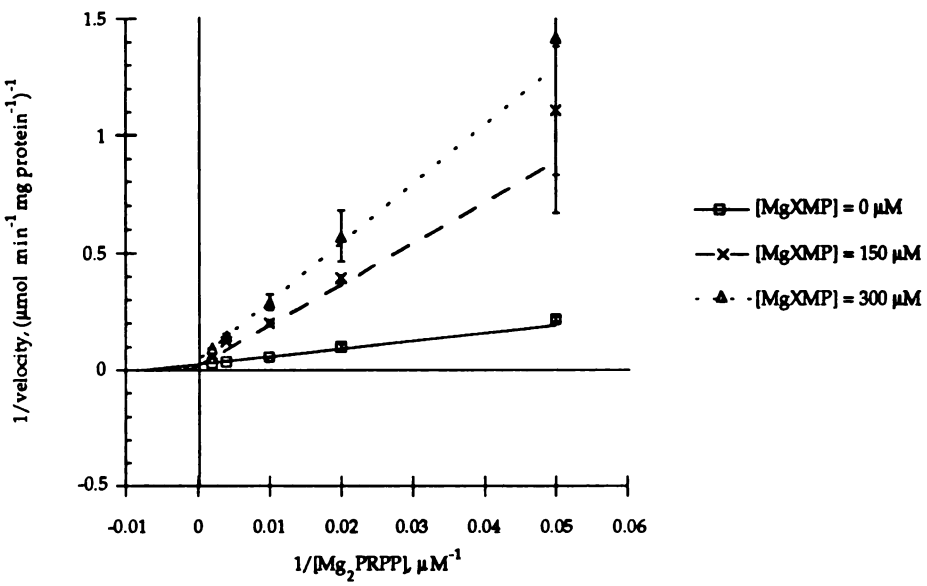

Figure 3.13b. Product inhibition by MgXMP on the reaction: xanthine + $Mg_2PRPP \rightarrow MgXMP + MgPP_i$, with Mg_2PRPP as the variable substrate and with the concentration of xanthine held constant at 250 µM. All conditions were as described under Materials and Methods.

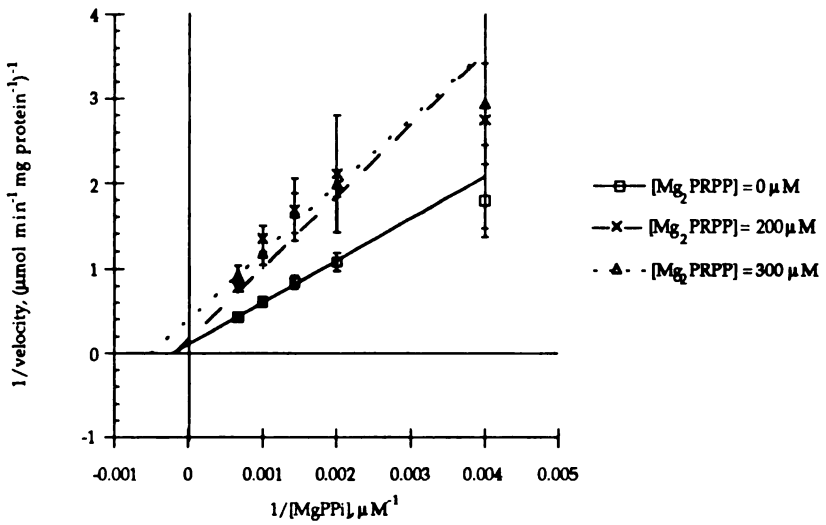

Figure 3.14a. Product inhibition by Mg_2PRPP on the reaction: MgXMP + $MgPP_i$ → xanthine + Mg_2PRPP, with $MgPP_i$ as the variable substrate and with the concentration of MgXMP held constant at 600 µM. All conditions were as described under Materials and Methods.

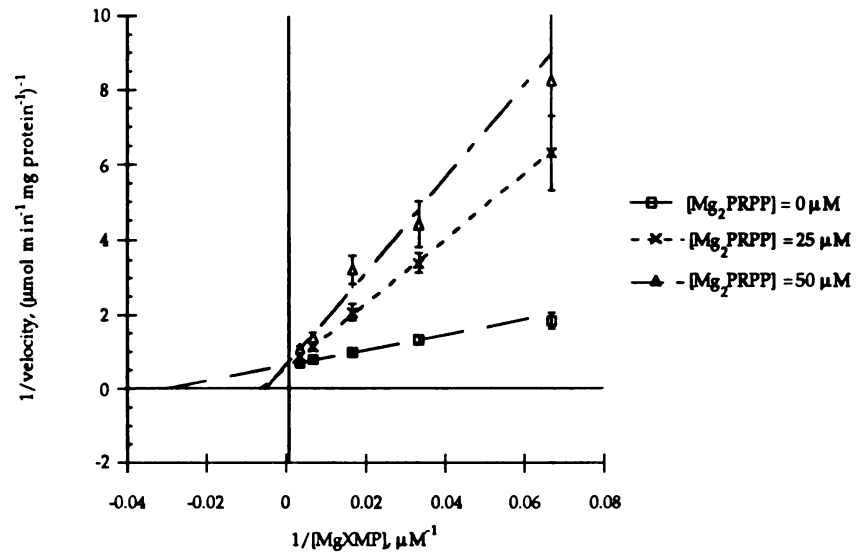

Figure 3.14b. Product inhibition by Mg_2PRPP on the reaction: MgXMP + $MgPP_i$ → xanthine + Mg_2PRPP, with MgXMP as the variable substrate and with the concentration of $MgPP_i$ held constant at 1000 µM. All conditions were as described under Materials and Methods.

CONCLUSIONS

The goals outlined in the introduction have been achieved. We were able to identify, clone and sequence the *T. foetus* HGXPRTase gene, which allowed us to characterize it at the genomic level and compare the predicted primary sequence with the primary sequence of other HGPRTases. The protocol utilized to isolate the *T. foetus* HGXPRTase gene will be useful in isolating genes encoding HGPRTases of other organisms (isolation of the gene encoding the GPRTase of *G. lamblia* is in progress now). We were also able to express the *T. foetus* HGXPRTase gene in *E. coli*, purify the recombinant enzyme to apparent homogeneity and show that it appears identical to the native *T. foetus* HGXPRTase. Finally, we were able to characterize the recombinant enzyme using both initial velocity and product inhibition studies.

The gene encoding the *T. foetus* HGXPRTase is a single copy gene and is the smallest eukaryotic gene encoding an HGPRTase. Alignment of the predicted amino acid sequence of the *T. foetus* enzyme with the amino acid sequence of other HGPRTases reveal that the overall similarity to to other HGPRTases is low, and as expected, the regions associated with higher homology are those regions of the enzyme which interact with PRPP. The size and amino acid alignment with the enzymes from *E. coli*, *V. harveyi* and *L. lactis* indicate that the *T. foetus* HGXPRTase is more closely related to the prokaryotic rather than eukaryotic enzyme. This is not unexpected since *T. foetus* is believed to be one of the earlier branches of the eukaryotic tree. Comparison of amino acid residues analogous to the residues of the human enzyme which interact with the purine base reveal that most residues are conserved and any differences are conservative substitutions. Thus, determination of the residues involved in purine base

specificity will have to rely on X-ray crystallographic studies of the *T. foetus* enzyme and HGPRTases of other organisms, such as the human (HGPRTase) and *G. lamblia* (GPRTase) enzymes. Once specific residues have been determined to be responsible for purine specificity, mutagenesis experiments can be used to complement the crystallographic results. X-ray crystallographic studies of the recombinant *T. foetus* enzyme are currently in progress.

The enzyme kinetic studies of the recombinant *T. foetus* enzyme have enabled us to propose a kinetic mechanism for this enzyme. The simplest model, supported by our data, is an ordered bi-bi mechanism with Mg_2PRPP binding first and the Mg-complexed purine nucleotide released last. This model is identical to the one proposed for the schistosomal HGPRTase (Yuan, et al., 1992), and it would be interesting to discover whether the HGPRTase of other parasites would also follow an ordered bi-bi mechanism. An unexpected result from the kinetic studies is the large K_m values for $MgPP_i$, which are five to ten times larger than the K_m values for Mg_2PRPP. Residues proposed to interact with Mg_2PRPP are highly conserved in all HGPRTases studied to date; nevertheless, the Mg_2PRPP binding pocket of the *T. foetus* HGXPRTase may have subtle differences in its three-dimensional structure that can be observed with X-ray crystallography. The large K_m values could indicate that $MgPP_i$ may not bind very well to the *T. foetus* HGXPRTase and ensure that the transfer of the phosphoribosyl group to the purine base is favored over purine nucleotide pyrophosphorolysis. Since *T. foetus* has no other means of meeting its purine base requirements, it would be essential that the purine salvaging activities of its HGXPRTase be favored. The pyrophosphate generated by the phosphoribosyltransferase reaction would be available for other purposes, such as being used a high energy compound for glycolysis. The human HGXPRTase is the only mammalian HGPRTase that has been studied extensively, and the

kinetic mechanism of this enzyme is an ordered bi rapid equilibrium random bi mechanism with the enzyme binding Mg_2PRPP first and releasing products in a random order. If all mammalian HGPRTases follow the same kinetic mechanism as the human enzyme then the key differences between the trichomonad and mammalian enzymes could be the order of product release, the ability of the *T. foetus* enzyme to use xanthine and the poor ability that the *T. foetus* enzyme has for binding $MgPP_i$. Similarities and diferences of the T. foetus HGXPRTase, the human and the bovine HGPRTases are presented in Table C.1.

The work described here has been fundamental to the continued examination of the *T. foetus* HGXPRTase as a model for structure-based drug design. The availability of large quantities of purified *T. foetus* HGXPRTase through the *E. coli* gene expression system will be essential to X-ray crystallographic studies and chemical labeling of active site residues of the enzyme. The information obtained from the kinetic studies will be used in conjunction with the results of the structural studies of the enzyme to design inhibitors with antitrichomonal activities.

Table C.1. Comparison of the *T. foetus* HGXPRTase with the human HGPRTase (Olsen and Milman, 1977; Eads, *et al.*, 1994; Giacomello and Salerno, 1978) and the bovine HGPRTase (Paulus, 1980).

	T. foetus	Human	Bovine
MW	21.1 kDa	26 kDa (subunit)	26 kDa (subunit)
pI	4.8	5.6, 5.7, 5.9	7.85, 8.10
substrate specificity	hypoxanthine guanine xanthine	hypoxanthine guanine	hypoxanthine guanine
amino acid residues involved in purine binding	Lys-134 Ile-157 (Tyr-156) Asp-163	Lys-165 Val-187 (Phe-186) Asp-193	———— ———— ————
Km (hypoxanthine)	1 μM	7.7 μM	0.99 μM
Km (guanine)	1.8 μM	————	0.42 μM
Km (xanthine)	31.2 μM	————	————
Km (Mg_2PRPP))	(H) 43.5 μM (G) 55.6 μM (X) 111.1 μM	(H) 66 μM	(H) 18.6 μM (G) 2.9 μM
Km (MgIMP)	1.1 μM	5.8 μM	————
Km (MgGMP)	199 μM	————	————
Km (MgXMP)	52.6 μM	————	————
Km ($MgPP_i$)	(MgIMP) 500 μM (MgGMP) 303.9 μM (MGXMP) 5070 μM	(MgIMP) 39 μM	————
kinetic mechanism	ordered bi-bi	ordered bi rapid equilibrium random bi	————

REFERENCES

1. Abraham, R., and Honigberg, B.M. (1964) Structure of *Trichomonas gallinae* (Rivolta). *J. Parasitol.* **50**, 608-619.
2. Adams, J.M. (1968) On the Release of the Formyl Group from Nascent Protein. *J. Mol. Biol.* **33**, 571-589.
3. Ainsworth, S. (1977) "Steady-State Enzyme Kinetics," University Park Press, Baltimore, Maryland.
4. Akinboade, D.A. (1980) Incidence of Bovine Trichomoniasis in Nigeria. *Rev. d'Elev. Med. Vet. Pays. Trop.* **33**, 381-384.
5. Ali, L.Z., and Sloan, D.L. (1982) Studies of the Kinetic Mechanism of Hypoxanthine-Guanine Phosphoribosyltransferase from Yeast. *J. Biol. Chem.* **257**, 1149-1155.
6. Allen, T., Hwang, H.Y., and Ullman, B. (1993) GenBank Accession Number L25412.
7. Allen, T.E., and Ullman, B. (1993) Cloning and Expression of the Hypoxanthine-guanine Phosphoribosyltransferase gene from *Trypanosoma brucei*. *Nucleic Acids Res.* **21**, 5431-5438.
8. Allen, T.E., and Ullman, B. (1994) Molecular Characterization and Overexpression of the Hypoxanthine-guanine Phosphoribosyltransferase Gene from *Trypanosoma cruzi*. *Mol. Biochem. Parasitol.* **65**, 233-245.
9. Ames, B., Durston, W., Yamasaki, E., and Lee, F. (1973) Cardinogens are Mutagens: a Simple Test Combining Liver Homogenates for Activation and Bacteria Detection. *Proc. Natl. Acad. Sci. USA* **70**, 2281-2285.
10. Bartlett, D.E. (1948) Further Observations on Experimental Treatments of Trichomonas foetus Infection in Bulls. *Am. J. Vet. Res.* **9**, 351-359.
11. Beck, J.T., and Wang, C.C. (1993) The Hypoxanthine-Guanine-Xanthine Phosphoribosyltranferase from *Tritrichomonas foetus* is a Unique Enzyme. *Mol. Biochem. Parasit.* **60**, 187-194.
12. Beck, J.T., Zhao, S., and Wang, C.C. (1994) Cloning, Sequencing, and structural Analysis of the DNA Encoding Inosine Monophosphate Dehydrogenase (EC 1.1.1.205) from *Tritrichomonas foetus*. *Experimental Parasitology* **78**, 101-112.
13. Ben-Bassat, A., Bauer, K., Chang, S.Y., Myambo, K., Boosman, A. *et al.* (1987) Processing of the Initiation methionine from Proteins: Properties of the *Escherichia coli* Methionine Aminopeptidase and Its Gene Structure. *J. Bacteriol.* **169**, 751-757.
14. Benchimol, M. (1994) Fine Structure of *Tritrichomonas foetus* as Seen Using Cryotechniques. *Microsc. Res. Tech.* **29**, 37-46

15. Benchimol, M., and de Souza, W. (1983) Fine Structure and Cytochemistry of the Hydrogenosomes of *Tritrichomonas foetus*. *J. Protozool.* **30**, 422-425.

16. Benchimol, M., Elias, C.A., and De Souza, W. (1982) *Tritrichomonas foetus*: Ultrastructural Localization of Basic Proteins and Carbohydrates. *Exp. Parasitol.* **54**, 135-144.

17. Berens, R.L., Marr, J.J., LaFon, S.W., and Nelson, D.J. (1981) Purine metabolism in *Trypanosoma cruzi*. *Mol. Biochem. Parasitol.* **3**, 187-196.

18. Bhatia, M.B., Vinitsky, A., and Grubmeyer, C. (1990) Kinetic Mechanism of Orotate Phosphoribosyltransferase from *Salmonella typhimurium*. *Biochemistry* **29**, 10480-10487.

19. Birnstiel, M.L., Busslinger, M., and Strub, K. (1985) Transcription Termination and 3' Processing: The End is in Site! *Cell* **41**, 349-359.

20. Breese, G.R., criswell, H.E., Duncan, G.E., Mueller, R.A. (1990) A Dopamine Deficiency Model of Lesch-Nyhan Disease-The Neonatal-6-OHDA-Lesioned Rat. *Brain Res. Bull.* **25**, 477-484.

21. Burgess, D.E., and Knoblock, K.F. (1989) Identification of *Tritrichomonas foetus* in Sections of Bovine Placental Tissue with Monoclonal Antibodies. *J. Parasitol.* **75**, 977-980.

22. Burgess, D.E., Knoblock, K.F., Daugherty, T., and Robertson, N.P. (1990) Cytotoxic and Hemolytic Effects of *Tritrichomonas foetus* on Mammalian Cells. *Infection and Immunity* **58**, 3627-3632.

23. Cerkasovová, A., Cerkasov, J., and Kulda, J. (1984) Metabolic Differences Between Metronidazole Resistant and Susceptible Strains of *Tritrichomonas foetus*. *Mol. Biochem. Parasitol.* **11**, 105-118.

24. Champney, W.S., Chittum, H.S., and Samuels, R. (1992) Ribosomes from Trichomonad Protozoa have Prokaryotic Characteristics. *Int. J. Biochem.* **24**, 1125-1133.

25. Chapman, A., Hann, A.C, Linstead, D., and Lloyd, D. (1985) Energy-dispersive X-ray Microanalysis of Membrane-associated Inclusions in Hydrogenosomes Isolated from *Trichomonas vaginalis*. *J. Gen. Microbiol.* **131**, 2933-2939.

26. Chin, M.S., and Wang, C.C. (1994) Isolation, Sequencing and Expression of the Gene Encoding Hypoxanthine-Guanine-Xanthine Phosphoribosyltransferase of *Tritrichomonas foetus*. *Mol. Biochem. Parasitol.* **63**, 221-229.

27. Chinault, A.C., and Caskey, C.T. (1984) The Hypoxanthine Phosphoribosyltransferase Gene: A Model for the Study of Mutation in Mammalian Cells. *Prog. Nuc. Acids Res. Mol. Biol.* **31**, 295-313

28. Christensen, R., Clark, B.L., and Parsonson, I.M. (1977) Incidence of *Tritrichomonas foetus* in Young Replacement Bulls Following Introduction into an Infected Herd. *Aust. Vet. J.* **53**, 132-134

29. Clark, B.L., Parsonson, I.M., White, M.E., *et al.* (1974) Control of Trichomoniasis in a Large Herd of Beef Cattle. *Aust. Vet. J.* **53**, 132-134

30. Cleland, W.W. (1963) The Kinetics of Enzyme-Catalyzed Reactions with Two or More Substrates or Products. I. Nomenclature and Rate Equations. *Biochim. Biophys. Acta* **67**, 104-137.

31. Cleland, W.W. (1977) Determining the Chemical Mechanisms of Enzyme-Catalyzed Reactions by Kinetic Studies. *Adv. Enzymol. Relat. Areas Mol. Biol.* **45**, 274-309.

32. Corbeil, L.B., Hodgson, J.L., Jones, D.W., Corbeil, R.R., Widders, P.R., *et al.* (1989) Adherence of *Tritrichomonas foetus* to Bovine Vaginal Epithelial Cells. *Infection and Immunity* **57**, 2158-2165

33. Craig, S.P., III, McKerrow, J.H., Newport, G.R., and Wang, C.C. (1988) Analysis of cDNA Encoding the Hypoxanthine-Guanine Phosphoribosyltransferase (HGPRTase) of *Schistosoma mansoni*; a Putative Target for Chemotherapy. *Nucl. Acids Res.* **16**, 7087-7101

34. Craig, S.P., III, Yuan, L., Bystroff, C., Focia, P., Fletterick, R. *et al.* (1992) The Human Hypoxathine-Guanine Phosphoribosyltransferase (HPRT) and the Targeted Inhibition of Parasitic Enzymes. *J. Cell. Biochem. Suppl.* **16A**, 145.

35. Craig, S.P., III, Yuan, L., Kuntz, D.A., McKerrow, J.H., and Wang, C.C. (1991) High Level Expression in *Escherichia coli* of Soluble, Enzymatically Active Schistosomal Hypoxanthine-Guanine Phosphoribosyltransferase and Trypanosomal Ornithine Decarboxylase. *Proc. Natl. Acad. Sci. USA* **88**, 2500-2504.

36. De Courcy, S.J., and Sevag, M.G. (1967) Population Dynamics and Results of Fluctuation Tests in a Study of the Role of Atabrine as an Antimutagen in Preventing Streptomycin Resistance in *Staphylococcus aureus*. *Antimicrob. Agents Chemother.* 235-244.

37. Diamond, L.S. (1957) The Establishment of Various Trichomonads of Animals and Man in Axenic Cultures. *J. Parasitol.* **43**, 488-490.

38. Diamond, L.S. (1964) Freeze-Preservation of Protozoa *Cryobiology* **1**, 95-102

39. DoCampo, R., Moreno, S., and Mason, R. (1984) Reduction of Nitrofurans and Metronidazole to Free Radical Intermediates by *Tritrichomonas foetus* Hydrogenosomes. *Abstract 1984 ASBC meeting St. Louis.*

40. Eads, J.C., Scapin, G., Xu, Y., Grubmeyer, C., and Sacchettini, J.C. (1994) The Crystal Structure of Human Hypoxanthine-Guanine Phosphoribosyltransferase with Bound GMP. *Cell* **78**, 325-334.

41. Eakin, A.E., Nieves, R., Tosado-Acevedo, R., Chin, M.S., Wang, C.C. *et al.* (1995) Comparative Complement Selection in Bacteria Enables Screening for Lead Compounds Targeted to a Purine Salvage Enzyme of Parasites. *Antimicrob. Agents Chemother* **39**, 620-625.

42. Edman, J.C., and Kwon-Chong, K.J. (1990) Isolation of the *URA5* Gene from *Cryptoccocus neoformans* var. *neoformans* and Its Use as a Selective Marker for Transformation. *Mol. Cell. Biol.* **10**, 4538-4544.

43. Filho, F.C.S., and de Souza, W. (1988) The Interaction of *Trichomonas vaginalis* and *Tritrichomonas foetus* with Epithelial Cells *in Vitro*. *Cell Structure and Function* **13**, 301-310.

44. Fish, W.R., Marr, J.J., and Berens, R.L. (1982) Purine metabolism in *Trypanosoma brucei gambiense Biochim. Biophys. Acta* **714**, 422-428.

45. Fitzgerald, P.R. (1986) Bovine Trichomoniasis. *Vet. Clinic No. Amer.: Food Animal Practice* **2**, 277-282.

46. Fitzgerald, P.R., Johnson, A.E., and Hammond, D.M. (1963) Treatment of Genital Trichomoniasis in Bulls. *J. Am. Vet. Med. Assoc.* **143**, 259-262.

47. Florent, A. (1947) Pouvoir Agglutinant du Mucus Vaginal Vis-À-Vis de *Trichomonas foetus* dans la Trichomonose du Bétail. *C.R. Seances Biol. Ses Fil.* **141**, 957-958.

48. Free, M.L., Gordon, R.B., Keough, D.T., Beacham, I.R., Emmerson, B.T. *et al.* (1990) Expression of Active, Human Hypoxanthine-Guanine Phosphoribosyltransferase in Escherichia coli and Characterisation of the Recombinant Enzyme. *Biochim. Biophys. Acta* **1087**, 205-211.

49. Giacomello, A., and Salerno, C. (1978) Human Hypoxanthine-Guanine Phosphoribosyltransferase: Steady State Kinetics of the Forward and Reverse Reactions. *J. Biol. Chem.* **253**, 6038-6044.

50. Goldstein, M., Anderson, L.T., Reuben, R., Dancis, J. (1985) Self-Mutilation in Lesch-Nyhan Syndrome. *Lancet* **1**, 338-339.

51. Goldstein, M., Kuga, S., Shimizu, Y., Meller, E. (1986) The Pathophysiological Functions Mediated by D1 Dopamine Receptors. *Adv. Exp. Med. Biol.* **204**, 189-195.

52. Gutensohn, W., and Huber, M. (1975) Irreversible Inactivation of Hypoxanthine Phosphoribosyltransferase by Periodate Oxidized Nucleotides. *Z. Physiol. Chem.* **356**, 431-436.

53. Gutensohn, W., Huber, M., and Jahn, H. (1976) Facilitated Purification of Hypoxanthine Phosphoribosyltransferase. *Hoppe-Seyler's Z. Physiol. Chem.* **357**, 1379-1385.

54. Gutteridge, W.E., and Coombs, G.H. (1977) "Biochemistry of Parasitic Protozoa," University Park Press, Baltimore, Maryland.

55. Gutteridge, W.E., and Gaborak, M. (1979) A Re-Examination of Purine and Pyrimidine Synthesis in the Three Main Forms of *Trypanosoma cruzi*. *Int. J. Biochem.* **10**, 415-422.

56. Hammond, D.M., and Bartlett, D.E. (1945) An Instance of Phagocytosis of *Trichomonas foetus* in Bovine Vaginal Secretions. *J. Parasitol.* **31**, 82.

57. Hanahan, D. (1983) Studies in Transformation of *Escherichia coli* with Plasmids. *J. Mol. Biol.* **166**, 557-580.

58. Harrap, G.J., and Watkins, W.M. (1970) Enzymes of *Trichomonas foetus*. Separation and Properties of Two β-galactosidases. *Biochem. J.* **117**, 667-675.

59. Henderson, J.F., Brox, L.W., Kelley, W.N., Rosenbloom, F.M., and Seegmiller, J.E. (1968) Kinetic Studies of Hypoxanthine-Guanine Phosphoribosyltransferase. *J. Biol. Chem.* **243**, 2514-2522.

60. Herrick, J.B. (1990) Food for Thought for Food Animal Veterinarians: Waiting for the Food and Drug Administration to Respond to its Advisory Committee's Recommendations. *J. Am. Vet. Med. Assoc.* **196**, 222-223.

61. Hershey, H.V., and Taylor, M.W. (1986) Nucleotide Sequence and Deduced Amino Acid Sequence of *Escherichia coli* Adenine Phosphoribosyltrnaferase and Comparison with Other Analogous Enzymes. *Gene* **43**, 287-293.

62. Hill, B., Kilsby, J., Rogerson, G.W., McIntosh, R.T., and Ginger, D.C. (1981) The Enzymes of Pyrimidine Biosynthesis in a Range of Parasitic Protozoa and Helminths. *Mol. Biochem. Parasitol.* **2**, 123-134.

63. Hill, D.L. (1970) Hypoxanthine Phosphoribosyltransferase and Guanine Metabolism of Adenocarcinoma 755 Cells. *Biochem. Pharmacol.* **19**, 545-557.

64. Hochstadt, J. (1978) Adenine Phosphoribosyltransferase From *Escherichia coli*. *Methods in Enzymol.* **51**, 558-567.

65. Hogue, M.J. (1938) The Effect of *Trichomonas foetus* on Tissue Culture Cells. *Am. J. Hyg.* **28**, 288-298.

66. Honigberg, B.M. (1978) Trichomonads of Veterinary Importance. In "Parasitic Protozoa". (J.P. Kreier, ed.), Vol. 2, pp. 163-273. Academic Press, New York, New York.

67. Honigberg, B.M., Mattern, C.F.T., and Daniel, W.A. (1971) Fine Structure of the Mastigont System in *Tritrichomonas foetus* (Riedmuller). *J. Protozool.* **18**, 183-198.

68. Ings, R.M., McFadzean, J.A., and Ormerod, W.E. (1974) The Mode of Action of Metronidazole in *Trichomonas vaginalis* and other Micro-organisms. *Biochem. Pharmacol.* **23**, 1421-1429.

69. Jinnah, H.A., Langlais, P.J., Friedman, T. (1992) Functional Analysis of Brain Dopamine Systems in a Genetic Mouse Model of Lesch-Hyhan Syndrome. *J. Pharmacol. Exp. Ther.* **263**, 596-607.

70. Jinnah, H.A., Page, T. Friedman, T. (1993) Brain Purines in a Genetic Mouse Model of Lesch-Nyhan Disease. J. Neurochem. 60, 2036-2045.

71. Jinnah, H.A., Wojcik, B.E., Hunt, M., Narung, N., Lee, K.Y., *et al.* (1994) Dopamine Deficiency in a Genetic Mouse Model of Lesch-Nyhan Disease. *J. Neurosci.* **14**, 1164-1175.

72. Jochimsen, B., Nygaard, P., and Vestergaard, T. (1975) Location on the Chromosome of *Escherichia coli* of Genes Governing Purine Metabolism. *Molec. Gsen. Genet.* **143**, 85-91.

73. Johnson, A.E. (1964) Incidence and Diagnosis of Trichomoniasisin Western Beef Bulls. *J. Am. Vet. Med. Assoc.* **145**, 1007-1010.

74. Johnson, P.J., D'Oliveira, C.E., Gorrell, T.E., and Muller, M. (1990) Molecular Analysis of the Hydrogenosomal Ferredoxin of the Anaerobic Protist *Trichomonas vaginalis*. *Proc. Natl. Acad. Sci. U.S.A.* **87**, 6097-6101.

75. Jolly, D.J., Okayama, H., Berg, P., Esty, A.C., Filpala, D. *et al.* (1983) Isolation and Characterization of a Full-length Expressible cDNA for Human Hypoxanthine Phosphoribosyltransferase. *Proc. Natl. Acad. Sci., USA* **80**, 477-481.

76. Kalckar, H.M. (1947) Differential Spectrophotometry of Purine Compounds by Means of Specific Enzymes. I. Determination of Hydroxypurine Compounds. *J. Biol. Chem.* **167**, 429-443.

77. Kanaaneh, J., Craig, S.P.III., and Wang, C.C. (1994) Differential Inhibitory Effects of GMP-2'.3'-Dialdehyde on Human and Schistosomal Hypoxanthine-Guanine Phosphoribosyltransferases. *Eur. J. Biochem.* **223**, 595-601.

78. Kaslow, D.C., and Hill, S. (1990) Cloning Metabolic Pathway Genes by Complementation in *Escherichia coli* Isolation and Expression of *Plasmodium falciparum* Glucose Phosphate Isomerase. *J. Biol. Chem.* **265**, 12337-12341.

79. Kelley, W., and Wyngaarden, J. (1983) "Clinical Syndromes Associated with Hypoxanthine-Guanine Phosphoribosyltransferase Deficiency," 5th, McGraw-Hill, New York, New York.

80. Kimsey, P.B., Darien, B.J., Kendrick, J.W., and Franti, C.E. (1980) Bovine Trichomoniasis: Diagnosis and Treatment. *J. Am. Vet. Med. Assoc.* **177**, 616-619.

81. King, A., and Melton, D.W. (1987) Characterisation of cDNA clones for Hypoxanthine-Guanine Phosphoribosyltransferase from the Human Malarial Parasite, *Plasmodium falciparum*: Comparisons to the Mammalian Gene and Protein. *Nucl. Acids Res.* **15**, 10469-10481.

82. Kirby, H. (1951) Observations on the Trichomonad Flagellate of the Reproductive Organs of Cattle. *J. Parasitol.* **37**, 445-459.

83. Kozak, M. (1984) Compilation and Analysis of Sequences Upstream from the Translational Start Site in Eukaryotic mRNAs. *Nucl. Acids Res.* **12**, 857-872.

84. Krug, E.C., Marr, J.J., and Berens, R.L. (1989) Purine Metabolism in *Toxoplasma gondii*. *J. Biol. Chem.* **264**, 10601-10607.

85. Kulda, J., and Honigberg, B.M. (1969) Behavior and Pathogenicity of *Tritrichomonas foetus* in Chick Liver Cell Cultures. *J. Protozool.* **16**, 479-495.

86. Kulda, J., Cerkasov, J., Demes, P. (1984) Tritrichomonas foetus: Stable Anaerobic Resistance to Metronidazole *in Vivo*. *Exp. Parasitol.* **57**, 93-193.

87. Laemmli, U.K. (1970) Cleavage of Structural Proteins during the Assembly of the Head of Bacteriophage T4. *Nature* **227**, 680-685.

88. Lahti, C.J., D'Oliveira, C.E., Gorrell, T.E., and Müller, M. (1992) Beta-Succinyl CoA Synthetase from Trichomonas vaginalis is a Soluble Hydrogenosomal Protein with an Amino-Terminoal Sequence that Resembles Mitochondrial Presequences. *J. Bacteriol.* **174**, 6822-6830.

89. Laue, T.M., and Rhodes, D.G. (1990) Determination of Size, Molecular Weight and Presence of Subunits. *Methods in Enzymol.* **182**, 566-587.

90. Lemoine, L.A., Hart, L.T., Larson, A.D., and McCorkle-Shirley, S. (1983) Costa as a Glycogen Store and Probable Site of Energy Generation in *Tritrichomonas foetus*. *Am. J. Vet. Res.* **44**, 713-714.

91. Lesch, M., and Nyhan, W. (1964) A Familial Disorder of Uric Acid Metabolism and Central Nervous System Function. *Am. J. Med.* **36**, 561-570.

92. Levine, N.D. (1961) "Protozoan Parasites of Domestic Animals and of Man," Burgess Publishing Company, Minneapolis, Minnesota.

93. Lindblom, G.P. (1961) Carbohydrate Metabolism of Trichomonads: Growth, Respiration, and Enzyme Activity in Four Species. *J. Protozool.* **8**, 139-150.

94. Lindmark, D.G., and Jarroll, E.L. (1982) Pyrimidine Metabolism in *Giardia lamblia* trophozoites. *Mol. Biochem. Parasitol.* **5**, 291-296.

95. Lindmark, D.G., and Müller, M. (1974) Superoxide Dismutase in the Anaerobic Flagellates, *Tritrichomonas foetus* and *Monocercomonas* sp. *J. Biol. Chem.* **249**, 4634-4637.

96. Lindmark, D.G., and Müller, M. (1976) Antitrichomonad Action, Mutagenicity, and Reduction of Metronidazole and Other Nitroimidazoles. *Antimicro. Agents Chemother.* **10**, 476-482.

97. Linstead, D.J., and Bradley, S. (1988) The Purification and Properties of Two Soluble Reduced Nicotinamide: Acceptor Oxidoreductases from *Trichomonas vaginalis*. *Mol. Biochem. Parasitol.* **27**, 125-134.

98. Lloyd, D., Lindmark, D.G., and Müller, M. (1979) Respiration of *Tritrichomonas foetus*: Absence of Detectable Cytochromes. *J. Gen. Microbiol.* **115**, 466-469.

99. Lloyd, K.G., Hornykiewicz, O., Davidson, L., Shannak, K., Farley, I., *et al.*, (1981) Biochemical Evidence of Dysfunction of Brain Neurotransmitters in the Lesch-Nyhan Syndrome. *N. Engl. J. Med.* **305**, 1106-1111.

100. Lo, H.S., and Wang, C.C. (1985) Purine Salvage in *Entamoeba histolytica*. *J. Parasitol.* **71**, 662-669.

101. Lockwood, B.C., North, M.J., Scott, K.I., Bremner, A.F., and Coombs, G.H. (1987) The Use of a Highly Sensitive Electrophoretic Method to Compare the Proteinases of Trichomonads. *Mol. Biochem. Parasitol.* **24**, 89-95.

102. Maion, G., and Chamberland, S. (1992) Co-Purification of *Toxoplasma gondii* Guanine, Hypoxanthine and Xanthine Phosphoribosyltransferases Using Affinity Chromatography. *Abstr. Mol. Parasitol. Meet. Woods Hole, Massachussetts.*

103. Marr, J.J., Berens, R.L., and Nelson, D.J. (1978) Purine Metabolism in *Leishmania donovani* and *Leishmania braziliensis*. *Biochim. Biophys. Acta* **44**, 360-371.

104. McLaughlin, J., Lindmark, D.G., and Müller, M. (1978) Inorganic Pyrophosphatase and Nucleoside Diphosphatase in the Parasitic Protozoon, *Entamoeba histolytica*. *Biochem. Biophys. Res. commun.* **82**, 913-920.

105. McLoughlin, D.K. (1965) Dimetridazole, a Systemic Treatment for Bovine Venereal Trichomoniasis. I. Oral Administration *J. Parasitol.* **51**, 835-836.

106. McLoughlin, D.K. (1967) Drug Tolerance by *Tritrichomonas foetus*. *J. Parasitol.* **53**, 646-648.

107. McLoughlin, D.K. (1968) Dimetridazole, a Systemic Treatment for Bovine Venereal Trichomoniasis. II. Intravenous Administration. *J. Parasitol.* **54**, 1038-1039.

108. McLoughlin, D.K. (1970) Dimetridazole, a Systemic Treatment for Bovine Venereal Trichomoniasis. III. Trials with Cows. *J. Parasitol.* **56**, 39-40.

109. McLoughlin, D.K., and Chute, M.B. (1968) Drug Resistance in *Eimeria tenella*. VII. Acriflavin-mediated Loss of Resistance to Amprolium. *J. Parasit.* **54**, 696-698.

110. McLoughlin, D.K., and Chute, M.B. (1969) Effect of Quinacrine Hydrochloride and Acriflavine Hydrochloride on Development and Stability of Resistance to Dimetridazole by *Tritrichomonas foetus*. *J. Parasitol.* **55**, 426-428.

111. Mertens, E. (1991) Pyrophosphate-dependent Phosphofructokinase, an Anaerobic Glycolytic Enzyme? *Fed. Eur. Biochem. Soc. Lett.* **285**, 1-5.

112. Mertens, E., Van Schaftingen, E., and Müller, M. (1989) Presence of a Fructose-2,6-Biphosphate-Insensitive Pyrophosphate: Fructose-6-Phosphate Phosphotransferase in the Anaerobic Protozoa *Tritrichomonas foetus*, *Trichomonas vaginalis* and *Isotricha prostoma*. *Mol. Biochem. Parasitol.* **37**, 183-190.

113. Michaels, R.M. (1968) "Chemotherapy of Trichomoniasis," Academic Press, New York, New York.

114. Miller, C.G., Strauch, K.L., Kukral, A.M., Miller, J.L., Wingfield, P.T. *et al.* (1987) N-terminal Methionine-specific Peptidase in *Salmonella typhimurium*. *Proc. Natl. Acad. Sci. USA* **84**, 2718-2722.

115. Miller, R.L., and Linstead, D. (1983) Purine and Pyrimidine Metabolizing Activities in *Trichomonas vaginalis* Extracts. *Mol. Bochem. Parasitol.* **7**, 41-51.

116. Mitsuhashi, S., Harada, K., and Kameda, M. (1961) Elimination of Transmissible Drug-Resistance by Treatment with Acriflavine. *Nature* **189**, 947.

117. Monteiro-Leal, L.H., da Cunha-e-Silva, N.L., Benchimol, M., and de Souza, W. (1993) Isolation and Biochemical Characerization of the Costa of *Tritrichomonas foetus*. *Eur. J. Cell Biol.* **60**, 235-242.

118. Moreno, S.N.J., Mason, R.P., Muniz, R.P.A., Cruz, F.S., and Docampo, R. (1983) Generation of Free Radicals from Metronidazole and other Nitroimidazoles by *Tritrichomonas foetus J. Biol. Chem.* **258**, 4051-4054

119. Morgan, B.B. (1946) "Bovine Trichomoniasis." rev. ed. Burgess, Minneapolis, Minnesota.

120. Müller, H.E., and Saathoff, M. (1972) The Pathogenic Role of Trichomonas foetus Neuraminidase. *Zentralbl. Bakteriol., Parasitenkd., Infektionskr. Hyg., Abt. 1: Orig* **222**, 275-279.

121. Müller, M. (1983) Mode of Action of Metronidazole on Anaerobic Bacteria and Protozoa. *Surgery* **93**, 165-171

122. Müller, M. (1992) Energy Metabolism of Ancestral Eukaryotes: A Hypothesis Based on the Biochemistry of Amitochondriate Parasitic Protists. *BioSystems* **28**, 33-40.

123. Müller, M. (1993) The Hydrogenosome *J. Gen. Microbiol.* **139**, 2879-2889.

124. Müller, M., and Lindmark, D.G. (1974) Enzymes Involved in Succinate Formation in *Tritrichomonas foetus*. *Program Abstr. 49th Annu. Meet. Am. Soc. Parasitol.* 43.

125. Musick, W.D.L. (1981) Structural Features of the Phosphoribosyltransferases and Their Relationship to the Human Deficiency Disorders of Purine and Pyrimidine Metabolism. *CRC Critical Reviews in Biochemistry* **11**, 1-34.

126. Natalini, P., Ruggieri, S., Santarelli, I., Vita, A., and Magni, G. (1979) Baker's Yeast UMP:Pyrophosphate Phosphoribosyltransferase-Purification, Enzymatic and Kinetic Properties. *J. Biol. Chem.* **254**, 1558-1563.

127. Neuhard, J., and Nygaard, P. (1987) Purines and Pyrimidines. In "*Escherichia coli* and *Salmonella typhimurium*." (Neidhardt, F.C. ed.), pp.445-473. Washington DC.

128. Nilsson, D., and Lauridsen, A.A. (1992) Isolation of Purine Auxotrophic Mutants of Lactococcus lactis and Characterization of the Gene hpt Encoding Hypoxanthine Guanine Phosphoribosyltransferase. *Mol. Gen. Genet.* **235**, 359-364.

129. Olsen, A.S., and Milman, G. (1974) Chinese Hamster Hypoxanthine-Guanine Phosphoribosyltransferase. Purification, Structural and Catalytic Properites. *J. Biol. Chem.* **249**, 4030-4037.

130. Olsen, A.S., and Milman, G. (1977) Human Hypoxanthine Phosphoribosyltransferase. Purification and Properties. *Biochemistry* **16**, 2501-2505.

131. Parsonson, I.M., Clark, B.L., and Dufty, J. (1974) The Pathogenesis of *Tritrichomonas foetus* Infection in the Bull. *Aust. Vet. J.* **50**, 421-423.

132. Parsonson, I.M., Clark, B.L., and Dufty, J.H. (1976) Early Pathogenesis and Pathology of *Tritrichomonas foetus* Infection in Virgin Heifers. *J. Comp. Path.* **86**, 59-66.

133. Paulus, V.A., Ingalls, R.G., Vasquez, B., and Bieber, A.L. (1980) Studies of an Unusually Basic Hypoxanthine-guanine Phosphoribosyltransferase. *J. Biol. Chem.* **255**, 2377-2382.

134. Pratt, D., and Subramani, S. (1983) Nucleotide Sequence of the *Escherichia coli* Xanthine-Guanine Phosphoribosyl Transferase Gene. *Nucleic Acids Res.* **11**, 8817-8823.

135. Queen, S.A., Jagt, D.V., and Reyes, P. (1988) Properties and Substrate Specificity of a Purine Phosphoribosyltransferase from the Human Malaria Parasite, *Plasmodium falciparum*. *Mol. Biochem. Parasitol.* **30**, 123-134.

136. Rhyan, J.C., Stackhouse, L.L., and Quinn, W.J. (1988) Fetal and Placental Lesions in Bovine Abortion Due to *Tritrichomonas foetus*. *Vet. Pathol.* **25**, 350-355.

137. Romanowska, E., and Watkins, W.M. (1963) Fractionation of Neuraminidases in Extracts of *Trichomonas foetus*. *Biochem. J.* **87**, 37P-38P.

138. Roos, D. (1994) Personal Communication.

139. Rosenbloom, F., Kelley, W., Miller, J., Henderson, J., and Seegmiller, J. (1967) Inherited Disorder of Purine Metabolism: Correlation Between Central Nervous System Dysfunction and Biochemical Defects. *J. Am. Med. Ass.* **202**, 103-106.

140. Rustia, M., and Shubik, P. (1972) Induction of Lung Tumors and Malignant Lymphomas in Mice by Metronidazole. *J. Natl. Cancer. Inst.* **48**, 721-729

141. Ryley, J.F. (1955) Studies on the Metabolism of the Parasite Flagellate *Trichomonas foetus*. *Biochem. J.* **59**, 361-369.

142. Salerno, C., and Giacomello, A. (1981) Human Hypoxanthine Guanine Phosphoribosyltransferase: The Role of Magnesium Ion in a Phosphoribosylpyrophosphate-Utilizing Enzyme. *J. Biol. Chem.* **256**, 3671-3673.

143. Sambrook, J., Fritch, E.F., and Maniatis, T. (1989), *Molecular Cloning: A Laboratory Manual*, Cold Spring Harbor Laboratory Press, Cold Spring Harbor, New York.

144. Scapin, G., Grubmeyer, C., and Sacchettini, J.C. (1994) Crystal Structure of Orotate Phosphoribosyltransferase. *Biochemistry* **33**, 1287-1294.

145. Schulz, G.E. (1992) Binding of Nucleotides by Proteins. *Curr. Opin. Struct. Biol.* **2**, 61-67.

146. Schwartzman, J.D., and Pfefferkorn, E.R. (1982) *Toxoplama gondii*: Purine Synthesis and Salvage in Mutan Host Cells and Parasites. *Exp. Parasitol.* **53**, 77-86.

147. Searle, S.M.J., and Müller, M. (1991) Inorganic Pyrophosphatase of *Trichomonas vaginalis*. *Mol. Biochem. Parasitol.* **44**, 91-96.

148. Seegmiller, J. (1980) "Diseases of Purine and Pyrimidine Metabolism," 8th, Saunders, Philadelphia, Pennsylvania.

149. Seegmiller, J., Rosenbloom, F., and Kelley, W. (1967) Enzyme Defect Associated with a Sex-Linked Human Neurological Disorder and Excessive Purine Synthesis. *Science* **155**, 1682-1684.

150. Segel, I.H. (1975) "Enzyme Kinetics: Behavior and Analysis of Rapid Equilibrium and Steady-State Enzyme Systems," John Wiley & Sons, New York, New York.

151. Shahabuddin, M., and Scaife, J. (1990) The Gene for Hypoxanthine Phosphoribosyltransferase of *Plasmodium falciparum* Complements a Bacterial *HPT* Mutation. *Mol. Biochem. Parasit.* **41**, 281-288.

152. Shorb, M.S., (1964) The Physiology of Trichomonads. In "Biochemistry and Physiology of Protozoa" (Hutner, S.H., ed.), Vol. 3, pp. 383-457. Academic Press, New York, New York.

153. Short, J.M., Fernandez, J.M., Sorge, J.A., and Huse, W.D. (1988) λZAP: A Bacteriophage Lambda Expression Vector with *in vivo* Excision Properites. *Nucl. Acids Res.* **16**, 7583-7600.

154. Showalter, R.E., and Silverman, M.R. (1990) Nucleotide Sequence of a Gene, *hpt*, for Hypoxanthine Phosphoribosyltransferase from *Vibrio harveyi*. *Nucl. Acids Res.* **18**, 4621

155. Skirrow, S.Z., and BonDurant, R.H. (1988) Treatment of Bovine Trichomoniasis with Ipronidazole. *Aust. Vet. J.* **65**, 156.

156. Skirrow, S.Z., BonDurant, R.H., Farley, J., and Correa, J. (1985) Efficacy of Ipronidazole Against Trichomoniasis in Beef Bulls. *J. Am Vet. Med. Assoc* **187**, 405-407.

157. Sledge, W.E., Larson, A.D., and Hart, L.T. (1978) Costae of *Tritrichomonas foetus*: Purification and Chemical Composition. *Science* **199**, 186-188.

158. Smith, J.L., Zaluzec, E.J., Wery, J.P., Niu, L., Switzer, R.L. *et al.* (1994) Structure of the Allosteric Regulatory Enzyme of Purine Biosynthesis. *Science* **264**, 1427-1433.

159. Sogin, M.L. (1989) Evolution of Eukkaryotic Microorganisms and Their Small Subunit Ribosomal RNAs. *Am. Zool.* **29**, 487-499.

160. Sogin, M.L. (1991) Early Evolution and the Origin of Eukaryotes. *Curr. Opinion Genet. Develop.* **1**, 457-463.

161. Sogin, M.L., Gunderson, J.H., Elwood, H.J., Alonso, R.A., and Peatie, D. (1989) Phylogenetic Meaning of the the Kingdom Concept: an Unusual Ribosomal RNA from *Giardia lamblia*. *Science* **243**, 75-77.

162. Southern, E.M. (1975) Detection of Specific Sequences Among DNA fragments Seperated by Gel Electrophoresis. *J. Mol. Biol.* **98**, 503-517.

163. Srivastava, S.K., and Beutler, E. (1971) Purification and Kinetic Studies of Adenine Phosphoribosyltransferase From Human Erythrocytes. *Arch. Biochem. Biophys.* **142**, 426-434.

164. Stealey, J.R., and Watkins, W.M. (1972) Separation of α-L-Fucosidases in Extracts of *Trichomonas foetus*. *Biochem. J.* **126**, 16P-17P.

165. Steinbuchel, A., and Müller, M. (1986) Anaerobic Pyruvate Metabolism of *Tritrichomonas foetus* and *Trichomonas vaginalis* hydrogenosomes. *Mol. Biochem. Parasitol.* **20**, 57-65.

166. Steinbuchel, A., and Müller, M. (1986) Glycerol, a Metabolic End Product of *Trichomonas vaginalis* and *Tritrichomonas foetus*. *Mol. Biochem. Parasitol.* **20**, 45-55.

167. Takeda, M., and Webster, R.E. (1968) Protein Chain Initiation and Deformylation in B. subtilis Homogenates. *Biochemistry* **60**, 1485-1494.

168. Thomas, C.B., Arnold, W.J., and Kelley, W.N. (1973) Human Adenine Phosphoribosyltransferase. Purification, Subunit Structure, Amino Acid Composition, and Substrate Specificity. *J. Biol. chem.* **248**, 2529-2535.

169. Timofeev, B.A. (1962) Facteur de Diffusion et L'Hyaluronidase dans Les *Trichomonas Porcins* et *Trichomonas foetus* (Riedmuller, 1928). *Tr. Vses. Inst. Eksp. Vet.* **28**, 300-306.

170. Ullman, B. (1994) Personal Communication.

171. Vasanthakumar, G., van Ginkel, S., and Parish, G. (1994) Isolation and Sequencing of a cDNA encoding the Hypoxanthine-Guanine Phosphoribosyltransferase from *Toxoplasma gondii*. *Gene* **147**, 153-154.

172. Verham, R. (1985) The Purine and Pyrimidine Metabolism in *Tritrichomonas foetus*. Dissertation UCSF.

173. Victor, J., Greenberg, L.B., and Sloan, D.L. (1979) Studies of the Kinetic Mechanism of Orotate Phosphoribosyltransferase from Yeast. *J. Biol. Chem.* **254**, 2647-2655.

174. Viscogliosi, E., Philippe, H., Baroin, A., Perasso, R., and Brugerolle, G. (1993) Phylogeny of Trichomonads Based on Partial Sequences of Large Subunit rRNA and on Cladistic Analysis of Morphological Data. *J. Euk. Microbiol.* **40**, 411-421.

175. Walsh, C.J., and Sherman, I.W. (1968) Purine and Pyrimidine Synthesis by the Avian Malaria Parasite, *Plasmodium lophurae*. *J. Protozool.* **15**, 763-770.

176. Wang, A.L., and Wang, C.C. (1985) Isolation and Characterization of DNA from *Tritrichomonas foetus* and *Trichomonas vaginalis*. *Mol. Biochem. Parasitol.* **14**, 323-335.

177. Wang, C.C., and Aldritt, S.L. (1983) Purine Salvage Networks in *Giardia lamblia*. *J. Exp. Med.* **158**, 1703-1712.

178. Wang, C.C., and Simashkevich, P.M. (1981) Purine Metabolism in the Protozoan Parsite *Eimeria tenella*. *Proc. Natl. Acad. Sci. U.S.A.* **78**, 6618-6622.

179. Wang, C.C., Verham, R., Rice, A., and Tzeng, S. (1983) Purine Salvage by *Tritrichomonas foetus*. *Mol. Biochem. Parasitol.* **8**, 325-337.

180. Wang, C.C., Verham, R., Tzeng, S., Aldritt, S., and Cheng, H. (1983) Pyrimidine Metabolism in *Tritrichomonas foetus*. *Proc. Natl. Acad. Sci., U.S.A.* **80**, 2564-2568.

181. Watanabe, T., and Fukasawa, T. (1961) Episome-mediated Transfer of Drug Resistance in Enterobacteriaceae. II. Elimination of Resistance Factors with Acridine Dyes. *J. Bact.* **81**, 679-683.

182. Watkins, W.M. (1959) Enzymes of *Trichomonas foetus*. The Action of Cell-free Extracts on Blood-group substances and Low-Molecular-Weight Glycosides. *Biochem. J.* **71**, 261-274.

183. Watkins, W.M., and Morgan, W.T.J. (1954) Inactivation of the H Receptors on Human Erythrocytes by an Enzyme obtained from *Trichomonas foetus Br. J. Exp. pathol.* **35**, 181-190.

184. Watts, R.W.E. (1985) Defects of Tetrahydrobiopterin Synthesis and Their Possible Relationship to a Disorder of Purine metabolism (the Lesch-Nyhan Syndrome). *Adv. Enzyme Regul.* **23**, 25-58.

185. Weinrich, D.H., and Emmerson, M.A. (1933) Studies on the Morphology of *Tritrichomonas foetus* (Riedmuller) (Protozoa, Glagellata) from American cows. *J. Morphol.* **55**, 193-206.

186. Williams, O.J., McEwan, D., Bertram, J.D., and Gilfedder, J. (1987) Treatment of Trichomoniasis. *Aust. Vet. J.* **64**, 159-160.

187. Wilson, S.K., Kocan, A.A., Gaudy, E.T., and al., e. (1979) The Prevalence of Trichomoniasis in Oklahoma Beef Herds. *Bovine Pract.* **14**, 109-110.

188. Yuan, L., Craig, S.P., III, McKerrow, J.H., and Wang, C.C. (1990) The Hypoxanthine-Guanine Phosphoribosyltransferase of *Schistosoma mansoni*. *J. Biol. Chem.* **265**, 13528-13532.

189. Yuan, L., Craig, S.P., III, McKerrow, J.H., and Wang, C.C. (1992) Steady-State Kinetics of the Schistosomal Hypoxanthine-Guanine Phosphoribosyltransferase. *Biochemistry* **31**, 806-810.

APPENDIX A: PREPARATION OF NUCLEIC ACIDS FROM *TRITRICHOMONAS FOETUS*

T. foetus strain KV_1 was axenically cultured in Diamond's TYM medium pH 7.2, supplemented with 10% heat inactivated horse serum and 1% antibiotic/antimycotic mixture at 37°C (Diamond, 1957; Verham, 1985). The composition of one liter of TYM media is as follows:

	g/liter H_2O
Tryptose	20.0
Yeast extract	10.0
Maltose	5.0
Cysteine HCl	1.0
Ascorbic Acid	0.2
K_2HPO_4	0.8
KH_2PO_4	0.8

The pH of the media was adjusted to 7.2 with KOH, and the media was sterilized either by filtration through a sterile 0.22 µm filter or by autoclaving for 20 min at 121°C. 10% heat inactivated horse serum and 1% antibiotic/antimycotic mix is added to the media prior to use. The stock antibiotic/antimycotic solution (100X) consists of 10,000 U/ml penicillin, 10,000 µg/ml streptomycin and 25 µg fungizone.

The parasites are passaged in fresh media in a 1:10 ratio after 16-24 hours growth. Stabilates of *T. foetus* were achieved using dimethylsulfoxide as the cryoprotectant (Diamond, 1964).

The method used to prepare DNA and RNA from *T. foetus* was that used by Wang and Wang (Wang and Wang, 1985) and is described here briefly. Cultures were grown to early stationary phase, and the cells were harvested by centrifugation. The cell pellet was washed with ice-cold PBS and resuspended in 10 volumes of 4 M guanidinium thiocyanate. Cesium chloride was added to the lysate to a final concentration of 0.4 g/ml. 2.5 ml of 5.7 M CsCl and 0.1 M EDTA, pH 8.0 was placed at the bottom of ultracentrifuge tubes for the Beckman SW41 rotor as a cushion, and 10 ml of the CsCl-cell lysate mixture was carefully layered on top of the cushion. The tube was centrifuged in a Beckman SW41 rotor at 34,000 rpm at 20°C for 16 h. DNA was located in the lower third of the tube, and RNA was the clear gelatinous pellet found at the bottom of the tube. After the DNA containing fraction was transferred to another tube, it was precipitated with 2.5 volumes of ice-cold ethanol, purified with chloroform:isoamyl alcohol (49:1) extractions, and reprecipitated with one-tenth volume of 3 M NaOAc and 2.5 volumes of ice-cold ethanol. The RNA was resuspended with 0.3 M NaOAc, pH 6.0, extracted with phenol:chloroform, precipitated with 2.5 volumes of ice-cold ethanol, and stored in ethanol at -80°C.

APPENDIX B: VISUALIZATION OF DNA BLOTS BY CHEMILUMINESCENCE

Reagents:

Buffer 1: 100 mM Tris-HCl pH 8.0 + 150 mM NaCl

Tropix buffer: 2.1 g $NaHCO_3$ dissolved in 500 ml H20. The pH of the solution is adjusted to 9.5 with NaOH prior to adding $MgCl_2$ to a final concentration of 1 mM.

Blocking solution: 0.5% blocking reagent (provided by manufacturer) in buffer 1.

Detection solution: 20 µl of AMPPD (reagent is purchased from Tropix, Bedford, MA) in 10 ml of the Tropix buffer.

After the DNA blot has been washed, following hybridization to the probe, it was rinsed with buffer 1 and incubated in the blocking solution at room temperature for 30 min. The blot was again rinsed with buffer 1, incubated with a 1:4000 dilution of the rabbit antidigoxigenin antibody in buffer 1 at room temperature for 30 min. and washed twice at room temperature in buffer 1. Finally, the blot was washed twice in tropix buffer at room temperature and then developed using the detection solution. The blot was drained, wrapped in Saran wrap, incubated at 37°C for 30 min, and exposed to X-ray film.

APPENDIX C: PREPARATION OF SINGLE-STRANDED PHAGEMID DNA TEMPLATE FOR SEQUENCING

Cells transformed with phagemid were grown in LB media (Sambrook, *et al.*, 1989), with ampicillin at a final concentration of 50 µg/ml, to $OD_{600} \approx 0.6$ in . Two milliliters of this culture were infected with M13K07 helper phage (at a multiplicity of infection of at least 10). The phage infected culture was incubated at 37°C with aeration for 1 h. Twenty milliliters of 2YT broth (Sambrook, *et al.*, 1989), containing 25 µg/ml ampicillin and 35 µg/ml kanamycin, were inoculated with 500 µl of the phage infected culture, and incubated at 37°C with aeration for 6-12 hs.

The first step in harvesting the phagemid DNA was to pellet the cells, and transfer the supernatant to another tube. Next the phagemid was precipitated by the addition of 125 µl of 5 M ammonium acetate and 125 µl of 40% PEG 8000 to each ml of supernatant. The resulting mixture was incubated on ice for at least 15 min (overnight is fine), and followed by centrifugation at 11,000 rpm at 4°C for 30 min. All of the supernatant was removed, and the pellet was resuspended in 1 ml of TE. The phagemid was precipitated a second time following the above mentioned procedure.

The phagemid DNA was liberated from the protein coat by extraction with phenol, pH 8:chloroform, which was followed by a chloroform extraction. The phagemid DNA was precipitated by addition of one-tenth a volume of 5 M ammonium acetate and 2-2.5 volumes of ice-cold ethanol.

APPENDIX D: PROTOCOL FOR PROTEIN GELS

Solutions:

Resolving buffer (1.5 M Tris pH 8.8): 18.21 g Trizma base/100 ml H_2O. Adjust pH to 8.8 with HCl.

Stacking buffer (0.5 M Tris pH 6.8): 6.07 g Trizma base/100 ml H_2O. Adjust pH to 6.8 with HCl.

30% Acrylamide/bis-acrylamide: 29 g acrylamide and 1 g bis-acrylamide/100 ml H_2O.

8X Running buffer (25 mM Tris, 191 mM glycine and 0.1% SDS:

12.1 g Trizma base, 57.4 g glycine and 4 g SDS/500 ml H_2O.

PAGE stain solution: 0.08% Coomassie Blue, 25% ethanol and 8 % acetic acid.

PAGE destain solution: 25% ethanol and 8 % acetic acid.

The recipe for a 12% acrylamide gel is as follows:

H_2O	5 ml
1.5 M Tris, pH 8.8	3.75 ml
30% Acryl/bis-acryl.	6 ml
10% SDS	150 µl
10 % AP	75 µl
TEMED	10 µl

This is enough for 3-4 minigels. If the solution is degassed, it will polymerize rapidly.

The recipe for a 4% acrylamide gel (stacker) is as follows:

H_2O	3 ml
0.5 M Tris, pH 6.8	1.25 ml
30% Acryl/bis-acryl.	665 µl
10% SDS	50 µl
10% AP	25 µl
TEMED	5 µl

Electrophoresis with the mini-gels is usually performed at a constant current of 20-30 mA/gel.